

**Effects of activation of the Unfolded Protein Response
in *Drosophila melanogaster***

DISSERTATION
zur Erlangung des Doktorgrades
der Mathematisch-Naturwissenschaftlichen Fakultät
der Christian-Albrechts-Universität zu Kiel

vorgelegt von
Gu Tian
aus China

Kiel, 2017

Referent: Prof. Dr. Thomas Roeder

Koreferent: Prof. Dr. Holger Heine

Tag der mündlichen Prüfung: 13,10,2017

Zum Druck genehmigt: 13,10,2017

gez. Dekan:

Table of contents

List of tables	1
List of figures	2
List of abbreviations	5
1.Introduction	7
1.1 ER stress and Unfolded Protein Response	7
1.1.1 IRE1/XBP1 pathway of the UPR	9
1.1.2 PERK pathway of the UPR	10
1.1.3 Atf6 pathway of the UPR.....	11
1.2 Functions of the unfolded protein response in innate immunity.....	12
1.3 Insulin/IGF signaling and relationship with UPR.....	13
1.4 Drosophila is a well-suited model system to study unfolded protein response mechanisms	15
1.5 Aims of this study.....	18
2.Materials and Methods	20
2.1 Materials	20
2.1.1 Drosophila strains and cultivation	20
2.1.2 Fly standard medium	21
2.1.3 GAL4/UAS crossing.....	21
2.1.4 Solutions.....	22

2.1.5 Antibodies	22
2.1.6 Oligonucleotides	23
2.1.7 Enzymes	23
2.1.8 Chemicals	24
2.1.9 Equipment.....	25
2.2 Methods	26
2.2.1 Lifespan measurements	26
2.2.2 Body fat quantification.....	26
2.2.3 Glucose measurements	27
2.2.4 Glucose tolerance test	28
2.2.5 Immunohistochemistry and imaging	28
2.2.6 Quantification of circulation and total DILP2 content	31
2.2.7 Constructing the UAS-Atf6 transgenic line and general molecular biology methods	32
2.2.8 Statistical analysis	39
3.Results.....	40
3.1 Activation of UPR via different branches induces substantial changes in different organs of the fruit fly	40
3.1.1 UPR activation changes the morphology of trachea in Drosophila larvae.	40
3.1.2 UPR activation changes the morphology of the intestinal tissue	49
3.1.3 UPR activation changes the morphology of the fat body in Drosophila.	

.....	52
3.2 Activation of XBP1s in trachea and fat body increased expression levels of drosomycin dramatically.	55
3.3 Analyses of activated UPR in regulation of insulin and glucose homeostasis	59
3.3.1 Overexpression of XBP1s and PERK influence DILP2 in IPCs.	59
3.3.2 Influence of overexpression of UPR on circulating and total DILP2 level	60
3.3.3 Influence of overexpression of UPR inducers on glucose tolerance.....	63
3.3.4 Influence of overexpression of UPR inducers on life span.....	65
3.3.5. Overexpression of PERK in IPCs decreases body size, weight and causes development delay	65
3.4 Influence of overexpression of ORMDL in Drosophila IPCs	67
4. Discussion	69
4.1 Specific activation of key UPR components influence the morphology of organs	70
4.2 Specific-expression of key UPR components activate the innate immune system	73
4.3 Specific-expression of key UPR components regulates insulin-like peptide release.....	74
Summary	78
Zusammenfassung	80
Reference	82

Appendix	95
Acknowledgement	101
Curriculum vitae	102
Declaration	103

List of tables

Table 1. Fly stock, genotype and donator	20
Table 2. Oligonucleotides used for PCRs.....	23
Table 3. Enzymes	23
Table 4. Chemicals	24
Table 5. Equipment	25
Table 6. PCR reaction reagents	33
Table 7. General Cycle conditions of PCR	34

List of figures

Figure 1. Three different sensors jointly coordinate the UPR in mammals.....	9
Figure 2. The GAL4/UAS system.....	17
Figure 3. Dissection of larvae by ventral filleting method	29
Figure 4. Map and construction of the pBID-UASC vector.....	35
Figure 5. Ectopic activation of XBP1s and of PERK in the trachea system was lethal.	41
Figure 6. Effects of ectopic expression of Ire1 and Atf6 on Drosophila tracheal cells' morphology.....	42
Figure 7. Ectopic activation of Xbp1s and PERK in the tracheal system.	43
Figure 8. Overexpression of XBP1s and PERK inhibit the growth of the terminal trachea branching in Drosophila.....	45
Figure 9. Immunohistochemical staining of terminal trachea in UPR overexpressing larvae.....	46
Figure 10. Susceptibility of UPR activated larvae to hypoxia.....	48
Figure 11. UPR signaling activated in the gut induced structural changes in cell shapes and nuclear sizes.....	50
Figure 12. Ire1 overexpression increased lifespan in males feeding DSS.	52

Figure 13 . Overexpression of XBP1s and PERK in the fat body changed morphology of the fat body cell significantly	53
Figure 14. Staining of fat body in overexpression of UPR components.....	54
Figure 15. Ectopic activation of PERK in the fat body	55
Figure 16. Spliced xbp1 (xbp1s) overexpression in the airway increases levels of drosomycin in larvae dramatically	57
Figure 17. Relative expression levels of xbp1s increased in larvae trachea under ER-stress condition.....	58
Figure 18. Spliced xbp1 (xbp1s) overexpression in the fatbody increases the level of drosomycin in larvae.....	58
Figure 19. Regulation of AMP gene expression in response to xbp1s activation in the airways.....	59
Figure 20. Overexpression of xbp1s and PERK in insulin-producing cells affect cell morphology.	60
Figure 21. Activation of signaling components of UPR in IPCs influence circulating DILP2 contents and total DILP2 contents in flies	62
Figure 22. Activation of signaling components of UPR in IPCs influence glucose tolerance in adult flies	64
Figure 23. XBP1s overexpression in IPCs influenced life span of flies	65
Figure 24. Overexpression of PERK in IPCs decreases body size and weight of flies	66
Figure 25. Overexpression of perk in IPCs causes development delay.....	67

Figure 26. Influence on DILP2 contents and glucose tolerance of overexpression of
ORMDL in Drosophila IPCs68

List of abbreviations

ANOVA	Analysis of variance
ATF6	Activating transcription factor 6
BSA	Bovine serum albumin
bp	Base pairs
CCA	Coupled Colorimetric Assay
cDNA	Complementary deoxyribonucleic acid
cm	centimeter
CO ₂	Carbon dioxide
d	day
DAPI	4',6-diamidino-2-phenylindole
Dilps	<i>Drosophila</i> insulin like peptides
DNA	Deoxyribonucleic acid
DNase	Deoxyribonuclease
dNTP	Deoxyribonucleotide triphosphate
EtOH	Ethanol
FB	Fat Body
g	gram
GFP	Green fluorescent protein
h	hour
HL3	Hemolymph-like buffer
IPCs	Insulin Producing Cells
kb	kilobase pairs
L	Liter
PBS	Phosphate buffered saline
PERK	Protein kinase RNA (PKR)-like ER Kinase
RNase	Ribonuclease
RNA	Ribonucleic acid
Rpl32	Ribosomal protein 32
rpm	Rotations per minute
RT-PCR	Reverse transcription-polymerase chain reaction
RT	Room temperature
SE	Standard error
TAG	Triacylglycerin
TBE	Tris/Borate/EDTA
mg	milligram
min	minutes
ml	Millilitres
mM	millimolar
mRNA	Messenger ribonucleic acid
UAS	Upstream activation sequence

UPR	Unfolded Protein Response
xbp1s	X-box binding protein-1
ns	not significant
WT	wild-type
sec	Seconds

1.Introduction

1.1 ER stress and Unfolded Protein Response

Proper functioning of the Endoplasmic Reticulum (ER) is essential for eukaryotic cell survival, since most secreted and transmembrane proteins are synthesized, folded and undergo further maturation in the ER lumen (Ghaemmaghami et al. 2003; Kanapin et al. 2003). The folding process in the ER is highly dynamic and if this machinery is overloaded, the cell will experience ER-stress. One of the common causes of ER-stress is that the protein folding capacity in the ER is exceeded and accumulation of unfolded or misfolded proteins in the ER lumen occurs. In response of this disturbed ER homeostasis, an evolutionarily conserved cell stress response, the unfolded protein response (UPR) is activated. The UPR is an intracellular signaling pathway, which can effectively cope with stress in the ER, protect cells from the toxic effects of accumulated proteins and restore homeostasis (Hetz et al. 2012; Rutkowski et al. 2010).

The UPR has three main functions, restoring normal physiology of the cell by halting protein translation, degrading misfolded proteins, and activating the signaling pathways that induce production of molecular chaperones required for proper protein folding. If these objectives are not achieved within a certain time span or the disruption is prolonged, the UPR aims towards apoptosis.

A variety of stressors can induce ER stress, including altered environmental conditions (changes in nutrients or oxygen) or intracellular insults (carcinogens or oncogenic mutations) and mutations that impair the inherent folding properties of an encoded protein (Kozutsumi et al. 1988). Hence, it is often closely linked to autophagy, hypoxia signaling, mitochondrial biogenesis, or reactive oxygen species (ROS) responses. Chronicity of ER stress leads to UPR-induced apoptosis and in turn to an imbalance of

tissue homeostasis. If UPR fails to relieve ER stress and the accumulation of unfolded proteins persists, cell death pathways are activated. Deregulated UPR is associated with a variety of human diseases including diabetes, cancer and neurodegenerative disorders (Wang et al. 2012).

In recent years, numerous studies have associated UPR with various neurodegenerative disorders, cancer, diabetes and infectious diseases, which has helped to attract attention to this field (Zhao et al. 2006). Accordingly, a better understanding of the complexity of the ER stress response and the UPR could lead to novel therapeutic approaches. Nevertheless, the mechanisms how cells activate apoptosis and promote tissue homeostasis after chronic ER stress remain poorly understood. Sustained overactivation of the UPR has been implicated in prion diseases as well as in several other neurodegenerative diseases, and inhibiting the UPR could develop into a treatment strategy for these diseases (Moreno et al. 2013). Diseases amenable to UPR inhibition thus include the neurodegenerative disorders Creutzfeldt–Jakob, Alzheimer, Parkinson and Huntington.

The UPR consists of three different branches (Fig. 1). Thus, the mechanisms that have been identified to reduce the level of misfolded proteins in the ER, are regulated by three ER membrane-embedded sensors: 1) the inositol-requiring protein-1 (IRE1), 2) the protein kinase RNA (PKR)-like ER kinase (PERK) and 3) the activating transcription factor-6 (ATF6). All these three adaptive signaling cascades can be activated by perturbed ER homeostasis (Rutkowski et al. 2007; Rutkowski et al. 2006).

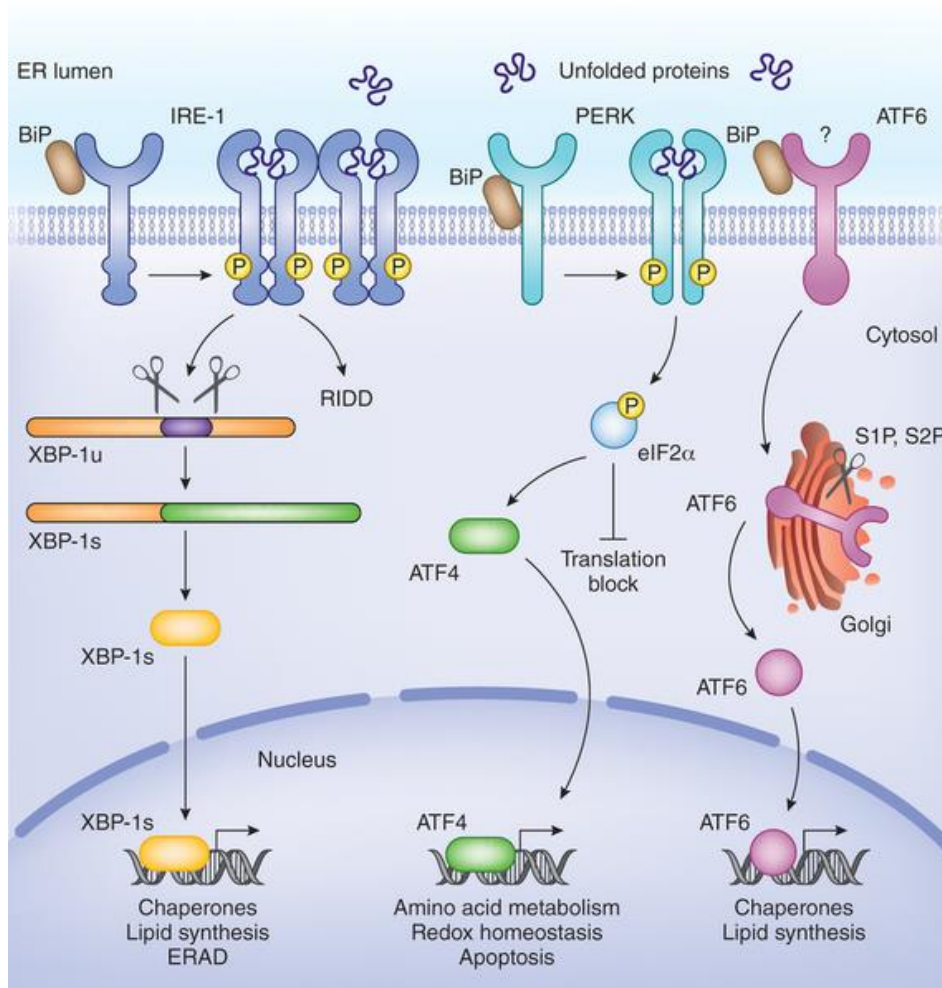


Figure 1. Three different sensors jointly coordinate the UPR in mammals.

Three sensors in the ER lumen are operative: inositol-requiring enzyme 1 (IRE1), protein kinase R-like ER kinase (PERK) and activating transcription factor 6 (ATF6) (from Janssens et al. 2014).

1.1.1 IRE1/XBP1 pathway of the UPR

Inositol requiring protein-1 (Ire1) is the evolutionarily most conserved arm of the UPR and was first identified in yeast (*Saccharomyces cerevisiae*) as a UPR signal transducer by using UPR inducible reporter activity as a read-out (Mori et al. 1993). It was first found that IRE1 is an essential mediator of ER chaperone induction after ER stress, as such conditions prompt the activation of this transmembrane signaling protein by forcing oligomer formation (Cox et al. 1993; Korennykh et al. 2009).

Misfolded proteins in yeast initiate UPR signaling through IRE1, which is an ER-tethered endonuclease. In unstressed cells, IRE1 is kept inactive through its interaction with the ER-chaperone BiP. The interaction between IRE1/ BiP acts as a molecular sensor of ER-stress. Activated IRE1 cleaves the HAC1 mRNA to initiate mRNA splicing. Once spliced HAC1 is produced, it induces the transcription of ER chaperones and other components to reduce ER-stress.

In metazoans, this overall mechanism is conserved but more complex (Fig. 1). Different from yeast, mammals have two isoforms of IRE1 (IRE1 α and IRE1 β), both of them are involved in the splicing of Xbp1 mRNA (Tirasophon et al. 1998; Niwa et al. 1999). In animals, IRE1 activates at least three branches of signaling activities and cleaves the mRNA of xbp1, which is a functional homologue of Hac1 (Yoshida et al. 2001; Calfon et al. 2002). Xbp1 unspliced mRNA (Xbp1u) is translated under normal conditions and is rapidly degraded (Calfon et al. 2002; Yoshida et al. 2006). Upon detection of ER stress, IRE1 directly binds to misfolded peptides in the ER lumen and its RNase domain on the cytoplasmic side is activated. IRE1 cuts the precursor Xbp1 mRNA twice, thus excising an intervening fragment or intron. The 5' and 3' mRNA fragments are then ligated, generating a spliced mRNA (Xbp1s) that encodes an activator of UPR target genes. The intron of XBP1 mRNA has 26 bp nucleotides in mammals and has 23 bp nucleotides in *Drosophila*. Interestingly, Xbp1u, which has a nuclear exclusion signal and degradation motif, binds to Xbp1s and sequesters it from the nucleus to the cytoplasm for degradation, thus acting as negative feedback regulator of Xbp1s (Yoshida et al. 2006; Ryoo et al. 2007). Splicing of Xbp1 causes a frame shift in the reading frame and has different functional properties. Xbp1s mRNA is more stable and works as a potent activator of UPR target genes (Yoshida et al. 2001), whereas the protein encoded by the precursor mRNA Xbp1u is labile and represses UPR target genes.

1.1.2 PERK pathway of the UPR

PERK is an ER-localized type I transmembrane protein, as an ER transducer it has a

similar structure and function compared with Ire1. It has a luminal stress-sensing domain and a cytosolic serine/threonine kinase domain. Much like IRE1, PERK is activated by autophosphorylation following the release of BIP. BIP is an immunoglobulin heavy-chain binding protein and is involved in all of the three branches of UPR. Under non-stress conditions, heat shock protein 90 (HSP90) and BIP bind to PERK to stabilize and prevent activation (Marcu et al. 2002). When cells are suffering ER stress, BIP binds to unfolded and misfolded proteins, permitting the release of PERK for homodimerization and autophosphorylation (Bertolotti et al. 2000; Liu et al. 2000). Activated PERK also phosphorylates eukaryotic translational initiation factor eIF2 α (Lu et al. 2014). The normal eIF2 α helps to charge 40S ribosomal subunits with initiator methionyl tRNAs, which is essential for translational initiation. Thus, eIF2 α phosphorylation inhibits the new protein synthesis, selectively upregulates the translation of specific target mRNAs including ATF4 (activating transcription factor 4) (Harding et al. 2000). Since the ATF4 mRNA possesses upstream open reading frames (ORFs) to escape translational suppression, ATF4 translocates to the nucleus where it activates a third set of UPR target genes. These include GADD34 (growth-arrest DNA damage gene 34), which feedbacks to inhibit PERK, which can induce apoptosis in cells with irrecoverable levels of ER stress.

1.1.3 ATF6 pathway of the UPR

ATF6 is a type II transmembrane protein that also plays an important role in the UPR. This protein has a transmembrane domain and a DNA binding domain that tethers the protein at the ER membrane under unstressed conditions. Under these unstressed conditions, ATF6 is inactive as it binds with BIP. When the luminal domain of ATF6 senses ER stress, ATF6 is released from BIP and translocate from the ER to the Golgi. In the Golgi, ATF6 is sequentially cleaved by the Golgi resident site-1 protease (S1P) and S2P to generate an active transcription factor (Ye et al. 2000). There are two homologues of ATF6 in the mammalian genome, single knockout mice are viable but double knockouts are embryonically lethal, indicative of redundancy of function in the

two genes (Yamamoto et al. 2007). By contrast, the *Drosophila* genome encodes a single ATF6 homolog. Like the mammalian counterpart, it has a DNA binding domain and an ER luminal domain. The sequence of the *Drosophila* Atf6 is similar to those of mammals. If this gene is required for a proper ER stress response in adult tissues remain to be validated.

1.2 Functions of the unfolded protein response in innate immunity

The innate immune system is an important subsystem of the overall immune system that comprises cells and mechanisms that defend the host from infection by other organisms (Litman et al. 2005). To function properly, an immune system distinguishes a variety of agents, such as pathogens, from the organism's own healthy tissue. Deregulation of the immune system can result in autoimmune diseases, inflammatory diseases and cancer (O'Byrne et al. 2001). Antimicrobial peptides (AMPs) are innate host defense molecules that are effective in fighting bacteria (Gram-positive, Gram-negative), fungi (yeasts and filamentous) and parasites, and in some cases also enveloped viruses (Zasloff et al. 2002). *Drosophila melanogaster* has multiple innate defense reactions, many of which are shared with mammals. These reactions include the presence of physical barriers together with local and systemic immune responses. In addition to systemic antimicrobial responses, cells of most of the barrier epithelia of *Drosophila* produce AMPs that provide a local first line of defense against microorganisms (Ferrandon et al. 1998). AMPs represent highly conserved, innate immune elements that protect the host from microbial pathogens, while also signaling a variety of downstream responses that further fortify innate and adaptive immunity (Pasupuleti et al. 2012; Nakatsuji et al. 2012). UPR signaling is related to the innate and adaptive immune response at many levels. In some immune cell types UPR sensors are constitutively active in the absence of traditional UPR gene induction, which is necessary for antigen presentation and immunoglobulin synthesis. Previous studies have shown that AMP production increases not only in response to microbial

challenges, but also in response to perturbations of the endoplasmic reticulum (ER), where AMPs orchestrate a host of ER-initiated stress responses (Park et al. 2011).

Studies have shown that the Toll signaling pathway is highly important for recognition and defense against microbial infection in *Drosophila*, therefore Toll receptors are crucial for organismal defense in innate immunity (Lemaitre et al. 1996). In insects, one of the principal responses to microbial infection is the transcriptional induction of a battery of genes encoding antimicrobial peptides. Nevertheless, up to now the regulatory mechanisms that control the inducible AMP expression in barrier epithelia are not well understood.

1.3 Insulin/IGF signaling and relationship with UPR

Diabetes mellitus (DM) is a metabolic disorder caused by varying or persistent hyperglycemia due to reduced insulin action. DM has already become a chronic metabolic disease with “epidemic” proportions. Its global prevalence was estimated to be 6.4% worldwide (285 million adults in 2010) and is predicted to rise to approximately 7.7% (439 million) by 2030 (Shaw et al. 2010). With the emerging worldwide epidemic of diabetes and obesity, work in this field has attracted more and more attention (Baker et al. 2007; Birse et al. 2011).

Type 1 diabetes (T1D) as a form of DM results from the failure of insulin-producing β cells, the loss of cells leads to a decrease in insulin production, unsuppressed glucose production, a high blood sugar levels in the body and weight loss (Lehuen et al. 2010; Mathis et al. 2001). Type 2 diabetes mellitus (T2DM) is another form of DM, which is a multifaceted disease involving multiple pathophysiological defects. T2DM is associated with a combination of insulin resistance and an impaired insulin-producing cells function, which results in impaired glucose tolerance (Nolan et al. 2011). The study in this thesis is highly relevant to type 1 diabetes.

Many recent studies have shown that this disease impairs insulin/IGF signaling (IIS) pathways in general, which play central roles in metabolism, growth and development in metazoans, including the fruit fly *Drosophila melanogaster* (Brogiolo et al. 2001; Baker and Thummel 2007; Giannakou and Partridge 2007). *Drosophila* is considered to be one of the most important model systems for studying the insulin signaling pathway and much progress has been made in *Drosophila* in order to understand the role of the insulin receptor signaling pathway and the interaction with other pathways, as well as their role in growth, protein synthesis and metabolism (Saucedo et al. 2003; Cheng et al. 2011). In *Drosophila*, eight insulin-like peptides (DILP 1-8) and only one receptor (dInR) have been identified (Fernandez et al. 1995; Brogiolo et al. 2001; Garelli et al. 2012). Of these peptides, DILP2, 3, and 5 are secreted from insulin producing cells (IPCs) in the brain, which take the role of the mammalian pancreatic beta cells. DILP6, DILP 3 as another ILP is produced in the fat body. Previous studies indicated altered expression of genes encoding DILP2, 3, 5, and 6 results in modulated IGF signaling and profound metabolic and longevity consequences (Broughton et al. 2005, 2008; Gronke et al. 2010; Bai et al. 2012). The functional roles of dILPs have been clarified based on a series of studies, however the control of dILPs production and release from IPCs by multiple factors has come into the research focus only recently. While genetic studies have indicated that adult IPCs are likely the primary endocrine tissue responsible for DILP secretion and signaling, the underlying molecular mechanism of how does IPCs work are unknown.

Insulin/IGF signaling pathway is very sensitive to alterations in ER homeostasis. Growing experimental evidence suggests that dysregulation of the endoplasmic reticulum responses contributes to type 1 diabetes pathogenesis that eventually lead to insulin-producing cells apoptosis (Mathis et al. 2001; Eizirik et al. 2009; Todd et al. 2008; Eizirik et al. 2013). In the organism, an acute or chronic stimulation of β cells by nutrients such as glucose leads to a large amount of insulin production, which places a continuous demand on the ER for proper protein synthesis, folding, trafficking, and secretion. When the folding capacity of the ER is exceeded, misfolded or unfolded

proteins accumulate in the ER lumen, and the unfolded protein response (UPR) is activated in these insulins producing cells (Cnop et al. 2005). The UPR can effectively preserve ER homeostasis of insulin-producing cells via enhanced protein-folding ability, increases chaperone availability, and enhances the degradation of misfolded proteins.

In recent studies, observations suggested that ER stress and UPR signaling through IRE1 can improve insulin sensitivity (Ramirez-Alvarado et al. 2010). Moreover, studies using genetically obese or high-fat diet (HFD)-induced obese mice identified an increase in UPR markers in the liver and in adipose tissues (Ozcan et al. 2004). In addition, elevated ER stress markers are detected in the liver and adipose tissue of obese insulin-resistant individuals (Boden et al. 2008). UPR signaling may increase the protein-folding capacity to improve insulin signaling, whereas IRE1-mediated Jun N-terminal kinase (JNK) activation could cause insulin resistance (Hotamisligil et al. 2010). Therefore, these observations indicate that there exists a link between insulin/IGF signaling (IIS) pathways and UPR signaling pathway, although the underlying mechanisms are poorly understood.

1.4 *Drosophila* is a well-suited model system to study unfolded protein response mechanisms

For more than a century, *Drosophila* has served as a powerful model organism for research at almost all levels of biology (Rincon-Limas et al. 2012). Especially fly genetics has been systematically and successfully applied to study mechanisms of numerous fundamental biological processes, including development, signaling processes, nervous system development and even the molecular aspects of human diseases (Bernards et al. 2001; Picher-Martel et al. 2016; Bier et al. 2005). As one of the most popular model organisms, it has a great number of advantages compared with other invertebrate models. The fruit fly has a very short life cycle and the large number of offspring is also advantageous for genetic research, because new fly lines

are quick and easy to make. Moreover, genetic manipulations are much easier to perform in fruit flies, because they offer some unique features, such as balancer chromosomes and binary expression control systems. Moreover, they have a relatively small, well-characterized genome, which was fully sequenced more than a decade ago. Although the manipulations I mentioned above can be performed in other animal models such as mice, mutations in flies can be generated much more easily and the complexity of genetic interventions is unmatched. Most of all, the fruit fly genome contains about 14,000 genes that share a high degree of homology with the corresponding human genes (Chen et al. 2008). During the past century, enormous resources of *Drosophila* have been produced, all of these accumulated research resources are available for studies using *Drosophila melanogaster*. A large collection of *Drosophila* stocks including P-element insertions (Bellen et al. 2004), genomic gene-defined deficiencies (Parks et al. 2004; Thibault et al. 2004), induced mutations and RNA interference mediated gene-specific knockdown lines (Dietzl et al. 2007) are mostly available from the Bloomington Stock Centre or the Vienna *Drosophila* Resource Centre (VDRC). Moreover, FlyBase (<http://flybase.org>) has provided freely an online repository of biological data and comprehensive knowledge about *Drosophila*.

Over the years, fly researchers have developed an impressive array of genetic tools that made *Drosophila melanogaster* an even better animal model for research. Among these tools, the availability of powerful binary and ternary expression systems is a unique advantage for using *Drosophila* as a research model including the GAL4/UAS system, the LexA/LexAop system (Sen-Lin et al. 2006) or the QF/QUAS systems (Potter et al. 2010). These systems allow fly researchers to target expression of a specific gene into a specific set of cells, and even activate or deactivate the gene at specific times. Among these systems, the GAL4/UAS expression system is the most widely used one (Brand and Perrimon 1993). The GAL4/UAS system consists of two main components: the yeast GAL4 transcriptional activator expressed in a specific pattern and a transgene

under the control of a UAS promoter that is largely silent in the absence of GAL4 (Fig. 2). These two essential components, GAL4 and UAS are separately inserted into two transgenic fly lines, both of them have usually no effect on the host organism. After crossing, their progeny has the gene of interest expressed in a specific cell or tissue result as defined by the GAL4 line. In addition to the accessible spatial control, many extremely versatile updates of the GAL4/UAS system has been achieved using as temporal control, such as the introduction of Gene Switch or TARGET systems, which is activated by a hormone induce or by a permissive temperature (Osterwalder et al. 2001; Suster et al. 2004).

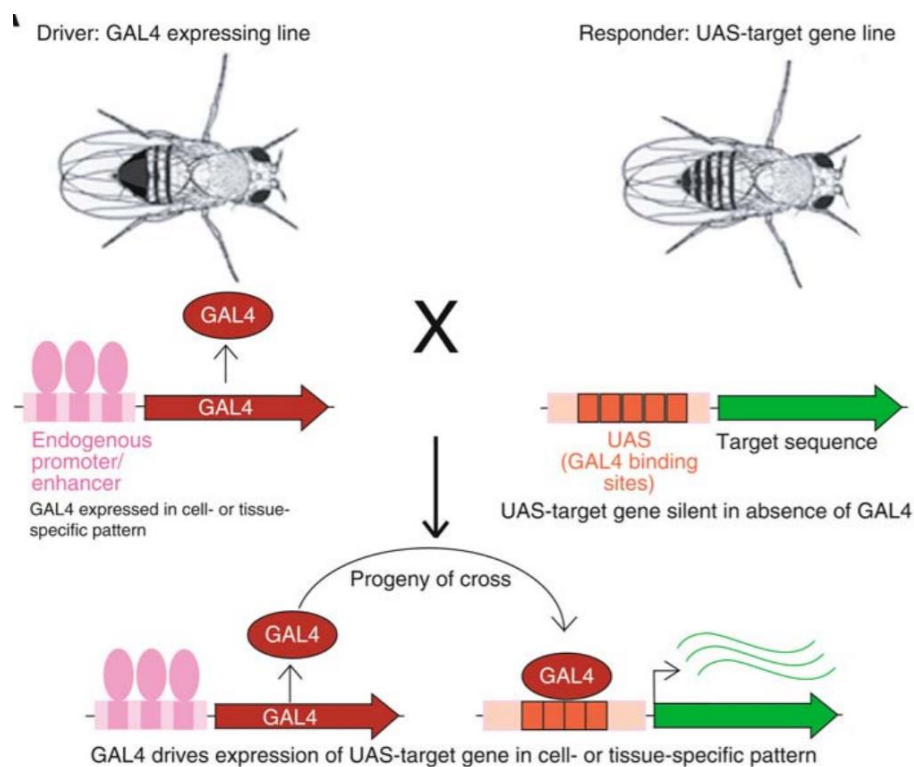


Figure 2. The GAL4/UAS system.

If the GAL4 driver line is crossed with the UAS responder line, in the F1-generation, the target gene is only expressed in a cell- or tissue-specific pattern. Adopted from (Elliott et al. 2008).

A growing interest has been drawn to the UPR since it is associated with various human diseases. In understanding the role of the UPR in disease, it has become increasingly important to use animal models that mimic more closely physiological conditions *in situ*. The UPR signaling pathway has three branches activated by three stress sensors: IRE1, PERK and ATF6, all these components are largely conserved between *Drosophila* and humans (Hollien et al. 2006). Unlike many pharmacological experiments done with homogeneous populations of cultured human cells, *Drosophila* can supply disease environments that closely mimick human conditions. Given the powerful genetic and molecular tools available in *Drosophila*, this system offers many exciting opportunities to investigate the connection between ER stress, cell death and disease. Consequently, the fact that the basic UPR pathways are highly conserved, together with the availability of many human disease models in this organism, makes *Drosophila* a powerful tool for studying UPR.

1.5 Aims of this study

The major aim of this project was to study the roles of the three branches of the unfolded protein response by their ectopic activation using *Drosophila melanogaster* as a model organism. My study comprises three major aspects. First, based on using the Gal4/UAS system to enhance the expression of IRE1, XBP1s, PERK, or ATF6 specifically in different *Drosophila* tissues, and to observe whether the activation of single UPR branches lead to changes at the molecular, the morphological or the physiological level.

Moreover, the interaction between the UPR signaling pathway and the innate immune response should have been investigated, primarily using transcript quantification of central molecules of the innate immune system in different organs of the fly that represent systemic and local immune responses.

Finally, based on many studies, which reported that UPR plays an important role in the

pathogenesis of diabetes and the regulation of insulin secretion in pancreatic beta cells, I aimed to decipher the role of UPR activation on insulin release and associated signaling events. For this, the GAL4/UAS system should be used to overexpress *XBP1s*, *IRE1*, *PERK* and *ATF6* in IPCs of the adult brain only. Using this approach, a novel and informative diabetes model should be installed.

2. Materials and Methods

2.1 Materials

2.1.1 *Drosophila strains and cultivation*

Without any special statements, all flies were maintained on standard medium, at 65% humidity under a 12 h light/dark cycle. Temperature was maintained at 25 °C during the day phase, while it was kept at 20 °C during night. All newborn flies were incubated in standard medium for 3 days at densities of 25-30 adults in each vial before they were used for assays. Stock flies were kept homozygous or balanced, using chromosome specific balancers, to avoid changes in genotypes due to recombination. If not further mentioned, fly stocks were obtained from the Bloomington stock center.

Table 1. Fly stock, genotype and donator

stock name	genotype	donator
w1118	w1118	Bloomington 5905
xbp1s-UAS	w;Sco/CyO;UAS-xbp1-Spliced/TM6B	Gift
ire1-UAS	w;Sco/CyO;UAS-ire1/TM6B	Gift
Perk-UAS	P{w[+mC]=lacW}Tor[k17004]/CyO	Gift
ppk-GAL4	w [*]; P{w[+mC]=ppk-GAL4.G}2	Bloomington 32078
ppk-GS-GAL4	w [*]; P{w[+mW.hs]=Switch2}GSG3330-1/CyO	Bloomington 40994
ppk-GAL80ts-GAL4	P{w[+mC]=tubP-GAL80} LL1	made in the lab
NP1-GAL4	w [1118]; P{w[NP1-Gal4}	D. Ferrandon
ppl-GAL4	w [1118]; P{w[ppl-Gal4}	Pierre Leopold
ppl-GS-GAL4	w1118; (Switch1)106 GS	Ronald Kühnlein
DILP2-HA-Gal4	w1118; UAS-dcr2; ilp2gd2HF(attP2), dipl2-15-1-HGal4	Sangbin PARK
dORMDL	P {w, UAS-dORMDL}	made in the lab

2.1.2 Fly standard medium

Normal medium

The ingredient of the fly standard food comprised 6.25% yeast, 6.25% cornmeal, 1% agar powder, 2% glucose and 3% molasses and syrup. All components were combined in sterile water and stirred to dissolve followed by sterilization by autoclaving for 15 minutes. After cooling to 70°C, 3% nipagin (in ethanol) and 1% propionic acid were added to the medium as preservatives to protect media from being infected.

Mifepristone medium

100 µl of a stock solution of 3 mg/ml mifepristone in 80% ethanol was applied onto the surface of standard food medium in *Drosophila* wide vials. The mifepristone solution was allowed to sink into the medium overnight resulting in a final concentration of 120 µg/ml. Control food medium was prepared applying 100 µl 80% ethanol to the standard food medium. After adult flies were placed in the mifepristone containing vials, they were transferred to new vials after 3 or 4 days.

2.1.3 GAL4/UAS crossing

Crossings were raised at 25 °C, and the F1-generation was used for the analysis. Virgin female flies were crossed with male flies at 25 °C. A proportion of 2:1 (females to males) was used for crossing; genotypes were followed by genetic markers. Virginity was assured by isolating freshly hatched females in time, which were 5 h at 25 °C and 16 h at 18 °C. For combination of chromosomes, virgin female progeny carrying two chromosomes in a trans heterozygous combination were crossed with males carrying appropriate balancer chromosomes. Offspring being candidates for recombined chromosomes were selected, amplified and analyzed.

2.1.4 Solutions

Phosphate Buffered Saline Tween-20 (0.3% PBST): The following components were dissolved in 800 ml of distilled water: 8 g NaCl, 0.2 g KCl, 1.44 g Na₂PO₄, 0.24 g KH₂PO₄, 3 ml Tween-20. Subsequently, the pH was adjusted to 7.2 and additional distilled water was added up to 1 liter. The solution was autoclaved.

Paraformaldehyde in PBS (4% PFA): 2 g paraformaldehyde powder was dissolved in 50 ml PBS solution under continuous stirring at 45 °C. The fixing solution was aliquoted and stored at 4 °C after it became clear.

Hemolymph-like saline (HL3): 70 mM NaCl, 5 mM KCl, 4 mM MgCl₂·6H₂O, 1.5 mM CaCl₂·2H₂O, 10 mM NaHCO₃, 115 mM sucrose, 5 mM trehalose, 5 mM HEPES were dissolved in 800 ml deionized water, adjusted pH to 7.2 and brought to the final volume of 1 liter. The buffer was sterile filtered and stored at 4 °C

Elisa coating buffer (0.2 M sodium carbonate/bicarbonate buffer): 2.12 g of Na₂CO₃ and 6.72 g of NaHCO₃ were dissolved in 500 ml of distilled water. The pH value was adjusted to 9.4 and then the solution was filter-sterilized.

2.1.5 Antibodies

Rabbit monoclonal anti-Dilp2

Anti-Drosophila Coracle

Monoclonal Anti-WKD
anti-Rabbit DyLight™ 549

Anti-Mouse AlexaFluor 488

Anti-Mouse AlexaFluor 647

Mouse monoclonal anti-Flag

Mouse monoclonal anti-HA-Peroxidase

Gift from Manfred Schmid, ETH Zürich, Switzerland

Developmental Studies Hybridoma Bank

Gift

Jackson ImmunoResearch Europe, Hamburg, Germany

Jackson ImmunoResearch Laboratories

Jackson ImmunoResearch Laboratories

Sigma-Aldrich, Steinheim, Germany

Sigma-Aldrich, Steinheim, Germany

2.1.6 Oligonucleotides

Table 2. Oligonucleotides used for PCRs.

primers	sequence (5' to 3')
pBID-UASC ATF6-F-NotI	GAGAGCGGCCGCAAAATGACGCCATGTTT
pBID-UASC ATF6-R-KpnI	GAGAGGTACCTCAACGCTGACAAGAGGTGG
Droso-F	ACCAAGCTCCGTGAGAACCTT
Droso-R	TTGTATCTTCCGGACAGGCAG
Rpl32-F	CCGCTTCAAGGGACAGTATC
Rpl32-R	GACAATCTCCTTGCGCTTCT
dTor-F	GCCAGCAGTTCGTGAGTAT
dTor-R	TATGCGGACTCCAGTACGTTG
CG10816-F	CCATCGTTTTCTGCT
CG10816-R	CTTGAGTCAGGTGATCC
CG12763-F	GCTGCGCAATCGCTTCTACT
CG12763-R	TGGTGGAGTGGCTTCATG N
CG10146-F	CCCGGAGTGAAGGATG
CG10146-R	GTTGCTGTGCGTCAAG
Xbp1s-F	CCGAACTGAAGCAGCAACAGC
Xbp1s-R	GTATACCCTGCGGCAGATCC
DSCP	CGTGCCGCTGCCTTCGTT
SV40	CCTTAGAGCTTTAAATCTCTGTAGG

F: forward, R: reverse

2.1.7 Enzymes

Table 3. Enzymes

DNase (RNase free 1U/μl)	Invitrogen, Darmstadt, Germany
2x qPCRBIOSyGreen Mix Hi-ROX	PCR Biosystems, London, UK
Kpn1	Invitrogen, Darmstadt, Germany
Not1	Invitrogen, Darmstadt, Germany
T4 DNA Ligase	Thermo Scientific, Germany
Superscript IV TM Reverse Transcriptase	Invitrogen, Darmstadt, Germany
Pwo DNA Polymerase	Peqlab, Erlangen, Germany
RNase inhibitor (40U/μl)	Invitrogen, Darmstadt, Germany
Taq DNA Polymerase (5 U/μl)	Invitrogen, Darmstadt, Germany

2.1.8 Chemicals**Table 4. Chemicals**

Agar-Agar	Carl Roth, Karlsruhe, Germany
Agarose	Biozym, Oldendorf, Germany
Bacto™ yeast extract	Becton, Dickinson and Company, Erembodegem, Belgium
BODIPY (493/503)	Molecular Probes life technologies, Darmstadt, Germany
Chloroform	Carl Roth, Karlsruhe, Germany
DAPI	Invitrogen, Darmstadt, Germany
Ethanol	Carl Roth, Karlsruhe, Germany
dextran sulfate sodium	MP Biomedicals, Germany
dNTPs	Promega, Mannheim, Germany
GeneRuler™ 1kb DNA Marker	Fermentas, St.Leon-Roth, Germany
Glucose	Carl Roth, Karlsruhe, Germany
Glucose (HK) Assay Kit	Sigma-Aldrich, Steinheim, Germany
Goat serum	Sigma-Aldrich, Steinheim, Germany
HPLC water	Carl Roth, Karlsruhe, Germany
Isopropanol	Carl Roth, Karlsruhe, Germany
Mifepristone	Sigma-Aldrich, Steinheim, Germany
Molasses	Kanne Brottrunk GmbH & Co. KG, Selm-Bork, Germany
Nipagin	Carl Roth, Karlsruhe, Germany
NucleoSpin® RNAII Kit	Macherey-Nagel, Düren, Germany
Paraformaldehyde	Sigma-Aldrich, Steinheim, Germany
RNAmagic	Bio-Budget, Kredeld, Germany
SureClean	Bioline, Luckenwalde, Germany
Sucrose	Carl Roth, Karlsruhe, Germany
SYBR® Green	Invitrogen, Darmstadt, Germany
Triglyceride	Invitrogen, Darmstadt, Germany
TritonX-100	Sigma-Aldrich, Steinheim, Germany
Tween-20	Carl Roth, Karlsruhe, Germany
1-Step™ Ultra TMB-ELISA Substrate Solution	Sigma-Aldrich, Steinheim, Germany

2.1.9 Equipment**Table 5. Equipment**

Agarose Gel electrophoresis unit	Biometra GmbH, Göttingen, Germany
Centrifuge 5415D	Eppendorf, Hamburg, Germany
Centrifuge 5417R	Eppendorf, Hamburg, Germany
EV 245 Electrophoresis power supply	Consort, Belgium
GenePix™ 4000B scanner	Molecular Devices GmbH, München, Germany
Imager.Z1, Zeiss	Zeiss, Oberkochen, Germany
Leica TCS SP1 confocal Microsystems	Leica, Heidelberg, Germany
MagnaRack	Invitrogen, Darmstadt, Germany
NanoDrop (ND-1000UV)	Peqlab, Erlangen, Germany
Olympus SZX12 microscope	Olympus GmbH, Hamburg, Germany
Omni Bead Ruptor 24	Omni International Inc, Kennesaw, USA
PCR amplification	Bio-Rad Laboratories GmbH, München
Spectrophotometer	Multiscan MCC/340P version 2.32
StepOnePlus™ System	Applied Biosystems, Life Technologies
Thermocycler (Labcyler)	SensQuest GmbH, Göttingen, Germany
Vortex-2 Genie	Scientific Industries, INC., Bohemia, N.Y., USA

2.2 Methods

2.2.1 Lifespan measurements

Control and experimental flies were collected during 24 h after eclosion and divided into females and males and maintained in vials supplied with standard medium at 25 °C. No more than 30 flies of each line were kept in a vial to avoid too high density, a constant climate with 65% humidity and a 12:12 h light-dark cycle was kept. Experiments were performed in several replicates. Flies were transferred to a fresh medium every other day. Lifespan was analyzed daily, separately for males and female. For DSS survival assays, 3–5-day old flies were fed in an empty vial containing a piece of 2.5 cm X 3.75 cm of chromatography paper. 2% dextran sulfate sodium (DSS) and 5% sucrose solution was used to wet paper as feeding medium. Flies that were still alive were transferred to new vials with fresh feeding media every day.

2.2.2 Body fat quantification

For total triacylglycerol (TAG) content quantification in flies, the Coupled Colorimetric Assay (CCA) method was used as described previously (Hildebrandt et al., 2011). Glycerol trioleate was used as TAG standard for standard curve establishment, which was diluted in a series of 2-fold dilution with starting the quantity of 100 µg. Eight male flies or five female flies per replicate were subjected to thorough homogenization in a 2 ml screwcap tube containing 1 ml 0.05% Tween-20 and 4 ceramic beads by using a Bead Ruptor 24 at a speed of 3.25 m/s for 2 min. Homogenates were incubated at 70 °C for 5 min as a heat-inactivated step followed centrifugation for 3 min at 3000 rpm. Of the supernatant 50 µl sample were transferred to a 96 well microtiter plate and the various concentrations of TAG standard were treated in an identical way. Homogenate absorbance was measured at 562 nm in a Microplate Reader as blank values. Prewarmed Triglyceride solution (200 µl) was added to each homogenate sample and standard curve, then incubated at 37 °C with mild shaking for 30–35 min.

The absorbance was measured at 562 nm again and corrected by subtraction of blank values.

The final quantity of samples was calculated per mg of fly wet weight base on the standard curve. TAG contents of a representative experiment are depicted as average values of triplicate measurements with corresponding standard deviations. Experiments were repeated at least twice.

2.2.3 Glucose measurements

Proper regulation of carbohydrate homeostasis is critical for maintaining normal physiology. The two primary forms of circulating carbohydrates in *Drosophila* are glucose. To ensure accurate and reproducible glucose, a good quality of hemolymph droplets from fruit fly is the most important step, only the pure hemolymph derived from peripheral hemolymph could accurately reflect the state of circulatory carbohydrates. Several alternate methods for hemolymph collection have been described for both larvae and adults. The centrifugation approach in this study requires approximately 30–50 adult females (adult males contain less hemolymph per fly and thus require larger numbers) carefully punctured in the thorax using a needle after 3 h starvation. Punctured flies were placed in a 0.5 ml microfuge tube that contained a hole at the bottom of the tube. This tube was then placed within a 1.5 ml collection tube and centrifuged at $5,000 \times g$ for 5 minutes at 4 °C. Longer centrifugation times, higher speeds, and more flies could increase yield, but may also increase cellular or intestinal contamination.

Not less than 0.5 μ l of hemolymph per sample was isolated and diluted 1:10 in deionized water. A standard curve was established with a glucose solution with known glucose concentrations. The glucose standard solution was diluted in 2-fold serial dilutions starting from 1 mg/ml to 0.0625 mg/ml with deionized water, 3 μ l of each diluted solution was loaded in 50 μ l glucose assay reagent (which was supplied in the

glucose assay kit). The same volume of water was added to the 50 μ l glucose assay reagent was set as a blank. Mixed tubes and incubated them for 15 min at RT (25 °C). Subsequently, the absorbance was measured at 340 nm with a Nanodrop 1000.

2.2.4 Glucose tolerance test

Adult flies (7 days after eclosion) were fasted for 16 h on 1% agar before transferred to vials containing 10% glucose solution-soaked filters for 1 hour. Subsequently, flies was subjected to hemolymph extraction, replicate groups having consumed 10% glucose solution for 1 h were then transferred to vials containing water-soaked filters for 30' and 60', respectively prior to hemolymph extraction. Multiple experiments were performed with 30-50 flies/hemolymph extraction in each experiment. The method of glucose measurement was same as described for *Glucose measurement*.

2.2.5 Immunohistochemistry and imaging

Preparation and Immunohistochemistry of the different tissue in *Drosophila*.

Trachea

The larvae were transferred to a dissection dish with cold HL3 and the cuticle of larva was split by forceps and trachea were removed from the body wall placed in small tube.

Terminal trachea

Dissection of larvae was done by the ventral filleting method (Chen et al. 2016). The third instar larvae were placed in a petri dish containing the silicone elastomer layer filled with HL3. Larvae were first pinned ventral side up between the tracheal dorsal trunks at the posterior end, the second pin was inserted just under the pharynx at the anterior end (black arrowhead) between the left and right anterior dorsal trunks (black arrows). The ventral epidermis was then cut along the anterior-posterior axis (black dashed line) (Fig. 3A). The cut epidermis was pulled to the side and pinned down to

the dissection dish (asterisk) (Fig.3B). Internal tissues were pulled out by forceps; thin terminal branches of the trachea attached to the tissues were cut (arrows) to allow the tissue to be removed (Fig.3C, D). As internal tissues were removed, more pins (asterisks) were inserted to pin the epidermis flat. The major branches of the trachea were visible after removal of the internal tissues (enlarged in Fig.3E).

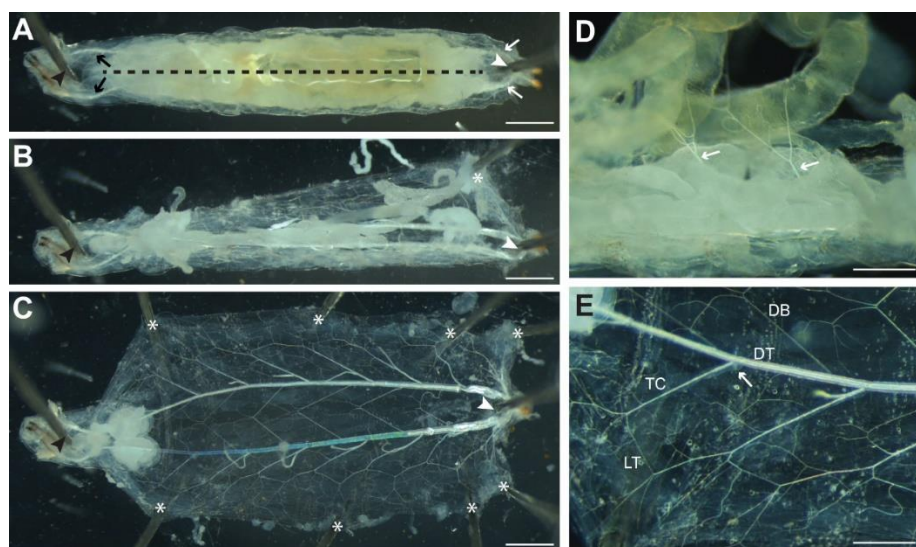


Figure 3. Dissection of larvae by ventral filleting method.

Whole larvae were fixed with needles, cut along the dotted line (A). The epidermis was pulled to the side and pinned down on the dissection dish. The other tissues were removed (B). More needles were used to fix the epidermis (C, D). The major branches of the trachea were observed after dissection (E). Adopted from (Chen et al. 2016).

Gut

Prepared dissection plates containing the agarose layer, which can prevent damaging the tips of the forceps during the dissection procedure were used. Flies were anaesthetized with CO₂ and transferred to the dissection dish immersed in the HL3 solution. Separation of the thorax from the abdomen was done by using forceps and grabbing the gut and pulling it out of the thorax gently. Then, Malpighian tubules, trachea and ovaries were removed, while being careful not to destroy the gut tissue during the dissection procedure.

Fat body

The third instar larvae were then washed in Schneider's solution or PBS to remove any surrounding food materials. These larvae were placed on ice to anaesthetize them and dissecting forceps were used to tear the cuticle of larvae. The exposed desired tissues (CNS, imaginal disc, gonads, fat body etc.) can now be dissected away. The fat body was transferred to a small tube for the next immunohistochemistry staining steps.

Brain

Adults brains were dissected in cold S2 cell culture medium (Schneiders Insect Medium). With gentle forceps manipulation, the brain was removed from the head cuticle and placed into 2% paraformaldehyde(PFA) in S2 Medium for 55 min at room temperature. The brains were placed in tubes and were washed with PBT (PBS with 0,5% (v/v) Triton-X100) 4 times for 10 minutes each. Incubation with the primary antibody (rabbit anti-dILP2 diluted 1:200 in PBT-NGS) for 1-4 h at RT was followed by 4 °C overnight after blocking with PBT-NGS (5% Goat serum) for 1,5 h at RT. Then it was washed 3 times for 30 min with PBT and incubated with the secondary antibody in PBT-NGS for 1-4h at RT followed incubate overnights at 4 °C. After washing 1-2 times 15 min each, the slides were prepared and observed.

Staining Assay

All above mentioned tissues of *Drosophila* were dissected under a microscope, then fixed in 4% PFA (except brain) for 30 min at room temperature, and rinsed three times for 5 min each in PBST (0.3% Triton X-100), blocked in blocking-buffer (1×PBS + 1% Triton X-100 + 5% goat serum) for 30 min at RT. Subsequently, the primary antibody was added to incubate overnight at 4 °C, after washing three times for 5 min each, the diluted secondary antibody was added and incubated for 3 h at RT in constant darkness. The material was washed three times for 10 min each, finally the tissue was mounted on slides by immersing in DAPI or 10% glycerol solution. Each image was photographed using Carl Zeiss fluorescent microscope (Imager.Z1, Zeiss) and Zeiss AxioVision 4.8 software.

2.2.6 Quantification of circulation and total DILP2 content

Detection of circulation and total DILP2 content of flies were achieved using the DILP2-HA-Gal4 effector lines (Géminard et al. 2009). The DILP2 tagged by both, FLAG (immunogen sequence DYKDDDDK) and HA (human influenza virus hemagglutinin, immunogen sequence YPYDVPDYA), was employed for this immunological work.

For hemolymph sample preparation, the posterior end of female and male flies' abdomen was dissected away. 10 dissected female or male bodies were transferred into a centrifuge tube containing 60µl of PBS, which was vortexed using a micro-tube holder at the max speed for >10 minutes, and then centrifuged at 1,000 ×g for 1 min. Then, 50 µl of supernatant (avoid crashing heads) were transferred into new tubes, which were utilized for circulating DILP2-HF measurement. The remaining flies were transferred to 2 ml screw-cap tubes, 500 µl of PBS with 1% Triton-X100 was added to the tubes and homogenized in the bead ruptor at 3.25m/s for 2 min with the help of ceramic beads. Vortexing the tubes using the micro-tube holder at the max speed for >5 minutes was done, followed by centrifugation at max. speed for 5 min. 50 µl of supernatant was utilized for total DILP2-HF measurements.

For the standard curve establishment, FLAG(GS)HA peptides (the peptide was synthesized by LifeTein LLC: DYKDDDDKGGGGSPYDVPDYA, Amidated, 1-4 mg, crude purity (57.8%) MW=2412.42 Daltons) was prepared at 2-fold gradually diluted concentrations (from 10 pg/50 µl onwards, 7 points totally), including a blank sample, to 50 µl of PBS or PBS with 1% Triton-X100 in PCR strips.

A 96-well ELISA polystyrene high binding microplate was coated with 100 µl of 2.5 µg/ml anti-FLAG antibody diluted in coating buffer (0.2 M sodium carbonate/bicarbonate buffer, pH 9.4) overnight at 4 °C, then the plate was washed with PBS with 0.2% Tween 20 (PBST 0.2%) twice. During each wash, the buffer was flicked off, and the plate was blotted on paper towels before refilling. After washing, the plate was blocked with 350 µl of 2% BSA (bovine serum albumin) in PBS by

incubation overnight at 4 °C. The blocked microtiter plate was washed with PBST three times, and dried on paper towels. Then, samples were transferred (standard curve samples) to microtiter plate, the plate was sealed and incubated in a humid chamber (with a wet paper towel) overnight at 4 °C. Following this, the supernatant was removed and the wells were washed six times with PBST. 100 µl of 1-Step Ultra TMB ELISA Substrate (Thermo Scientific 34029) was added to each well and incubated on a rotary shaker for 30 minutes at room temperature. Adding 100 µl of 2 M sulfuric acid per well was done to stop the reaction. Finally, measuring the absorbance at 450 nm (A_{450}) using the Spectra Max M5 photometer (Molecular Devices) was done immediately. To convert the concentration to the mass in a given volume, I used a molecular weight of 7829 Daltons for the mature IIP2HF protein. Data were analyzed in triplicates and shown as mean \pm S.D. for statistical analysis.

2.2.7 Constructing the UAS-Atf6 transgenic line and general molecular biology methods

Genomic DNA extraction

Drosophila larvae (5-10) were grinded in 200µl TE buffer and then added to 400µl lysis solution (DNA Extraction kit, MBI Fermentas), incubated at 65 °C for 5 min. 600 µl of chloroform was added to the previous solution and gently emulsified by inversion (3-5) times. After centrifugation at 10,000 rpm for 2 min, the upper aqueous phase containing the DNA was transferred to a new tube containing 800 µl of precipitation solution. This solution was mixed gently by several inversions at room temperature for 1-2 min and centrifuged at 10,000 rpm for 2 min. The supernatant was removed completely and the pellet was dissolved in 100 µl of 1.2 M NaCl solution by gentle vortexing. Cold ethanol was added to precipitate DNA, the solution was centrifuged at 10,000 rpm for 5 min. DNA was washed once with 70% ethanol, dried and resuspended in sterile deionized water by gentle vortexing.

PCR Amplification of the *Atf6* gene

PCR was used to amplify the *Atf6* gene sequence using a specific pair of primers containing the restriction enzyme sites that allow cloning onto the pBID vector. This part of the protein is believed to represent the active form of the protein that enters the nucleus.

Atf6, isoform B in *Drosophila melanogaster* (Sequence ID: ref|NP_610159.1|), was used as a template DNA sequence (Sequence is shown in the Appendices P98). A pair of primers containing two restriction enzyme sites (*NotI* and *KpnI*), which are also part of the multiple cloning site (MCS) of the pBID-UASC vector were used. Target gene amplification primers were designed as follows:

Forward *NotI* primer: GAGAGCGGCCGCCAAAATGACGCCATGTTT

Reverse *KpnI* primer: GAGAGGTACCTCAACGCTGACAAGAGGTGG.

Genomic DNA was used as a template to amplify the *Atf6* gene with these two primers.

PCR reaction reagent:**Table 6. PCR reaction reagents**

10X reaction buffer	2 μ l
dNTP mix (10 mM of each dNTP)	1 μ l
Taq DNA Polymerase (5 U/ μ l)	0.25 μ l
pBID-UASC ATF6-F-NotI (10 μ m/ μ l)	1 μ l
pBID-UASC ATF6-R-KpnI (10 μ m/ μ l)	1 μ l
template DNA (10-100 ng/ μ l)	1-2 μ l

nuclease-free water (adjusted to a final 50 μ l).

General Cycle condition of PCR amplification:

Table 7. General Cycle conditions of PCR

Step	Temperature	Duration	Cycle number
<i>Denaturation</i>	94 °C	1 min	1 cycle
<i>Denaturation</i>	94 °C	30 sec	
<i>Annealing</i>	50-55 °C	30 sec	35 cycles
<i>Elongation</i>	72 °C	3 min	
<i>Final extension</i>	72 °C	10 min	1 cycle
<i>Final soak</i>	4 °C	Hold	

Agarose gel electrophoresis

Agarose gels were prepared with 1% (w/v) agarose in electrophoresis buffer TBE (Tris/Borate/EDTA). To make DNA bands visible, 1 µl Ethidium Bromide (EtBr) was added to the agarose gels. Samples were mixed with loading buffer and loaded onto the sample lane together with the marker (usually marker in the first lane). An appropriate voltage was set and the electrophoresis was run. After approximately 35 min at lower voltage (80 V), the gel was subjected to higher voltage for 25 min (100 V). Subsequently, the agarose gel was put in an UV detector and the picture was recorded.

Restriction Enzyme Digestion

The *Atf6* amplification fragment was digested using the two restriction enzymes *Not1* and *Kpn1*, the enzyme sites include in the multiple cloning site of the vector (Fig. 4). The pBID-UASC plasmid was cut twice with the same two restriction enzymes that were used. Restriction enzymes and suggested buffers were used according to the manufacturer's instructions (Fermentas).

The pBID-UASC vector that allows both, phiC31 targeted transgene integration and incorporates insulator sequences to ensure specific and uniform transgene expression, contains a multicloning site (MCS) for insertion of target gene fragments (Wang et al. 2012).

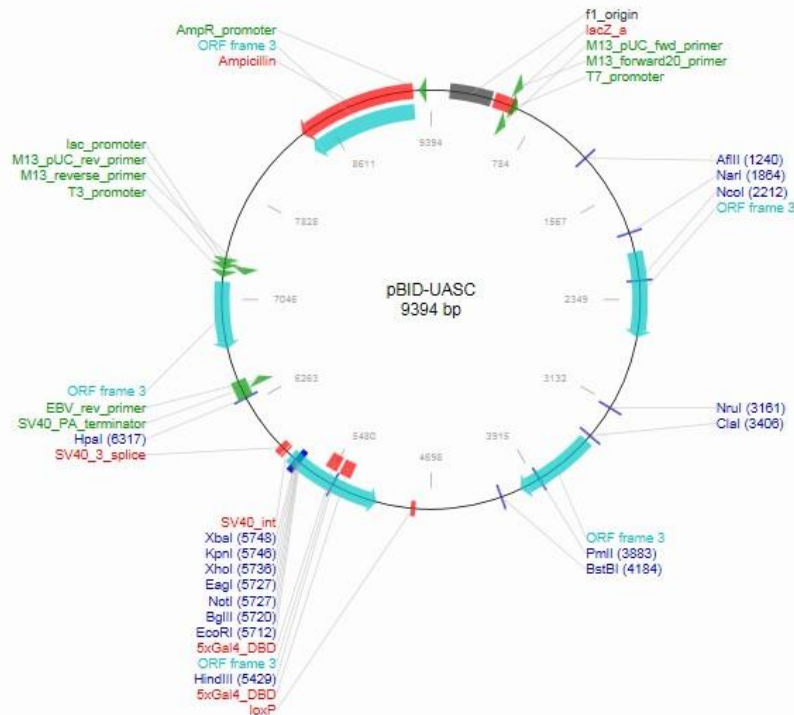


Figure 4. Map and construction of the pBID-UASC vector.

Whole sequence of vector and insert site are showed in Appendices (whole sequence showed on P95).

Ligation of *Atf6* gene in pBID-UASC vector

First the Nanodrop spectrophotometer was used to measure the concentrations of vector and insert. The ligation mixture was set up including vector DNA, insert, ligase buffer and T4 DNA ligase. The total volume was completed to 10 μ l with nuclease free water. The mixture was mixed gently and incubated at 4 $^{\circ}$ C overnight. Before transformation, the ligase was heat-inactivated by placing the tube containing the ligation mix in 65 $^{\circ}$ C incubator for 10 min.

Transformation into *E. coli* DH5 α

For most standard cloning approaches, transformation of the ligation reaction into

competent DH5alpha cells was performed. Bacteria were stocked at -80 °C and thawed on ice. The ligation mixture was added to competent cells incubated in ice for 5min. Then the tubes were heat-shocked by incubating them in an incubator at 42 °C for 90 sec and subsequently they were placed on ice again. The bacteria were cultured in LB medium with continuous shaking at 37 °C overnight. Ampicillin was added into LB under sterile condition (final concentration of ampicillin-sodium salt 100 mg/L). The *E. coli* suspension was spread on LB-amp-agar plates and incubated at 37 °C overnight. Finally, individual bacterial colonies were picked and checked for successful ligations.

Isolation of plasmid DNA (mini and midi)

For plasmid isolation, a single colony was selected and cultured in 4ml LB-amp liquid medium at 37 °C with continuous shaking overnight. For analytic purpose, 1.5 ml of an *Escherichia coli* culture was centrifuged for 5 min at 3500 rpm, resuspended in 200 µl TELT buffer with 1mg/ml lysozyme, incubated at room temperature for 5 min and boiled at 99 °C for 3 min in a thermomixer. After cooling on ice for 2 min, samples were centrifuged at 12000 rpm for 15 min at 4 °C, the supernatant was collected in a fresh tube and equal volume of isopropanol was added, incubated at room temperature for 5 min Plasmid DNA was pelleted by centrifugation at 13000 rpm for 15 min at 4 °C, washed with 500 µl of 70% ethanol, incubated at room temperature for 10 min and centrifuged at 13000 rpm for 15 min, air dried and resuspended in 30µl aqua bidest. For preparation of bigger amounts or highly pure plasmid DNA (e.g. for cell culture transfection), Nucleospin Plasmid AX-100 kit (Macherey Nagel) was used according to manufacturer's instructions.

Sequencing

The sequencing Service supplied by the Institute of Clinical Molecular Biology (IKMB) was used. The DNA was prepared according to the requirement of the partner. The sequences were obtained and verified using the alignment software BLAST (<https://blast.ncbi.nlm.nih.gov/Blast.cgi>) of the national centre of biotechnology

information (NCBI). (Sequence blasting result is showed in Appendices)

Injection of *Drosophila* embryos

Drosophila transgenic service supplied by Best Gene Inc was used. The injection line for plasmid integration was *w¹¹¹⁸*.

Total RNA extraction

Tissues of interest were dissected in HL-3 buffer on ice. After that, the dissected tissues were homogenized in 1 ml RNA magic for 1 min at 3.25 m/s speed, with the help of ceramic beads using the Bead Ruptor 24. Following addition of 200 µl of chloroform with shaking by hands 15 times, the mixture was centrifuged for 5 min at 15000 xg. The upper phase was transferred carefully into a clean tube, mixed with an equal volume of isopropanol. The mixture was centrifuged for 30 min at maximum speed at 4 °C after incubated at -20 °C overnight. The RNA pellet was washed twice with 500 µl cold 70% ethanol. Finally, all aqueous phase materials were discarded and air dried, the RNA resolved in RNase-free water and stored at -80 °C.

cDNA synthesis

RNA-concentrations were measured first with the Nanodrop. The following components were used: 250 to 500 ng of total RNA, 0.5 µl Oligo-dT7 I (10 pmol), 0.5 µl dNTPs mix (10 mM), HPLC water was added up to 6.75 µl. The mixture was incubated at 65 °C for 5 min, then placed on ice for at least 1 min. The following components were added in the mixture in the indicated order: 2µl 5 × FSB buffer, 0.25 µl RNase Inhibitor (10 U), 0.5µl DTT (0.1 M) and 0.5µl Superscript III Reverse Transcriptase (100 U). Gently mixed and incubated at room temperature for 5 min and then synthesized at 50 °C for 1 h. Finally, Stop Reaction 15 min 70 °C.

Purification of PCR Products

To purify PCR products, the reagent SureClean™ was used according to the

manufacturer's instruction. An equal volume of PCR products and SureClean solution was mixed thoroughly, incubated at RT for 10 min, and then centrifuged at maximum speed (21000 xg) for 10 min and the pellet retained. The pellet was washed twice in cold 70% ethanol at 2 × original volume, and resuspended it in 15 µl water. The final concentration and purity of cDNA was measured using a NanoDrop 100.

Relative quantification using the qRT-PCR

Primers were designed using appropriate software (<http://frodo.wi.mit.edu/>) and synthesized by Invitrogen. Before use, primers were resuspended in aqua bidest to a final concentration of 20 pmol/µl. For relative quantitative PCR, the reaction was performed using the StepOnePlus™ Real-Time PCR System for the primer efficiency check and relative expression level of gene of interest determination. For primer efficiency check, the template cDNA was treated as a series of 2-fold dilution from starting quantity of 50 ng/µl to the final of 3.125 ng/µl, while for the gene expression level determination, template cDNA was diluted to 20ng/µl. Then 5µl 2 x qPCR BIO SyGreen Mix Hi-ROX, 0.5 µl sense primer (5 µM), 0.5 µl anti-sense primer (5 µM), 1 µl template cDNA and 3 µl HPLC H₂O were mixed for one reaction. The amplification was run as below:

95 °C	10 min	
95 °C	15 sec	40 cycles
60 °C	20 sec	
72 °C	35 sec	
95 °C	5 min	
60 °C + 0.3 °C until 95 °C		
95 °C	15 sec	

The primer efficiencies were calculated according to $E=10^{-1/\text{slope}}$ formula (Pfaffl et al. 2001). Thus, the relative expression ratio (fold change) of a target gene was determined based on E and CT values in comparison to a reference gene. In triplicates,

the fold changes for each group were calculated by the formula below and represented as mean \pm S.D. for statistical analysis.

$$\text{Ratio} = \frac{(E_{target})^{\Delta CP_{target}(\text{control-sample})}}{(E_{ref})^{\Delta CP_{ref}(\text{control-sample})}}$$

In this case, rpl32 served as a reference gene for all of assays.

2.2.8 Statistical analysis

In all experiments, GraphPad Prism version 5 was mainly used for statistical analysis. The comparison between two groups was done with the unpaired two-tailed Student's *t*-test, if multiple comparisons were done, one-way ANOVA with Tukey post-hoc test were performed, while the two-way ANOVA was employed at the conditions with two different categorical independent variables on one continuous dependent variable. All histograms were represented as means \pm S.D. The survival curves of lifespan were analyzed with the Log-rank (Mantel-Cox) test. Statistical analysis of significant difference was defined as n.s. not significant, *P<0.05, **P<0.01 and ***P<0.001.

3.Results

3.1 Activation of UPR via different branches induces substantial changes in different organs of the fruit fly

3.1.1 UPR activation changes the morphology of trachea in *Drosophila* larvae.

3.1.1.1 Changes of morphology in the tracheal trunk

Using *Drosophila melanogaster* as a model, I studied the role of the three branches of the unfolded protein response by their ectopic activation. For this, I enhanced expression of IRE1, XBP1s, PERK, or ATF6, respectively in trachea of *Drosophila*. The trachea-specific driver line *ppk*-GAL4 was used to overexpress the corresponding genes in the tracheal system.

I have observed the development of offspring arising in the normal medium at 7 days after mating. Compared to the control (Fig. 5A), flies overexpressing XBP1s and PERK in the trachea could not develop into normal adults. Activation of XBP1s in the trachea induced lethality, there were no grown-up larvae in the experiments (Fig. 5B), whereas matching controls grew up normally. Similarly, ectopic expression of PERK induced also lethality. In the experimental vials (Fig. 5C), the first instar larvae were observed at the wall, outside of the medium, which is a typical for these animals. Therefore, both, PERK and XBP1s overexpression in the tracheal trunk induced lethality. IRE1 and Atf6-overexpression had no effect on larvae growth and developed.



Figure 5. Ectopic activation of XBP1s and of PERK in the trachea system was lethal. The offspring of the corresponding crossings were raised on normal medium for 7 days. Control larvae with the genotype *ppk-GAL4 > w¹¹¹⁸* (A) grew normally and formation of pupae started. XBP1s (B) and PERK (C) overexpression in the tracheal system of larvae led to death, with the genotype *ppk-GAL4 > UAS-Xbp1s* and *ppk-GAL4 > UAS-Perk*, respectively.

To further investigate how overexpression of these crucial UPR components affect the phenotype of the tracheal tissue, immunohistochemistry was used to highlight the structure of the tracheal cells boundaries and nuclei, since the cell shape is critical for function of individual cells. To label the septate junction proteins of the tracheal epithelia, immunohistochemical staining was performed with anti-*Drosophila* coracle antibodies as well as with DAPI. There are no morphological changes on tracheal structures in IRE1 and ATF6 overexpressing larvae (Fig. 6B, C). Since ectopic activation of XBP1s and of PERK in the trachea was lethal, there was a critical need for using inducible expression of transgenes in specific cells during development. In *Drosophila*, based on GAL4/UAS system (Duffy et al. 2002), to permit temporal as well as spatial control over UAS-transgene expression, I used a conditional RU486-dependent GAL4 protein (Gene Switch) system in *Drosophila*. Expression in the Gene Switch system is triggered only in the presence of the activator RU486 (mifepristone) (Osterwalder et al. 2001).

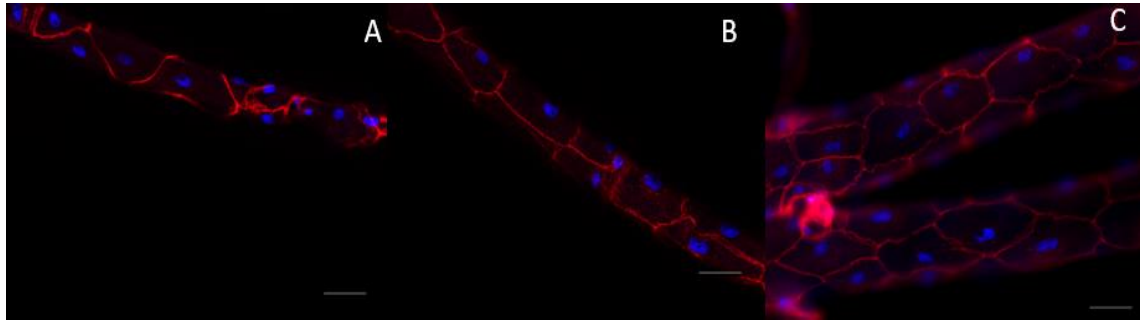


Figure 6. Effects of ectopic expression of Ire1 and Atf6 on *Drosophila* tracheal cells' morphology.

There was no morphological impact on tracheal trunk in Ire1 and Atf6-overexpression larvae. To label septate junction of cell the following primary antibody was used: anti-*Drosophila* coracle monoclonal antibody (1:200), secondary antibody was used: Anti-Mouse Alexa Fluor 488 (1:500) (red) and nuclei are labelled with DAPI (blue). Scale bar: 50 μ m. Genotypes: (A) *ppk*-GAL4 > *W*¹¹¹⁸ (B) *ppk*-GAL4 > UAS-*ire1* (C) *ppk*-GAL4 > UAS-*Atf6*

Here, I used a modified steroid-activated version of GAL4 to achieve inducible expression of target genes (Bloomington 40994) to generate the XBP1s/PERK-overexpression lines. After crossing, the first generations were raised on normal medium supplemented with the same dose of the diluent ethanol as the RU488 medium contained. Afterwards, larvae were transferred to the new vials containing inducible medium for 2 days. Dissection and immune-histochemical staining of larval trachea was performed before transfer and daily after induction by mifepristone. The morphology of control airway was influenced by neither the medium containing ethanol nor 2 days induction (Fig. 7A, B, C).

Xbp1s overexpression affects localization of septate junction proteins in the tracheal epithelium (Fig. 7F) strongly compared with trachea without mifepristone treatment (Fig. 7D) and those experiencing only one day of induction (Fig. 7E). A tight junction structure can be seen in the airway epithelial cells. After 2 days of RU488 induced PERK overexpression, septate junctions of individual cells could not be observed and a small fraction of nuclei were observed apparently not within the cells (Fig. 7I). There were

no changes of morphology in controls (Fig. 7G) and after one-day induction (Fig. 7H).

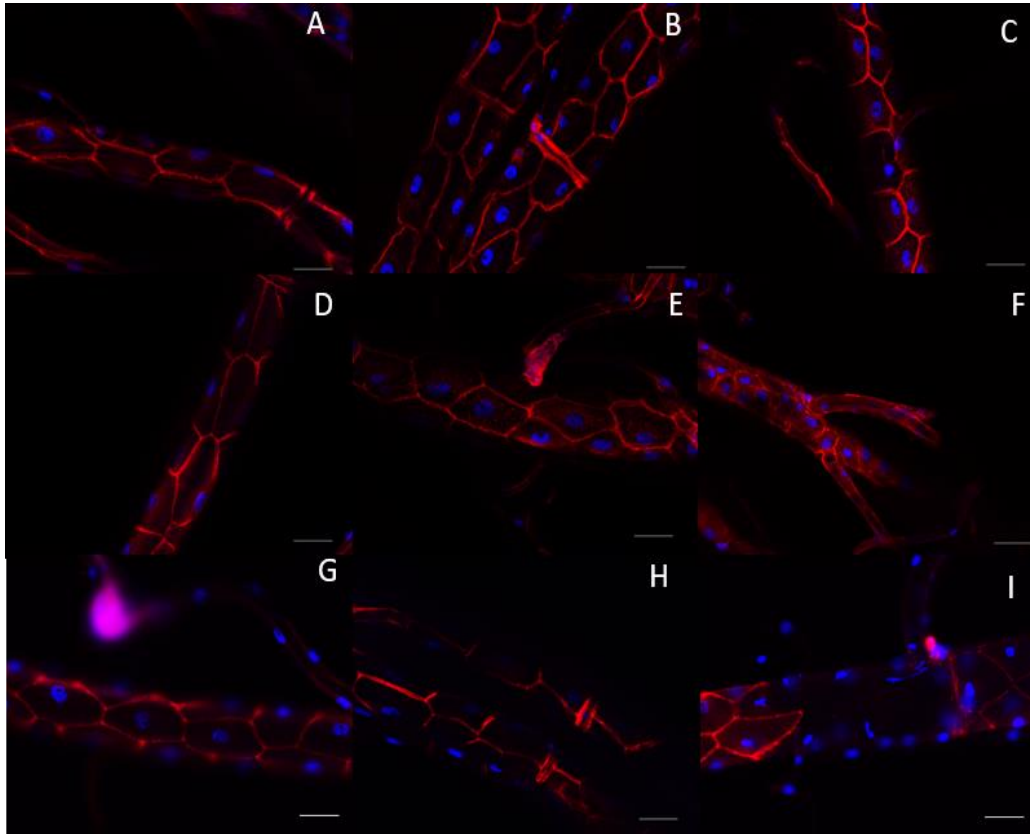


Figure 7. Ectopic activation of Xbp1s and PERK in the tracheal system.

Using the Gene Switch/UAS expression system, crossing RU486 induced tracheal driver line with *xbp1s*/PERK-overexpression line. (A; D; G) is control with low background expression in the absence of RU486. (B; E; H) and (C; F; I) show the trachea phenotype at the first day and second day after RU486 treatment. After 2 days treatment with mifepristone overexpression of *xbp1s* (F) and PERK (I) leads to significant changes of phenotype. To label cell septate junction, the following primary antibody was used: anti-*Drosophila* coracle monoclonal antibody (1:200), secondary antibody was used: Anti-Mouse Alexa Fluor 647 (1:500) (red) and nuclei are labelled with DAPI (blue). Scale bar: 50 μ m.

3.1.1.2 Morphological changes in terminal trachea

Drosophila terminal tracheal cells are a powerful genetic model to study the roles of genes required for generating cellular morphologies. The distinct cellular architectures

of terminal cells, along with the ease by which genetic analysis, make these cells an excellent model for investigating mechanisms of cellular outgrowth, branching, and intracellular tube formation. Therefore, terminal trachea was chosen as a model to understand signaling pathways leading to branched cell differentiation, outgrowth, and maturation (Jarecki et al. 1999; Ghabrial et al. 2006; Ruiz et al. 2012).

Quantitative analysis of terminal cell branch numbers, branch organization and individual branch shapes, can be used to provide information about the role of specific genetic mechanisms in the making of a branched cell. To analyse and quantify terminal cell morphology, I used ImageJ (<http://rsb.info.nih.gov/ij/>) plug-in NeuronJ (<http://www.imagescience.org/meijering/software/neuronj/>) to count the number and the lengths of branches.

In *Drosophila*, representative tracheation of the ventral nerve cord (VNC) can be observed from the body wall, in this assay I counted the number of terminal branching showed in the dotted box (Fig. 8) (Linneweber et al. 2014). In XBP1s and PERK overexpressing larvae, a significantly decreased number of terminal branches (Fig. 8D, C) was found compared with the control (Fig. 8A). There is no affection on the growth of terminal trachea in IRE1 (Fig. 8B) and ATF6 (Fig. 8E) overexpressing larvae. From the quantification of the total number of terminal branches by ImageJ, I concluded that overexpression of XBP1s and PERK inhibited the growth of terminal trachea branches in *Drosophila* larvae, but that IRE1 and ATF6 overexpression had no effect (Fig. 8F).

After dissection of larvae, immunostaining of terminal tracheal branching in *Drosophila* was performed with anti-WKD antibody. The ventral nerve cord (VNC) in red dotted box (Fig. 9G) showed the consistent result, XBP1s and PERK overexpressing (Fig. 9C, D) reduced branching in equivalent areas of the body wall compare with control (Fig. 9A). No obviously changes in IRE1, ATF6 larvae were seen (Fig. 9B, E).

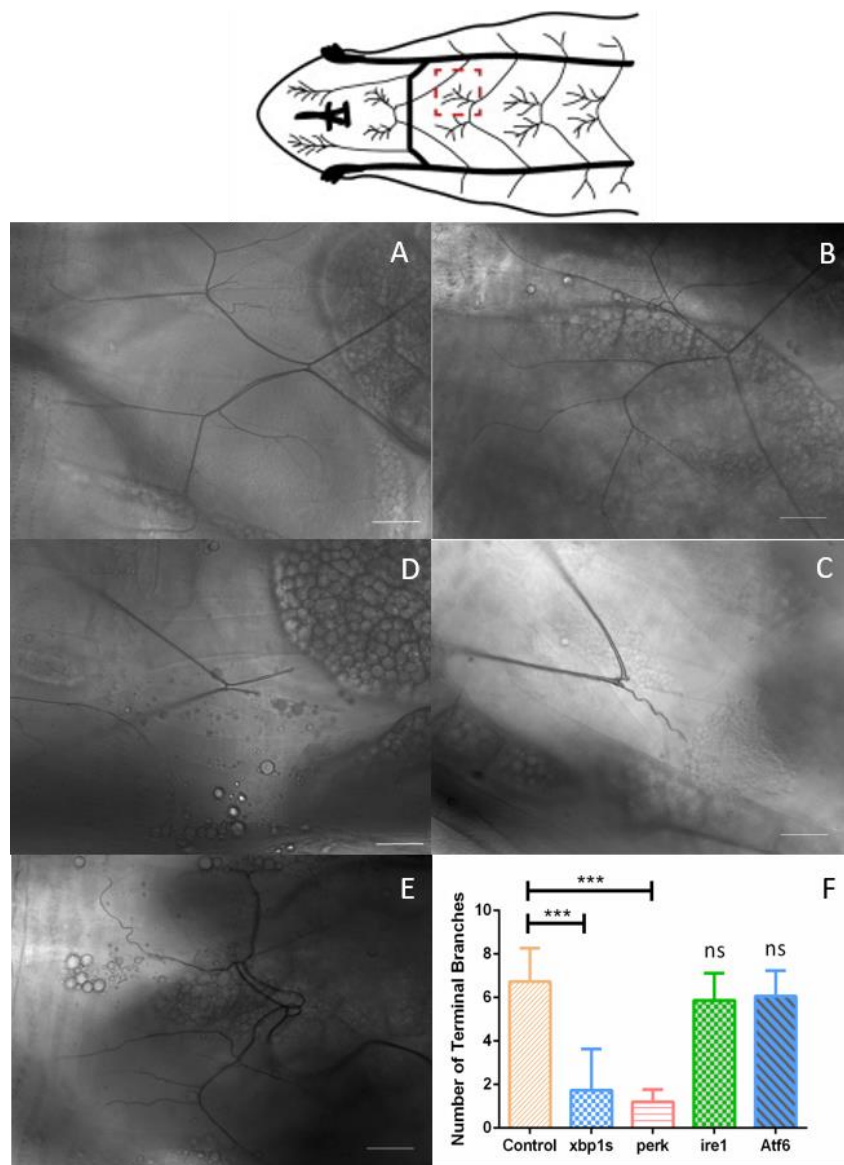


Figure 8. Overexpression of XBP1s and PERK inhibit the growth of the terminal trachea branching in *Drosophila*.

In *Drosophila*, representative tracheation of the ventral nerve cord (VNC) can be observed from the body wall, in this assay I counted the number of terminal branching showed in the red dotted box. XBP1s and PERK overexpression (D, C) decrease the terminal branching significantly compared with the control group (A). There is no affection on the growth of terminal trachea in IRE1 (B) and ATF6 (E) overexpressing larvae. (F) Total number of terminal branching quantified by ImageJ. Scale bar: 50 μ m. Genotypes: (A) DSRF-GAL4 > W¹¹¹⁸ (B) DSRF-GAL4 > UAS-ire1 (C) DSRF-GAL4 > UAS-xbp1s. (D) DSRF-GAL4 > UAS-PERK (E) DSRF-GAL4 > UAS-Atf6. Data are represented as means + SEM. n=15 for each sample. Unpaired two-tailed Student's t-test was used for analysis, ***p<0.001.

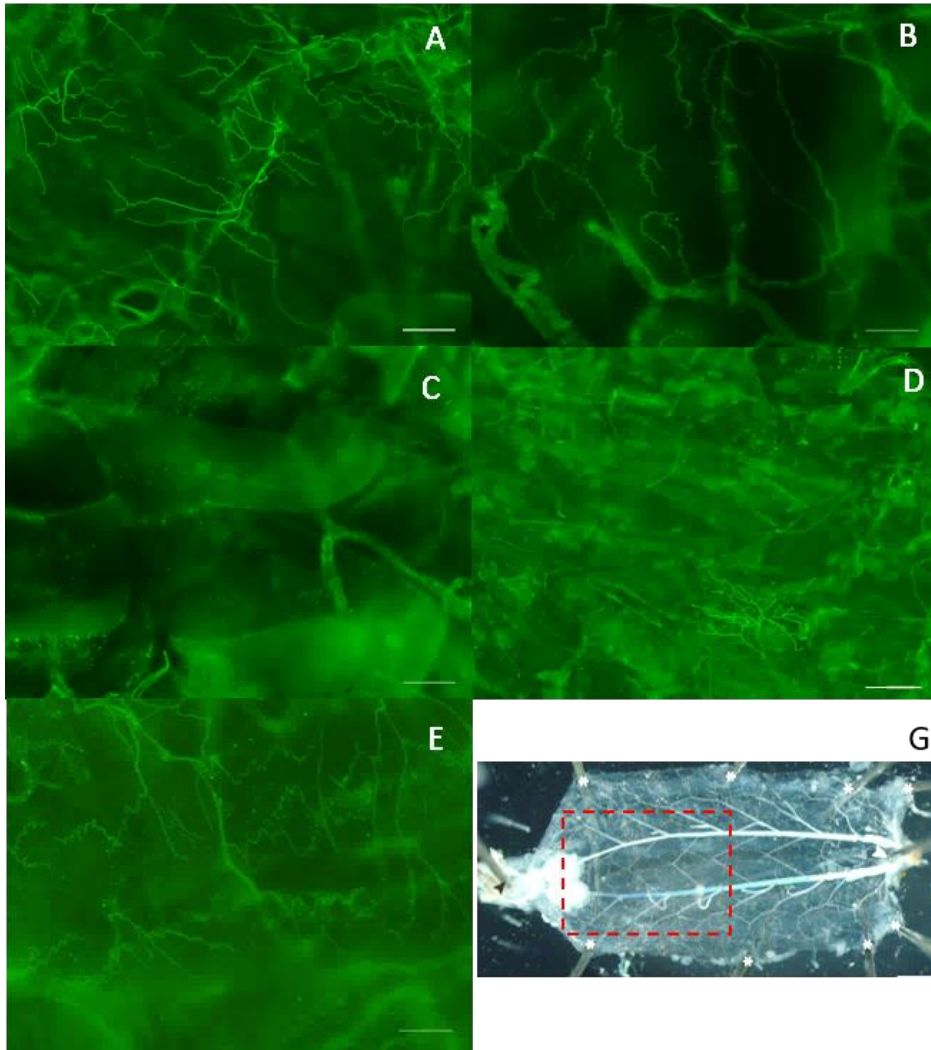


Figure 9. Immunohistochemical staining of terminal trachea in UPR overexpressing larvae.

The stained picture shows the body wall of larva in red dotted box (G). Reduced branching is apparent in equivalent areas of the body wall in XBP1s and PERK overexpressing larva (C, D) compared with control (A). No obviously changes in IRE1, ATF6 larvae were seen. Immunostaining of terminal trachea branching in *Drosophila* with the following primary antibody: Monoclonal Anti-WKD (1:200) and secondary antibody: anti-Rabbit Dylight 549 (1:500). Scale bar: 50 μ m. Genotypes: (A) DSRF-GAL4 > W¹¹¹⁸ (B) DSRF-GAL4 > UAS-ire1 (C) DSRF-GAL4 > UAS-xbp1s. (D) DSRF-GAL4 > UAS-PERK (E) DSRF-GAL4 > UAS-Atf6.

3.1.1.3 Susceptibility of UPR activated larvae to hypoxia.

In insects, the tracheal system is a network of air-filled tubes, which could distribute oxygen to organs and tissues throughout the body. The terminal tracheal cell is the only tracheal cell that has the capacity to produce cytoplasmic extension to deliver oxygen to target tissues (Chapman et al. 1998; Harrison et al. 2003). Cells at the tip of each branch acquire a terminal cell fate during tracheogenic (Affolter et al. 1994; Guillemin et al. 1996).

XBP1s and PERK overexpression led to decreasing numbers of terminal branches. Consequently, I evaluated the susceptibility of UPR activation in larval terminal trachea to hypoxia. 5% O₂ hypoxia in a suited chamber were used and experimental larvae were tested. Normally, larvae are buried in the medium until close to the start of pupation. To analyze the susceptibility to hypoxia, the total number of larva out of the medium was counted at the time point 5, 10, 15, 20, 30, 40, 60, 90 ... 300 min and then relative proportions were calculated. Ectopic activation of PERK in terminal trachea increased the susceptibility significantly since all third-instar larvae climbed out as soon as declining oxygen levels occurred (Fig. 10A). The proportion of Xbp1s overexpressing larvae climbing out reached 100% much quicker than controls, the hypoxia sensitivity was not as strong as in PERK overexpressing animals (Fig. 10B). After the susceptibility assay, vials were moved out of the hypoxia chamber and kept under normal oxygen conditions and about 80% of control larvae went back into the medium again. In contrast to the control, in both experimental groups, 82.33% of Xbp1s and 96.6% of PERK overexpressing larvae stayed out of medium (Fig. 10C).

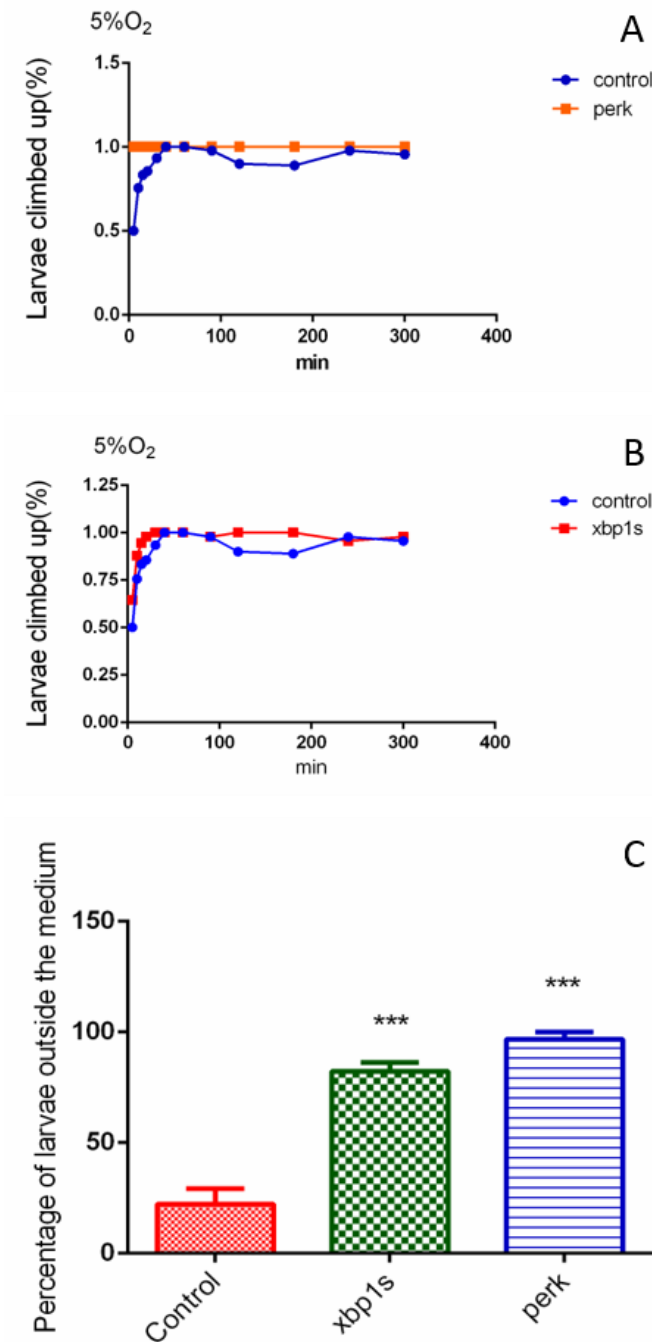


Figure 10. Susceptibility of UPR activated larvae to hypoxia.

Larval sensitivity to hypoxia was evaluated by counting the number of larvae climbing out of the medium after placing them into a 5% O₂ chamber. All third-instar larvae of the PERK overexpression group climbed out of the medium as soon as declining oxygen levels were experienced (A). The proportion of Xbp1s overexpressing larvae climbing out reached 100% quicker than the control (B). Proportion of Xbp1s (82.33%) and PERK (96.66%) overexpressing larvae being out of medium showed significant different from control (20.22%) 5 min after hypoxia treatment (C). n=30 Unpaired two-tailed Student's t-test was used for analysis, ***p<0.001.

3.1.2 UPR activation changes the morphology of the intestinal tissue

Using the driver line NP1-GAL4 adult enterocyte-specific expression was achieved. The intestinal epithelium from the adult midgut of *Drosophila melanogaster* was visualized by immunostaining, septate junction protein labeled by anti-coracle and nuclei labeled by DAPI.

After ectopic activation of UPR in the intestine, flies were prepared and stained. The impact of activation of UPR via different branches in the intestine was not as strong as in the airway system. As shown in Fig. 11 (white dotted box is labeled the area of cell while red dotted box labeled the nucleus), all intestinal cells with induction has obviously bigger nuclei (Fig. 11B-E) compared to control (Fig. 11A). The morphology of the intestine did not change obviously, except an increasing cell/nucleus ratio (Fig. 11F).

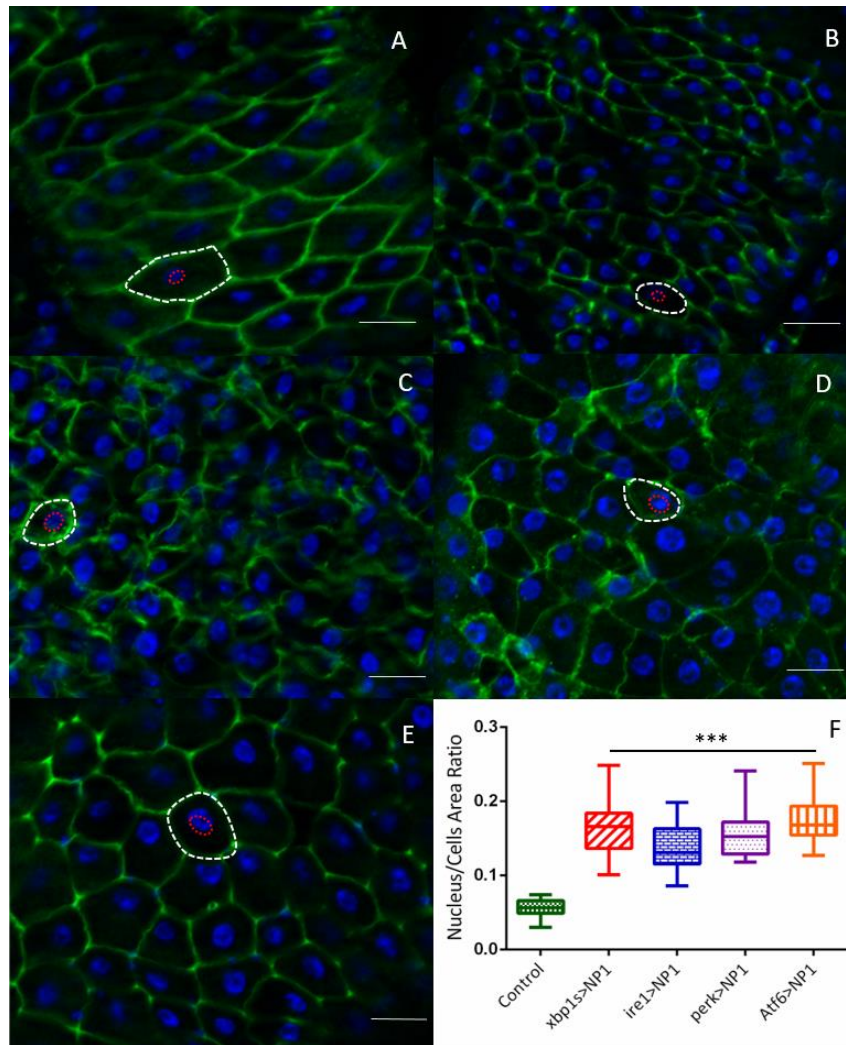


Figure 11. UPR signaling activated in the gut induced structural changes in cell shapes and nuclear sizes.

In IRE1, XBP1s and PERK overexpression (B, C, D), misslocalization of septate junction proteins and bigger nuclei were observed, compared with controls (A). In ATF6 overexpressing larvae, bigger sizes of nuclei could be observed (E). Quantification of nucleus/cells area ratio (F) indicated UPR signaling activation led to bigger sized nuclei in epithelial cells. Intestinal epithelium from the adult midgut of *Drosophila melanogaster* were visualized by anti-coracle (green) immunostaining and DAPI labeling of the nuclei (blue). Dashed lines represent the outline of cells and nuclei. Scale bar: 50 μ m. Genotypes: (A) NP1-GAL4 > w^{1118} (B) NP1-GAL4 > UAS-*ire1* (C) NP1-GAL4 > UAS-*xbp1s*. (D) NP1-GAL4 > UAS-*PERK* (E) NP1-GAL4 > UAS-*Atf6*. Data are represented as means \pm SEM. n=30 for each sample. Unpaired two-tailed Student's t-test was used for analysis, ***p<0.001.

3.1.2.1 Feeding of Dextran Sulfate Sodium influence life span extension in IRE1 overexpressing flies.

Numerous recent studies have revealed that UPR attempts to restore homeostasis from tissue damage, such as seen in inflammatory bowel diseases, but if unsuccessful it can trigger apoptosis. Feeding flies with 5% dextran sulfate sodium (DSS) causes injury in the intestines and complex interactions in the gut leading to excessive inflammation. In inflammatory bowel disease, IRE1-XBP1 has been shown to function protectively. Deletion of the *ire1* or the *xbp1s* gene in the mouse intestinal epithelium leads to an increased susceptibility to dextran sulfate sodium (DSS) induced colitis. Deletion of XBP1 in the mouse intestine also results in intestinal inflammation.

In general, 5-day-old female and male adult flies were used for life span assays, control groups were cultured in empty vials containing a piece of chromatography paper wetted with 5% sucrose solution as feeding medium, correspondingly experimental groups were fed with 5% *Dextran Sulfate Sodium* (DSS) dissolved in 5% sucrose. Flies that were still alive were transferred to new vials with fresh feeding media every day and the percentage of flies alive after each day is expressed as survival rate.

Under the DSS treatment, IRE1 overexpressing male flies significantly extended their lifespan compared to control flies, but not females (Fig. 12A). No significant changes were seen in the other overexpressing flies.

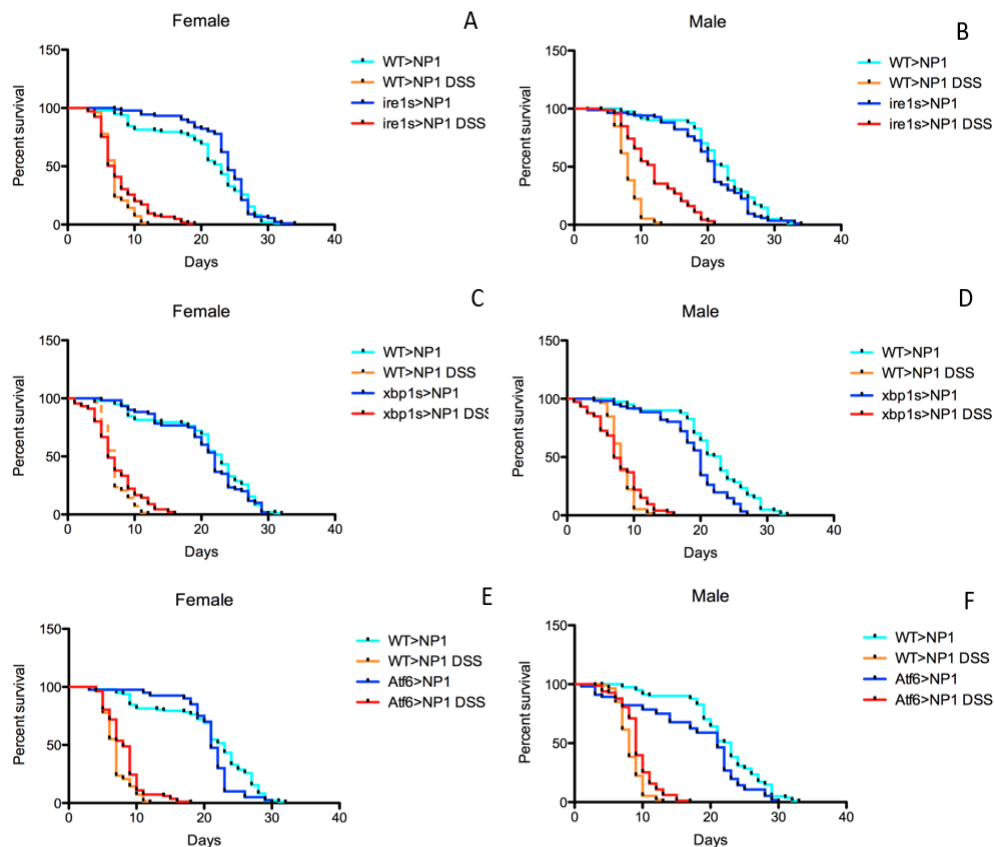


Figure 12. IRE1 overexpression increased lifespan in males feeding DSS.

Under DSS treatment, IRE1 flies significantly extended their lifespan in males (B, 10 days for the median survival, $n=105$) but not in females (A, 6 days for the median survival, $n=93$) and compared to control flies (female 6 days and male 8 days for the median survival, $n=140$, 112 , respectively). However, both of Xbp1s and Atf6 overexpressing flies have no effect on survival (C-F). Log-rank test for survival analysis showed significant differences, $p<0.001$.

3.1.3 UPR activation changes the morphology of the fat body in *Drosophila*.

To test whether tissue-specific overexpression of crucial UPR markers in *Drosophila* can influence the morphology of the fat body, I generated ectopically activated flies using the driver line *ppl-Gal4* and analyzed changes with microscopy. The abnormal morphology of fat body tissue in Xbp1s and PERK overexpression larvae was observed (Fig. 13B, C) compared to matching controls (Fig. 13A). To further investigate changes of the cell shapes I performed BODIPY and DAPI staining of the fat droplets and nuclei,

respectively in larvae. Consistent with direct observations mentioned previously, PERK overexpression induced a dramatic change of localization of fat body cells (Fig. 14D) as well as bigger, dissolved nuclei (Fig. 14H) compared to the controls (Fig. 14A). XBP1s overexpression (Fig. 14C) induced bigger nuclei than controls. To quantify the nucleus/cell area ratio I randomly selected 15 pictures comprising 6 biological replicates and measured areas of cells and nuclei (Fig. 14F). No changes were observed in IRE1 and ATF6 overexpression (Fig. 14B, E).

Afterwards, I used the inducible Gene Switch System to overexpress PERK in the fat body, thus the morphological changes could better be observed in a time dependent fashion. First, flies were maintained on normal medium supplemented with the same dose of the diluent ethanol. Following this, they were transferred to medium containing RU486, which can induce expression of PERK specifically in the fat body. Dissection and immunohistochemical staining was performed every day after induction by mifepristone. At the second and the third day, the fat body tissue including the cells septate junctions and nucleus became irregular (Fig. 15A-F). Altogether, these results reveal an obviously changed phenotype in fat body cells following PERK overexpression.

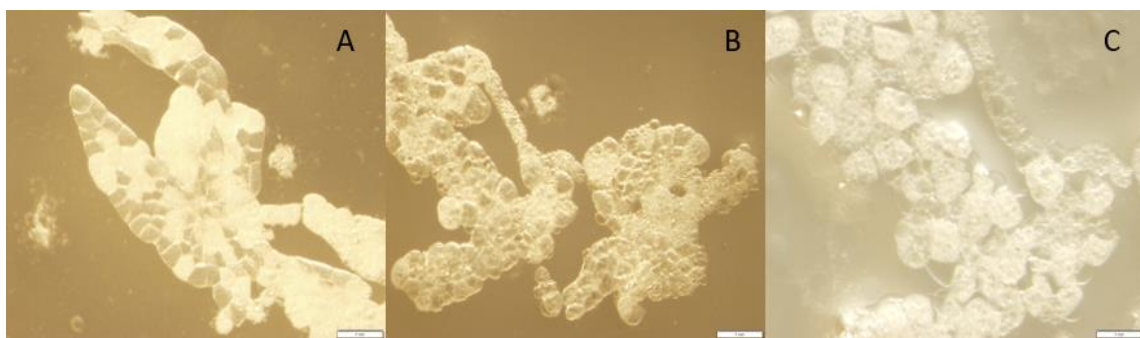


Figure 13 . Overexpression of XBP1s and PERK in the fat body changed morphology of the fat body cell significantly.

Scale bar: 1 mm. Genotypes: (A) *ppl-GAL4 > W¹¹¹⁸* (B) *ppl-GAL4 > UAS-xbp1s*. (C) *ppl-GAL4 > UAS-PERK*.

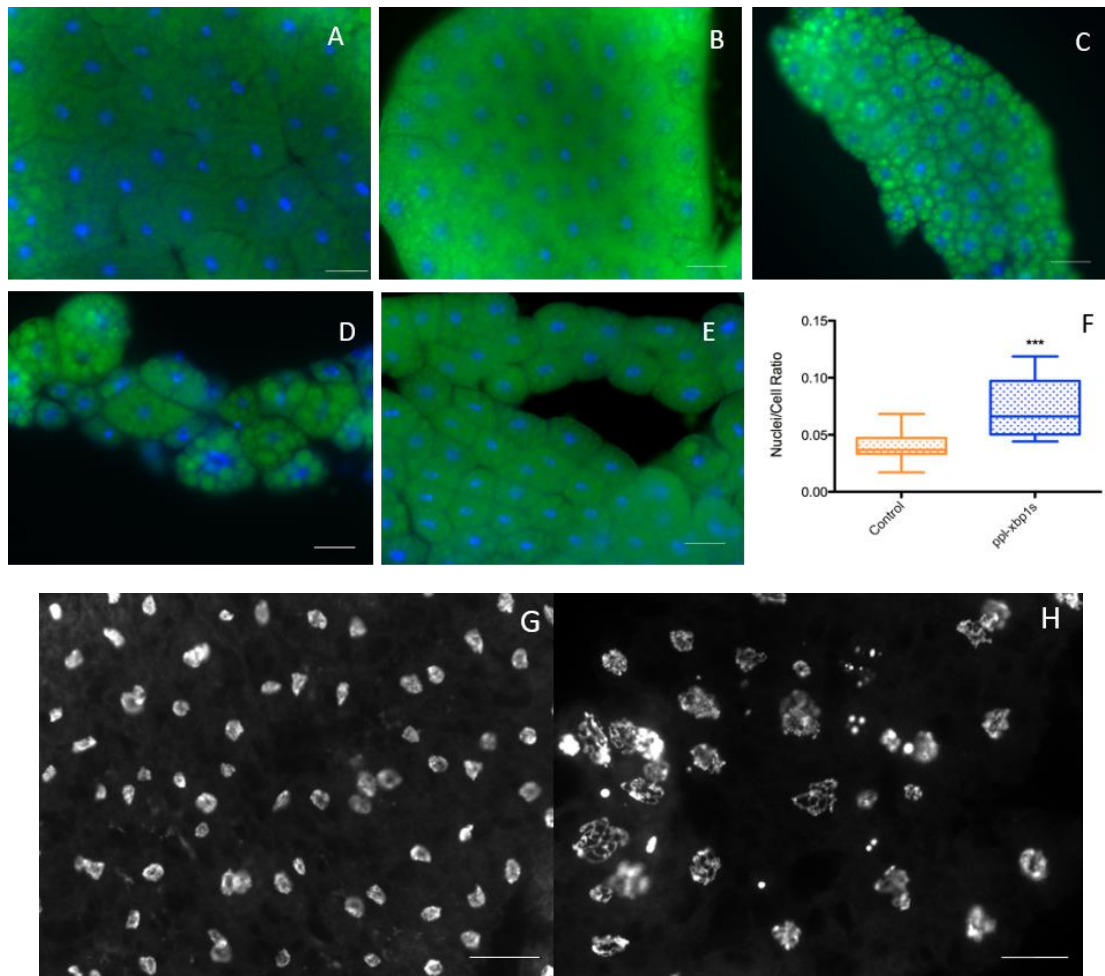


Figure 14. Staining of fat body in overexpression of UPR components.

PERK overexpression (D) induced a dramatic change of the fat body cell and nuclei structure (H) compared with the control (A, G). No changes were observed in IRE1 and ATF6 overexpressing fat bodies. To quantify the nucleus/cell area ratio (F) indicated UPR signaling activated lead to bigger size nucleus as observed in staining picture (C) in fat body cells when Xbp1s overexpression. Fat body of *Drosophila melanogaster* were visualized by Bodipy (green) and DAPI staining labeled the nuclei (blue). Scale bar: 50 μm . Genotypes: (A) NP1-GAL4 > W^{1118} (B) NP1-GAL4 > UAS-*ire1* (C) NP1-GAL4 > UAS-*xbp1s*. (D) NP1-GAL4 > UAS-*PERK* (E) NP1-GAL4 > UAS-*Atf6*. Data are represented as means \pm SEM. n=30 for each sample. Unpaired two-tailed Student's t-test was used for analysis, **p<0.01.

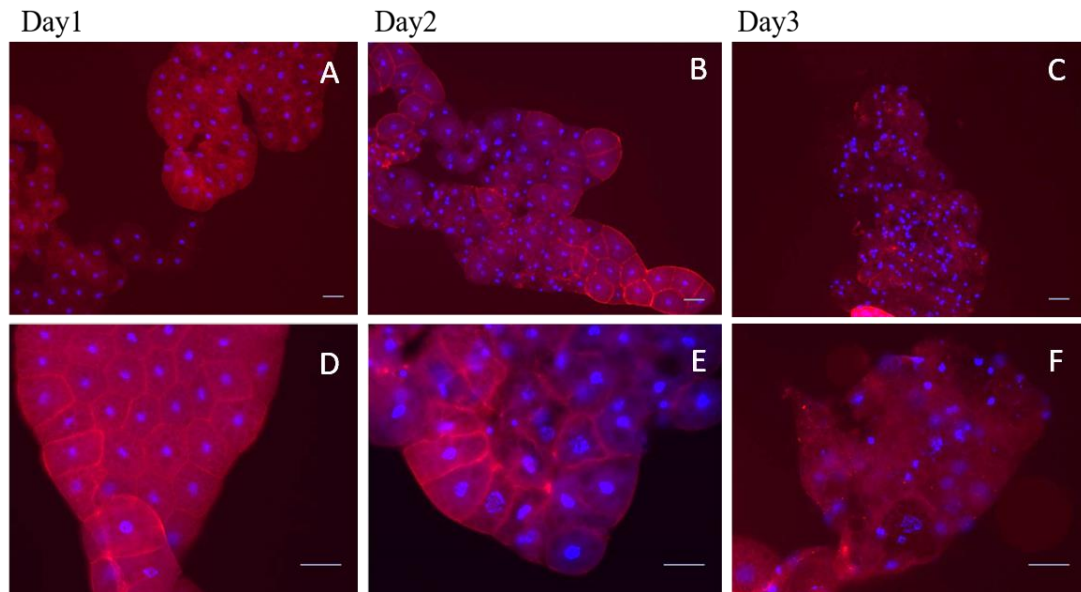


Figure 15. Ectopic activation of PERK in the fat body.

Using the Gene switch expression system, RU486 induced PERK-overexpression (*pp1GS-Gal4 > UAS-PERK*). After transfer of the animals to the medium containing RU486 to induce the expression of PERK, no change in the fat body was seen at the first day (A, D). At the second day (B, E) and the third day (C, F), the fat body tissue including the cell septate junction and nuclei became irregular. To label septate junction of cell the following primary antibody was used: anti-*Drosophila* coracle monoclonal antibody (1:200), secondary antibody was used: Anti-Mouse Alexa Fluor 647 (1:500) (red) and nuclei were labeled with DAPI (blue). Scale bar: 10 μm (A-C), 50 μm (D-E).

3.2 Activation of Xbp1s in trachea and fat body increased expression levels of *drosomycin* dramatically.

The innate and adaptive immune system defends the organism against a multitude of pathogens and infections. The UPR signaling intersects at many levels with the innate and adaptive immune response (Muralidharan et al. 2013).

Under non-infected conditions, AMPs are synthesized constitutively in specific tissues, particularly in barrier epithelia and systemically in the fat body in both insects and mammals (Selsted et al. 2005). Among the major eight AMP genes identified in

Drosophila, *drosomycin* is the best characterized one. Nevertheless, the regulatory mechanisms to induce AMP expression in barrier epithelia are not well understood.

To investigate the relationship between activation of different branches of the UPR and innate immunity, I analyzed relative expression levels of *drosomycin* in *Drosophila* trachea using real-time quantitative PCR. Xbp1s, ire1 and Atf6 overexpression in the airway epithelium of larvae using a Gal4-Gal80ts/UAS temperature induce system was employed.

The result of real-time quantitative PCR analysis showed that the relative expression of *drosomycin* was upregulated dramatically by overexpression of XBP1s in the tracheal system. The observed differences were only significant for XBP1s but not for IRE1 and Atf6 overexpression (Fig. 16). To test whether Xbp1s induced AMP expression could be not only observed in airway epithelial but also in Xbp1s overexpression in the fat body, I next assessed the relative *drosomycin* expression level by qRT-PCR. Consistent with the changes in the trachea, only activation of XBP1s induced significant and very high mRNA expression levels of *drosomycin* in the fat body (Fig. 18). Further experiments were done to learn whether the other AMP genes were also induced by Xbp1s. There was no up-regulation of relative expression levels detectable by qRT-PCR analysis for *diptericin* and *attacin*, respectively (Fig. 19).

Chronic hypoxia leads the production of reactive oxygen species (ROS), which are produced in several organelles, including the ER. Altered redox homeostasis in the ER cause ER stress (Sena and Chandel 2012; Cao and Kaufman 2014; Inagi et al. 2014). Third instar larva (WT) were exposed to 3-5% O₂ for 2, 4, 24 h and to CS (Cigarette Smoke) at 22 °C to induce ER-stress. To test whether the level of xbp1s in larvae increased under ER-stress conditions, I performed qRT-PCR to check the expression level of xbp1s in larval trachea. After 4 h of hypoxia treatment, the level of xbp1s increased compared to the control without treatment and the other conditions (Fig. 17). This result indicates that hypoxia treatment can induce the ER stress in the fly,

when UPR is activated to response this stress, meanwhile up-regulates the level of *xbp1s*.

From all these results, we could find that ectopic activation of Xbp1s in trachea and in the fat body induced expression of antimicrobial peptide genes, namely that of the AMP *drosomycin*. Thus, a strong activation of the innate immune response might be part of the UPR in these tissues.

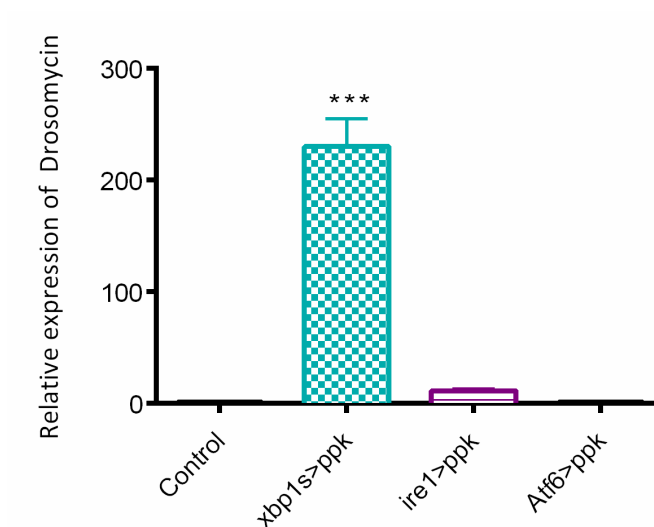


Figure 16. Spliced *xbp1* (*xbp1s*) overexpression in the airway increases levels of drosomycin in larvae dramatically.

Shown is a significantly increased level of *drosomycin* in *ppk*-Gal80ts-GAL4>UAS-*xbp1s* compare to the control (*ppk*-Gal80ts-GAL4>UAS-W¹¹¹⁸), no difference in *ppk*-Gal80ts-GAL4>UAS-*ire1* and *ppk*-Gal80ts-GAL4>UAS-*Atf6*. Data are presented as mean \pm SEM; one-way ANOVA was used for analysis, *** p <0.01.

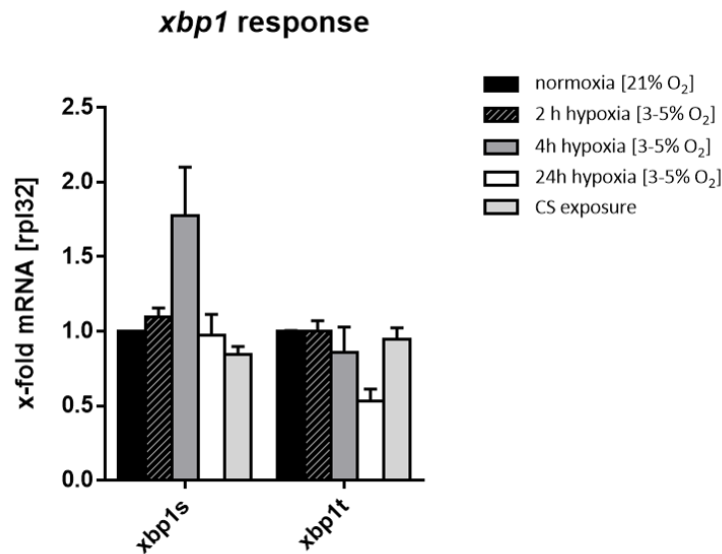


Figure 17. Relative expression levels of *xbp1s* increased in larval trachea under ER-stress condition.

Third instar larva (WT) were exposed to 3-5% O₂ for 2,4,24 h and CS (Cigarette Smoke) at 22°C. Control larvae were put in normoxia (21% O₂). After 4h of hypoxia stress, spliced *xbp1s* significantly increased. (n=3 replicates for each group).

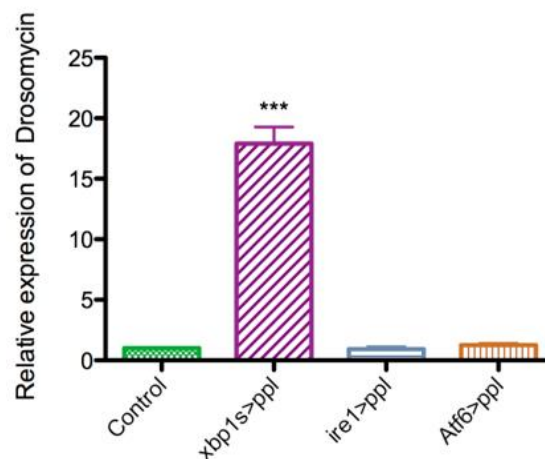


Figure 18. Spliced *xbp1* (*xbp1s*) overexpression in the fat body increases the level of *drosomycin* in larvae.

Activation of XBP1s in fat body increases expression level of *drosomycin* dramatically. The difference of *drosomycin* expression levels was only significant in *ppl*-Gal4>UAS-*xbp1s* but not in *ppl*-Gal4 >UAS-*ire1* and *ppl*-Gal4 > UAS-*Atf6* compared to control (*ppl*-Gal4 > UAS-W¹¹¹⁸). Data are presented as mean ± SEM; one-way ANOVA was used for analysis, ***p<0.01.

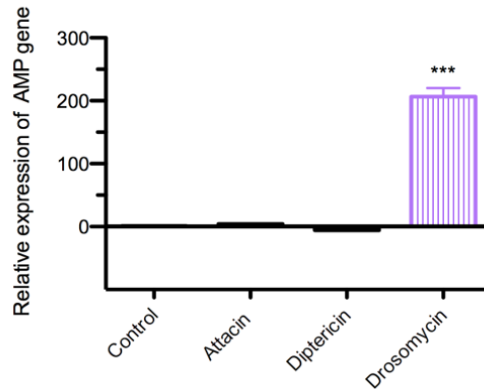


Figure 19. Regulation of AMP gene expression in response to Xbp1s activation in the airways.

A significantly increased level of *drosomycin* in *ppk-Gal80ts-GAL4 > UAS-xbp1s* compare to the control (*ppk-Gal80ts-GAL4 > UAS-W¹¹¹⁸*), no difference in the expression level of *Attacin*, *Diptericin*. Data are presented as mean \pm SEM; one-way ANOVA was used for analysis, *** $p < 0.01$.

3.3 Analyses of activated UPR in regulation of insulin and glucose homeostasis

3.3.1 Overexpression of XBP1s and PERK influence DILP2 in IPCs.

In larvae and adults of the *Drosophila* brain, DILP2, 3 and 5 are produced in a set of 14 median neurosecretory cells, so-called IPCs. (Brogiolo et al. 2001; Cao and Brown 2001; Rulifson et al. 2002; Geminard et al. 2009). These IPCs (Figure. 20A) are embedded in a cluster of median neurosecretory cells (MNCs) in the *pars intercerebralis* (PI). Among these insulin-like peptides (DILPs), DILP2 is the most highly expressed one and it is related to the fly's metabolism and lifespan (Broughton et al. 2005; Ikeya et al. 2002; Rulifson et al. 2002).

To investigate the relationship of UPR signaling pathways and insulin secretion, four crucial UPR markers (XBP1s, PERK, ATF6 and IRE1) were overexpressed in IPCs of the adult brain using the driver line *dilp2-Gal4*. IPCs were visualized by anti-DILP2 labeling

in the adult brain. It was found that IPCs labeled by anti-DILP2 staining decreased in XBP1s flies (Fig. 20C) compared with controls (Fig.20B). In PERK flies, there was an even stronger decrease in IPCs (Fig.20D).

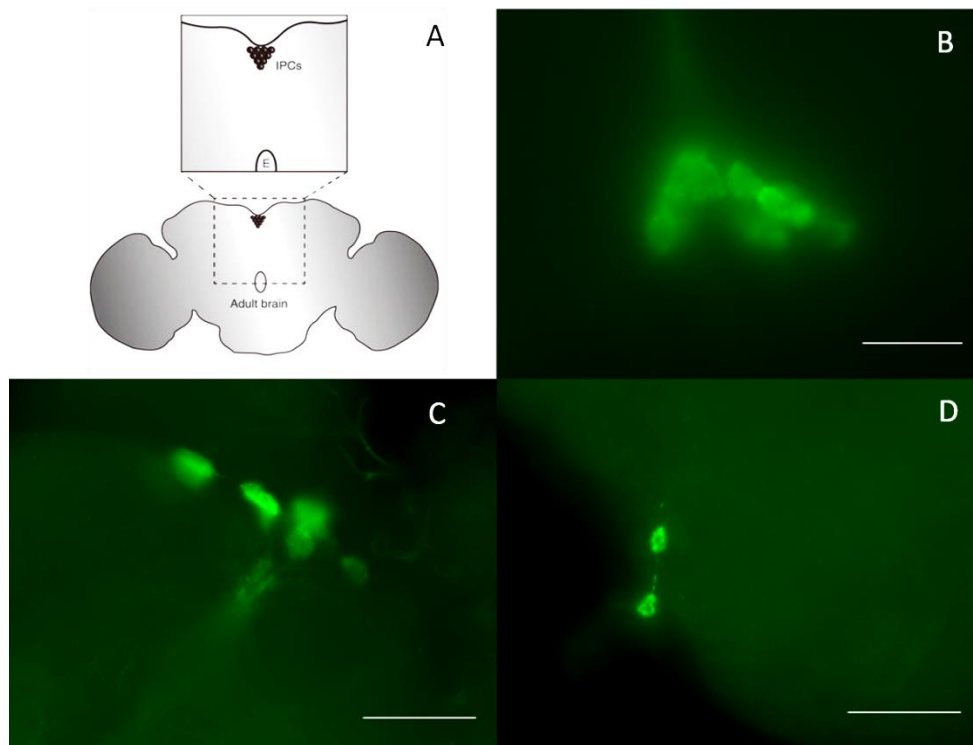


Figure 20. Overexpression of *xbp1s* and PERK in insulin-producing cells affect cell morphology.

A scheme of the adult brain indicates the position of the IPCs in the median neurosecretory cluster in the *pars intercerebralis* (A). To visualize insulin-producing cells in the adult brain by anti-Dilp2 (green) immunostaining. Genotype: *dilp2-HA-Gal4 > w¹¹¹⁸* (B), *dilp2-HA-Gal4 > UAS-xbp1s* (C), *dilp2-HA-Gal4 > UAS-perk* (D) Scale bar: 50μm.

3.3 2 Influence of overexpression of UPR on circulating and total DILP2 level

Insulin-like signaling is conserved in order to correlate metabolism with nutrient status in multicellular organisms (Sato-Miyata Y et al., 2015). Circulating insulin levels are often associated with hyperglycemia, insulin resistance, diabetes and some other impaired physiological conditions.

To provide insights into the roles played by three activated UPR branches in DILP2

secretion, I used the GAL4/UAS System to overexpress XBP1s, IRE1, PERK and ATF6 in IPCs of adult brain. Here, tissue-specific overexpression is achieved by crossing of UAS line with the driver line *dilp2-HA-Gal4*. To quantify total and circulating Dilp2 in adult flies we established an ELISA based on commercially available monoclonal antibodies and peptide standards harboring both HA- and FLAG- epitope tags (Park et al. 2014).

The circulating DILP2 content measurement assay showed that the level of circulating Dilp2 in XBP1s flies decreased both in female and male (Fig. 21A), same as the level of total Dilp2 (Fig. 21B). PERK flies showed normal levels in circulating insulin (Fig. 21E), but a dramatic decrease in total levels of insulin compared to the control (Fig. 21F). The decrease is mild in circulating Dilp2 in IRE1 overexpressing flies both in females and males (Fig. 21C). There were no changes in ATF6 overexpressing flies regarding the insulin levels (Fig. 21G, H).

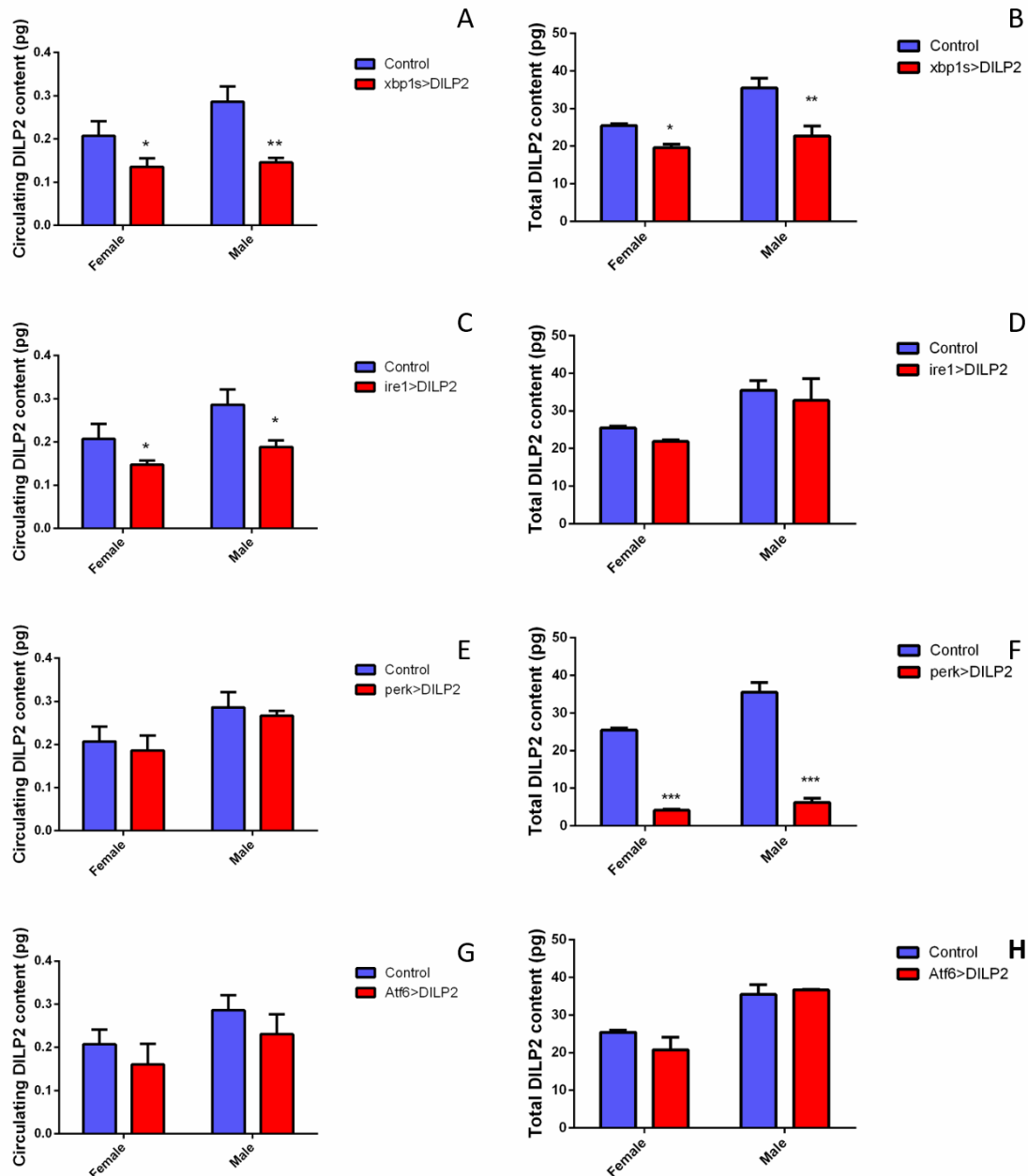


Figure 21. Activation of signaling components of UPR in IPCs influence circulating DILP2 contents and total DILP2 contents in flies.

The circulating DILP2 content measurement assay showed that the level of circulating Dilp2^{FLAG} proteins in XBP1s flies (*dilp2-HA-Gal4 > UAS-xbp1s*) decreased both in female and male (A) as same as the level of total Dilp2^{FLAG} proteins (B). PERK flies (*dilp2-HA-Gal4>UAS-perk*) showed normal level in circulating insulin (E), but a dramatically decreasing total level of insulin (F). Comparing to the control (*dilp2-HA-Gal4 > w¹¹¹⁸*). The decrease is mild in circulating in IRE1 flies (*dilp2-HA-Gal4 > UAS-ire1*) both in female and male(E). There was no change in Atf6 flies' (*dilp2-HA-Gal4 > UAS-Atf6*) insulin level (G, H). Data are presented as mean \pm S.D.; unpaired two-tailed Student's t-test was used for analysis, * $p < 0.05$, ** $p < 0.01$, *** $p < 0.001$.

3.3.3 Influence of overexpression of UPR inducers on glucose tolerance

It has been demonstrated that DILP2 regulates glucose homeostasis, the reduction of DILP2 in the hemolymph leads to an increased glucose content (Broughton et al. 2008). Furthermore, to fully understand how insulin affects glucose homeostasis, it is important to measure the organism's ability to clear increasing peripheral glucose levels.

To understand the role of the unfolded protein response (UPR) in glucose homeostasis via regulating insulin signaling, I created transgenic *Drosophila* lines with targeted UPR protein expression in insulin producing cells (IPCs) as mentioned above. The adult flies were challenged with an oral glucose tolerance test that was developed to investigate the ability to clear high glucose levels. Adult flies (10 days old) were fasted for 16 hours on 1% agar before subjected to oral glucose tolerance test (see Materials and Methods).

As shown in Fig. 22, control flies show similar glucose clearance kinetics after ingestion of glucose as seen in mammals (Guerra et al. 2001). Following this, the glucose tolerance assay testified a reduced capacity of glucose clearance in Xbp1s flies, since a higher level of glucose in the hemolymph was seen 60 min after oral feeding of glucose compared to control flies (Fig. 22A, B). Hence, xbp1s overexpression in flies' IPCs results in hyperglycemia. IRE1 overexpression in IPCs has a slightly higher glucose level than controls after oral glucose challenge (Fig. 22C, D). PERK overexpression in IPCs led to normal clearance of glucose (Fig. 22E, F). Moreover, ATF6 overexpression has no negative effect on glucose tolerance as compared to control flies (Fig. 22G, H). In females of PERK, IRE1 and Atf6 overexpressing flies, a higher glucose level after treatment with oral glucose was observed, but the level decreased to the normal level as in controls (Fig. 22C, E, G).

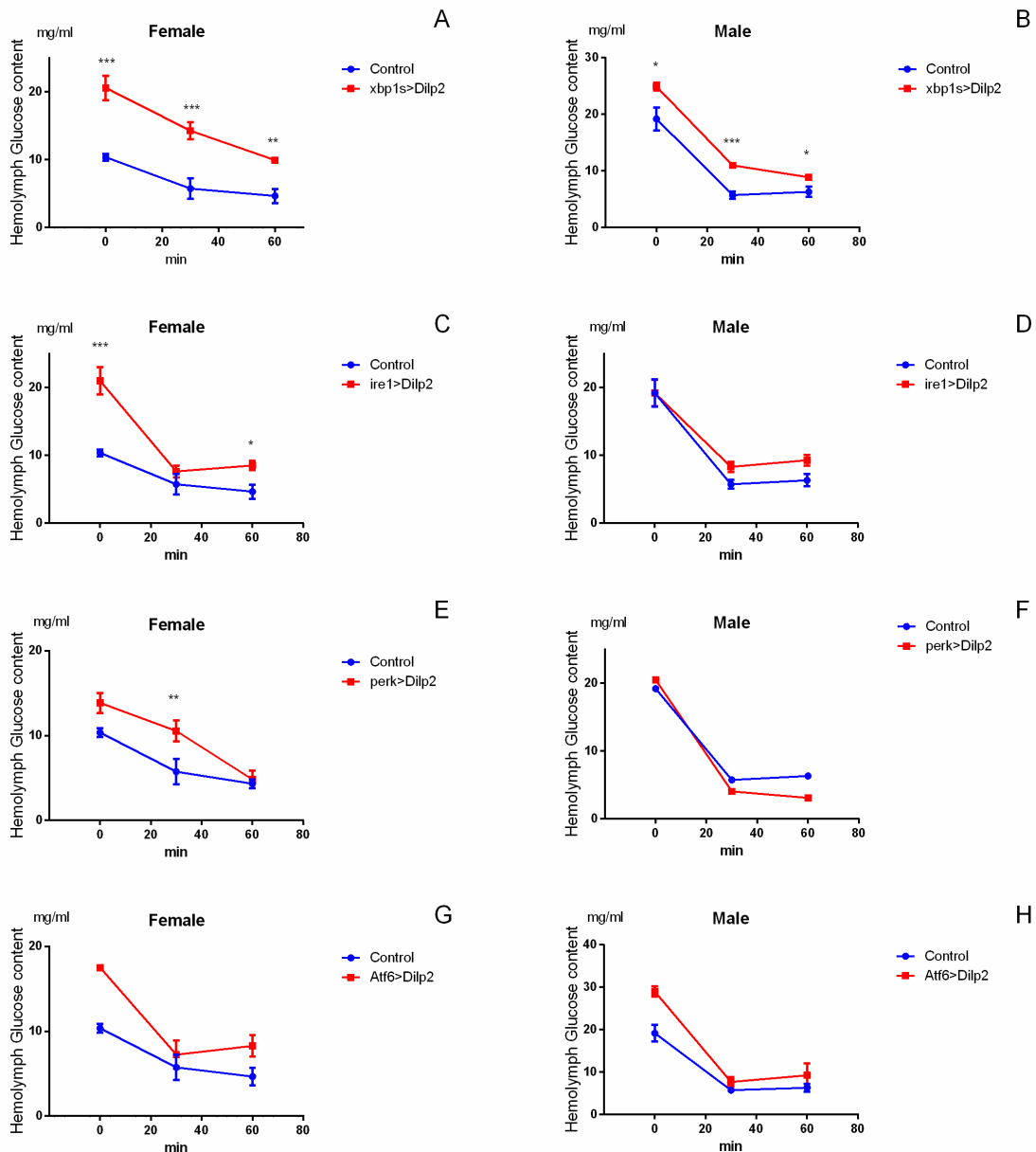


Figure 22. Activation of signaling components of UPR in IPCs influence glucose tolerance in adult flies.

Adult flies (10 days old) were fasted for 16 hours on 1% agar before subjected to the oral glucose tolerance test. Adult-specific, overexpression of Xbp1s (*dilp2-HA-Gal4 > UAS-xbp1s*) in IPCs renders those flies hyperglycemic and glucose intolerant as compared to controls (*dilp2-HA-Gal4 > w¹¹¹⁸*) either in females or males (A, B). Ire1 overexpression in IPCs (*dilp2-HA-Gal4 > UAS-ire1*) had a slightly higher glucose level than control after treatment with oral glucose (C, D). PERK overexpression in IPCs (*dilp2-HA-Gal4>UAS-perk*) could clear the glucose to the normal level after treatment with oral glucose (E, F). ATF6 overexpression (*dilp2-HA-Gal4 > UAS-Atf6*) has no negative effect on glucose tolerance response as compared to control flies (G, H). Data are presented as mean \pm SEM.; (N =3 independent hemolymph collections with 30-50

flies/collection). Unpaired two-tailed Student's t-test was used for analysis, * $p < 0.05$, ** $p < 0.01$, *** $p < 0.001$.

3.3.4 Influence of overexpression of UPR inducers on life span

Reducing the levels DILPs leads to an array of phenotypes including increased fasting glucose levels in the adult hemolymph, increased storage of lipid and carbohydrate, reduced fecundity, extension of median and maximal lifespan (Broughton et al. 2005). As the level of DILP2 is highly related to the fly's metabolism and lifespan, I performed survivorship studies to determine the impact of adult-specific expression of UPR inducers in IPCs on longevity. An increasing life span of Xbp1s overexpression flies was shown compared to controls (Fig. 23).

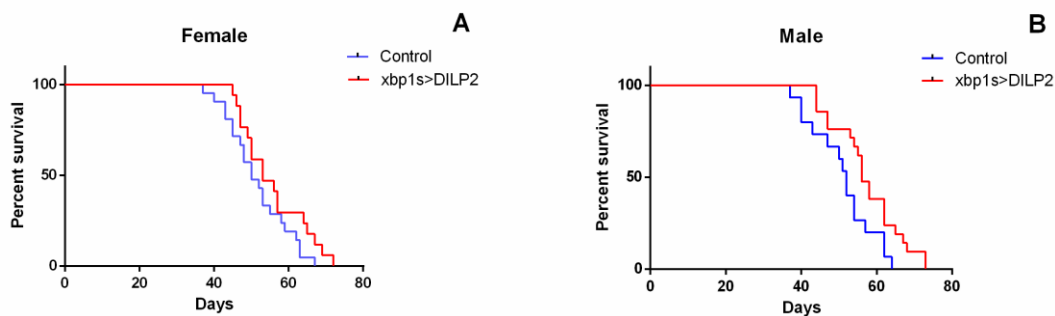


Figure 23. XBP1s overexpression in IPCs influenced life span of flies.

Overexpression Xbp1s in IPCs (*dilp2-HA-Gal4>UAS-xbp1s*) extends longer lifespan both in males (A, 55 days for the median survival, $n=29$) and females (B, 57 days for the median survival, $n=30$) compared to control flies (female 52 days and male 50 days for the median survival, $n=28, 30$ respectively). Log-rank test for survival analysis showed significant differences, $p < 0.001$.

3.3.5. Overexpression of PERK in IPCs decreases body size, weight and causes development delay

Previous studies showed that genetic manipulation of Dilp2 signaling affected lifespan, stress resistance, lipid levels, metabolism and the pattern of animal activity. Therefore, I performed a quantification of body size, weight and development delay of PERK

overexpressing flies (Fig. 24A, B). The PERK overexpressing flies had significantly reduced body weight (42% in females and 45% in males, respectively) (Fig. 24C). PERK overexpression led also to remarkable decreasing body sizes (44% in females and 39% in males compared to controls) (Fig. 24D, E). To investigate the effect of PERK-overexpression on development, I analyzed the timing of pupariation in larvae and compared it with the control. PERK expression in IPCs in flies resulted in a delay of 5 days in larval developmental rates when compared with the control flies (Fig.25).

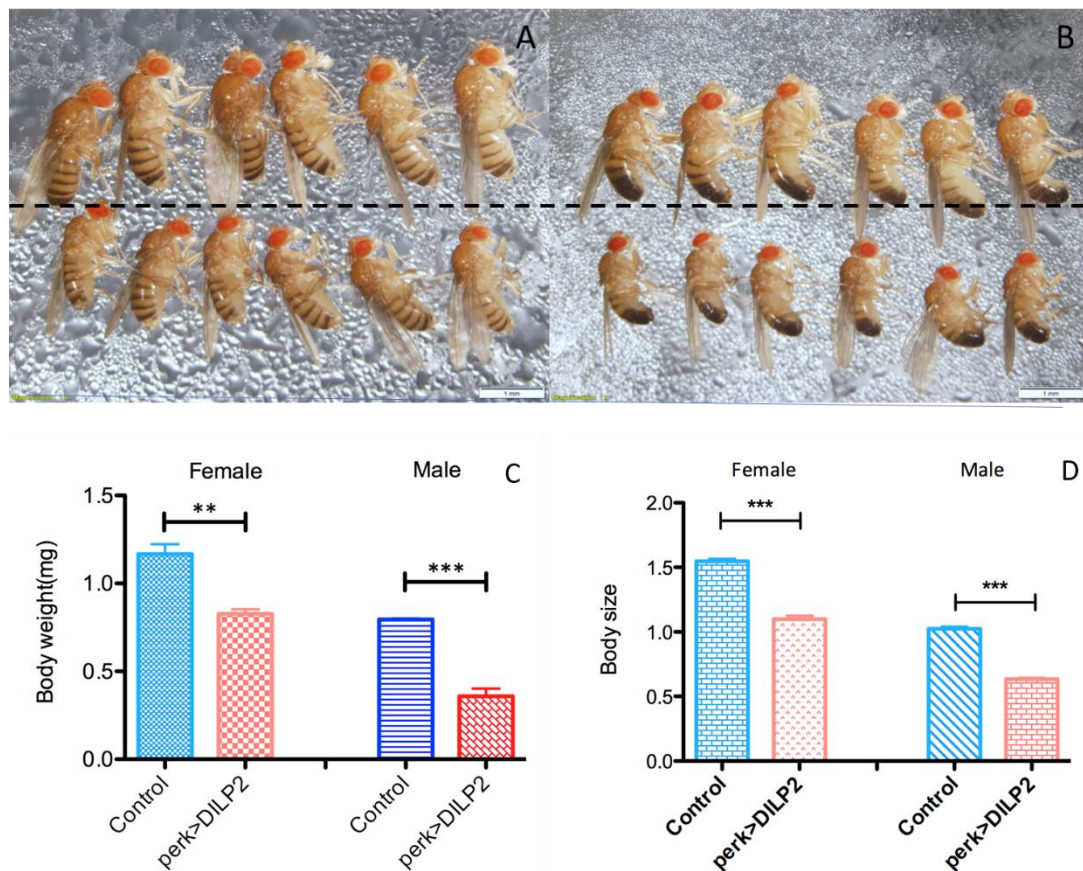


Figure 24. Overexpression of PERK in IPCs decreases body size and weight of flies.

3-5 days old adult flies' female (A) and male (B) were weighted and body sizes measured using ImageJ. The flies above the dotted line are controls (*dilp2-HA-GAL4 > W¹¹¹⁸*), the genotype of flies below the dotted line is *dilp2-HA-GAL4 > UAS-perk*. Compared to control, PERK-overexpressing flies had significantly decreased body weight, by 42% in females and by 45% in males (C), as well as decreased body sizes 44% in females and 39% in males. (PERK, n=20; Control, n=20). Student t-test was performed to analyze statistical significance. **p<0.01, ***p<0.001.

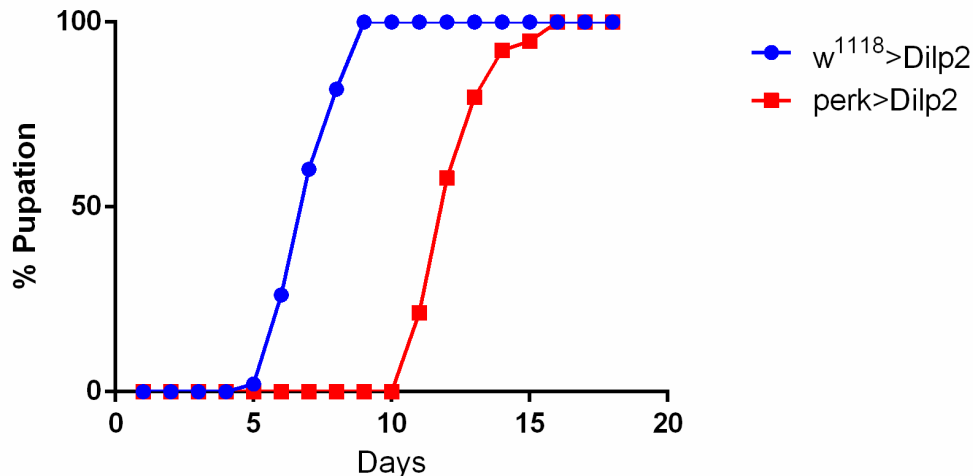


Figure 25. Overexpression of *perk* in IPCs causes development delay.

Drosophila larvae were raised on normal medium and their number was counted daily until pupation. PERK larvae (*dilp2-HA-GAL4 >UAS-perk*) had around 5 days delay compared with controls (*dilp2-HA-GAL4 > W¹¹¹⁸*). (PERK, n=102; control, n=128)

3.4 Influence of overexpression of ORMDL in *Drosophila* IPCs

ORMDL3 belongs to a gene family comprising three members in humans (ORMDL1, ORMDL2 and ORMDL3), as well as homologs in yeast, microsporidia, plants, *Drosophila*, and vertebrates (Hjelmqvist et al. 2002). The ORMDL genes encode transmembrane proteins anchored in the endoplasmic reticulum (ER), which is the most relevant candidate gene linking UPR and a risk factor for asthma and Type 1 diabetes mellitus (Moffatt et al. 2007; Bouzigon et al. 2008).

To investigate the impact of ORMDL overexpression in IPCs of the adult brain I crossed UAS-ORMDL with the driver line *dilp2-Gal4*. The circulating and total DILP2 content of ORMDL overexpression flies were not different from controls, both in females and males (Fig.26A, B). The glucose tolerance assay demonstrated a normal capacity of glucose clearance in ORMDL flies 60 min after oral feeding of glucose compared to control flies (Fig.26C, D).

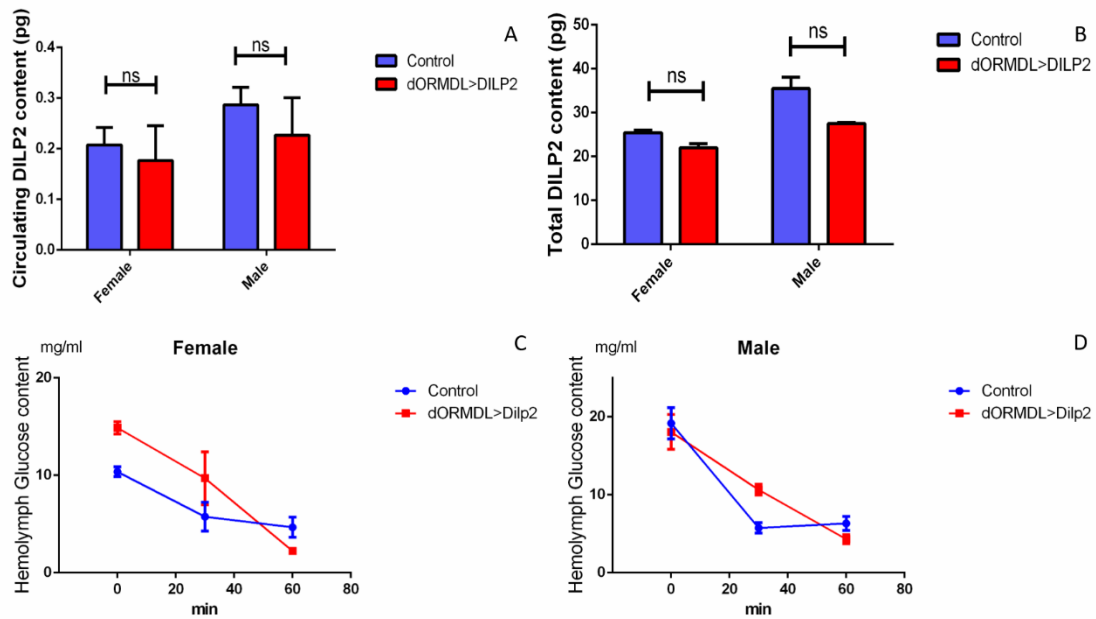


Figure 26. Influence on DILP2 contents and glucose tolerance of overexpression of ORMDL in *Drosophila* IPCs.

The circulating DILP2 content measurement assay showed that the level of circulating Dilp2^{FLAG} proteins in ORMDL flies was not different from controls, both in females and males (A). The same was true for the level of total Dilp2^{FLAG} proteins (B). ORMDL overexpression in IPCs had no effect on the glucose level after treatment with oral glucose either in females (C) or males (D). Student t-test was performed to analyze statistical significance. **p<0.01, ***p<0.001.

4. Discussion

The endoplasmic reticulum (ER) is an intracellular membrane system present in all eukaryotic cells. The UPR is a complex signaling pathway activated in response to ER stress. This cellular response system aims to alleviate ER-stress through regulation of DNA transcription, mRNA translation, and other cellular processes, if the stress can't be resolved it initiates apoptosis (Ron et al. 2007). Endoplasmic reticulum (ER) stress, can be caused by many reasons, including viral infections, protein misfolding and accumulation, as well as local oxidative stress or drastic depletion of ER calcium levels. Furthermore, it has been demonstrated that ER stress can be one of the reasons to induce cellular dysfunction (Rutkowski et al. 2010).

The UPR comprises of three signaling branches mediated by three ER transmembrane proteins: inositol-requiring protein 1 α (IRE1 α), protein kinase RNA-like ER kinase (PERK), activating transcription factor 6 (ATF6). X-box binding protein 1 (XBP1) splicing by activated IRE1 α has been considered as a crucial UPR activation markers. Moreover, dysfunction of the UPR causes numerous diseases, including neurodegenerative, inflammatory, metabolic, and cardiovascular diseases or even cancer (Kadowaki et al., 2013). Thus, a thorough research agenda in ER stress-induced signaling pathways may serve as a potent therapeutic avenue towards fighting of ER stress-related diseases.

4.1 Specific activation of key UPR components influence the morphology of organs

In this chapter, I will focus on discussing how morphological parameters of different tissues are affected by activation of UPR via different branches in *Drosophila*.

To study growth and development of *Drosophila*, with ectopically triggered overexpression of the of the XBP1s/IRE1 as well as of the perk in trachea, a lethal phenotype was observed. In order to evaluate the morphological changes, an inducible tracheal expression control system activated by mifepristone (RU488) had to be used. In larvae experiencing XBP1 overexpression, an abnormal phenotype of changed septate junctions structure of tracheal cells was found compared with matching controls. *In vitro* studies using human umbilical vein endothelial cells (HUVECs) indicated XBP1 splicing to be related to endothelial proliferation and overexpression of spliced XBP1 induced apoptosis (Zeng et al. 2009). My own results point in the same direction, as massive proliferation is seen directly after beginning of Xbp1s expression, which leads later to cell death and consequently to death of the entire organism. Similarly, in PERK-overexpressing larvae, an abnormal morphology was observed as well. After two days of mifepristone treatment, individual cell membranes disappeared, meanwhile small fractions of nuclei related structures were released from trachea cells implying modes of cell death, although a definite proof for this assumption is still lacking. This would mean that this type of UPR activation has a two phases response with proliferation coming first, followed by induced cell death processes.

It is well known that the UPR has two major functions, one is to inhibit protein translation to alleviate and resolve the ER stress, the other is to induce cell apoptosis in cases were the ER stress remains unresolved. PERK as one of the major branches of the UPR has been demonstrated to be able to independently trigger apoptosis (Demay et al. 2014). Therefore, a sustained expression of PERK in trachea may induce apoptosis,

thus leading to a dysfunctional airway system. Usually larvae are burrowed in the medium, but they leave it in response to oxygen deprivation. The percentage of larvae outside the medium correlates with the response towards hypoxia (Roeder et al. 2009). This also can well explain that first instar larvae climbed out of the medium and that they had a much stronger susceptibility to hypoxia (Wingrove et al. 1999; Vermehren et al. 2010). This observation would mean that the cell death induction occurs extremely early during development, thus leading to this lethal phenotype that is obviously dependent on a hypoxia-like response that results from dysfunction of the respiratory organ.

In addition, targeting expression to the terminal tracheal cells showed that XBP1s and PERK inhibit the growth of terminal trachea branches, whereas IRE1 and ATF6 overexpressing larvae were not affected structurally. The structural changes may be the cause of the enhanced susceptibility towards hypoxia that was observed in the corresponding animals, eventually also for the response seen for those animals experiencing UPR activation in the entire airway system. My observation that PERK-overexpressing larvae showed a trend towards staying out of the medium even in the absence of hypoxia implied that these animals have a massively decreased ability of utilize oxygen, which may directly result from structural impairments in the terminal tracheal cells. These terminal tracheal cells are the structures, where the actual gas exchange takes place, thus they take the central position for this highly important physiological task.

The impact of activation of UPR branches on the structure of the *Drosophila* gut was not as strong as seen in the airway system. The morphology of the intestine did not change obviously with the exception of an increasing cell/nucleus ratio.

The UPR plays a central role in the normal development and function of cells specialized in secretion, therefore highly secretory cells are extremely dependent upon an unfolded protein response in pursuit of their normal physiologic functions

(Hetz et al. 2012). The intestine has one of the most relevant secretory cells in metazoans. Especially intestinal epithelial cells, including Paneth and goblet cells, strongly depend on a well-functioning UPR due to their high demand on secretory proteins (Zhao et al. 2010). Unresolved ER stress has been found in inflamed intestinal epithelial cells and genome wide association studies identified UPR-associated genes as potential risk factors for inflammatory bowel disease (IBD) (Kaser et al. 2008). Despite the physiological divergence between vertebrates and insects, the intestine of *Drosophila melanogaster* is well suited for the research of intestinal stem cell physiology during aging, stress and infection because of the high degree of conservation between *Drosophila* and mammals with respect to the signaling pathways that control intestinal development, regeneration and disease. A fundamental question is how to find the balance between cytoprotective functions and apoptosis promoting functions of the UPR and how this balance can influence inflammation. We used the dextran-induced model of colitis to evaluate the effects of UPR components activation during acute intestinal inflammation (Dieleman et al. 1998). Life span assay showed IRE1 overexpression in the intestine can extend the lifespan of male flies fed with dextran sulfate sodium (DSS) to induce colitis, the average lifespan of female flies showed no significant extension but maximum lifespan increased by 6 days. Numerous studies demonstrated that activation of the UPR aims to restore homeostasis from tissue damage, as observed in inflammatory bowel disease (Senft et al. 2015). In IBD, activation of the IRE1-XBP1 axis has been shown to function protectively. Deletion of IRE1 gene in the mouse intestinal epithelium leads to an increased susceptibility to DSS induced colitis (Bertolotti et al 2001; Jamora et al. 1996). Thus, the experimental situation in *Drosophila* is one that should lead to a cell protection and therewith to an increased resistance towards strong intestinal stressors such as DSS. DSS treatment leads to a dramatic stressing of epithelial cells that, in turn, leads to activation of the stem cell activity in the intestine, thus replenishing the pool of functional enterocytes.

4.2 Specific-expression of key UPR components activate the innate immune system

The response of *Drosophila melanogaster* to various infections relies on a set of defense systems, including epithelia as first physical and immunological barriers. Antimicrobial peptides (AMPs) are of prime importance as effectors of the immune system. They are innate host defense molecules that are effective on bacteria, fungi and parasites, even enveloped viruses can be destroyed (Zasloff et al. 2002). Previous studies have demonstrated that AMP expression increases in response to infection but it can also increase in response to ER-stress (Park et al. 2011; Kaser et al. 2010).

Taking into account that AMPs are synthesized constitutively in specific tissues, particularly in barrier epithelia and the fat body, flies that specifically express key inducers of UPR components in airway and fat body were constructed. As already mentioned, UPR signaling pathway comprises three major branches, therefore this study can unravel which component of the UPR signaling plays a key role in UPR-induced AMP expression.

The result of real-time quantitative PCR analysis showed that the relative expression of *drosomycin* was upregulated dramatically by XBP1s overexpression in the tracheal system and in the fat body, whereas IRE1 and Atf6 had no effects. In *Drosophila*, eight AMP genes have been classified in three groups depending on their main microbial targets, including *Drosomycin*, *Defensin*, *Drosocin*, *Cecropins*, *Attacins*, *Diptericins*, etc. (Hoffmann et al. 2003; Rabel et al. 2004). I also selected several other AMP genes to examine if the relative expression level could be affected by XBP1s. Analysis of qRT-PCR showed no change of *diptericin* and *attacin* expression levels in the flies' airway. These results suggest that *xbp1s* specifically regulates *drosomycin* and no other AMPs, which implies that *drosomycin* takes a very special position among all *Drosophila* AMPs.

To identify naturally occurring signals that induce UPR and therewith an immune

response in these tissues, I focused on chronic hypoxia, which is known to lead to the production of reactive oxygen species (ROS), which are produced in several organelles, including the ER. Hypoxia has long been known to cause ER stress, possibly due to the elevated levels of ROS in hypoxic cells (Tu et al. 2002). Hypoxia is also considered to perturb ER homeostasis through an increase in unfolded protein within the ER lumen, causing dissociation of GRP78 from all three major UPR sensors (Kim et al. 2009). I could show that hypoxia treatment indeed activates ER stress, as the level of xbp1s increased compared to the control that was not treated accordingly. Thus, hypoxia appears to be a natural stressor that induces an immune response in the airways mediated by a specific activation of the unfolded protein response.

4.3 Specific-expression of key UPR components regulates insulin-like peptide release

Unlike type 2 diabetes, which is caused by the loss of insulin sensitivity, type 1 diabetes (T1D) is manifested by the absolute deficiency of insulin secretion due to the loss of insulin-producing cells by autoimmune responses against cell self-antigens (Wen et al. 2008). Endoplasmic reticulum (ER) stress plays an essential role in insulin producing-cells since they are equipped with highly developed endoplasmic reticulum (ER) to fulfill the requirement of secreting a large amount of insulin (Hertog et al. 2010; Lee et al. 2014). Based on this very peculiar demand to produce these extremely high amounts of insulin, ER-stress is commonly seen in IPCs and a well-functional UPR is essential in these cells. Thus, UPR is required to resolve the ER-stress in exactly these cells (Brozzi et al. 2016). While UPR can't restore the ER homeostasis, severe or long-term ER stress would further exacerbate β -cell death (Eizirik et al. 2008). Moreover, in mammals, the insulin transduction pathway increases the uptake of glucose into muscle, fat and liver cells and reduces the synthesis of glucose in the liver and hence is involved in maintaining glucose homeostasis.

In this part of the thesis, *Drosophila* was used as a model organism to study the interaction of insulin signaling and UPR signaling pathways, at the basis of insulin producing cells (IPCs). Brain located cells that secrete insulin-like peptides (DILP) are equivalent to the β cells in mammals (Özcan et al. 2006). In addition to understanding impaired insulin secretion and beta cell failure, this model of type 1 diabetes mellitus that I developed in the fruit fly may be very helpful for future research strategies and finally to find new ways to develop alternative therapeutic strategies.

In response to ectopic activation of the UPR, phenotypic changes of IPCs were observed in the adult brain, decreased IPCs cluster sizes in XBP1s and PERK overexpressing flies compare to the control, this reduction was more significant in PERK flies. For these structural reductions seen in XBP1 flies, an argument given by Allagnat and colleagues may answer it. The authors suggested that sustained production of spliced XBP1 (XBP1s) induces beta cell dysfunction by decreasing insulin gene expression, leading finally to apoptosis (Allagnat et al. 2010.). This may also explain the phenotype seen in PERK flies, since persistent PERK expression has been described as a signaling pathway that could independently trigger apoptosis (Demay et al. 2014). Why *xbp1s* and *perk* overexpression lead to these effects, and overexpression of *Atf6* and *Ire1* not, is not known.

The DILP2 content measurement assay showed that the level of circulating and total Dilp2 proteins was down-regulated in XBP1s overexpression flies, both in females and males. In consideration of the insulin/IGF signaling mechanism, decreased circulating insulin level should be associated with hypoglycemia, with all its consequences, such as influences on life span (Fridell et al. 2009). Following this, glucose tolerance assays testified the reduced capacity of glucose degradation in XBP1s flies. Previous studies indicated usually a reduced systemic insulin signaling is accompanied by a mild hyperglycemia and extended life span (Taguchi et al. 2008). Consistent with the expectation, I showed an increased longevity of XBP1s overexpressing adults and an attenuated ability of glucose clearance. In addition, ablation of IPCs significantly

impairs the ability of those flies to clear the glucose load and renders those flies' glucose intolerant (Rulifson et al. 2002; Kim et al. 2004), which further shows that the ectopic overexpression of xbp1s in IPCs is indeed a very useful Type 1 diabetes model.

Conversely, studies of PERK overexpression flies, a markedly down-regulation of total insulin level was detected compared to the normal flies, but circulating insulin was at normal levels, which is currently hard to explain. There was also no significant reduced ability of glucose clearance, further showing that release properties of IPCs were not changed substantially.

There was a developmental delay and smaller body sizes were observed only in PERK-overexpression animals. A growing body of studies showed that the UPR network impacts early differentiation stages before acquiring a specialized secretory phenotype (Hetz et al. 2010; Rutkowski et al. 2010). Accumulating evidence based on the genetic manipulation of key UPR components in mice revealed that the UPR pathway has an important role in maintaining protein homeostasis during embryonic development and in adult tissues (Cornejo et al. 2013). Therefore, the studies reported here would seem to indicate among the several key UPR components, XBP1s and PERK highly impact the development of these cells in early stages. Early studies have demonstrated that ablation of IPCs or interference with DILPs diminished growth showing smaller body sizes (Ikeya et al. 2002; Teleman et al. 2010). In addition, PERK/ATF4 also activated the JNK pathway through Rac1 and Slpr activation in apoptotic cells, leading to the expression of Dilp8. This insulin-like peptide is also related to developmental delays (Demay et al. 2014).

Genetic studies have suggested that ORMDL (orosomucoid 1-like protein) is a risk factor for a number of inflammatory conditions including asthma (Moffatt et al. 2007), primary biliary cirrhosis (Hirschfield et al. 2009), Type 1 diabetes mellitus (Barrett et al. 2009), and various others. The functions of the ORMDL proteins are currently unknown, but studies suggested that ORMDL3 is involved in ER-mediated Ca²⁺

homeostasis (Cantero-Recasens et al. 2009; McGovern et al. 2010). Disruptions to ER Ca^{2+} concentrations can cause protein misfolding, and accumulation of these unfolded proteins can lead to ER stress (Hotamisligil et al. 2010). It can also activate the ATF6 pathway as one of the branches of UPR signaling pathway (Miller et al. 2012). Overexpression of ORMDL in IPCs of the adult brain to investigate the impact in insulin producing. The circulating and total DILP2 content of ORMDL overexpression flies was not different from controls, both in females and males, ORMDL flies possess a good capacity of glucose clearance after oral feeding of glucose compared to control flies although the glucose levels are slightly higher. All these results suggest that ORMDL overexpression has a slight effect towards type 1 like phenotypes although the effects are not statistically significantly different from the matching controls.

Summary

In eukaryotic cells, endoplasmic reticulum (ER) stress occurs when misfolded proteins accumulate in the lumen of the ER. It is observed in many tissues in human diseases including cancer, diabetes, obesity, and neurodegeneration. The unfolded protein response (UPR) is an intracellular signaling system, which is activated in response to ER-Stress to restore homeostasis. The conservation of the UPR pathway, together with the availability of numerous genetic tools make *Drosophila melanogaster* a powerful model for studying the role of ER-stress and the physiological role of the UPR. The UPR comprises of three signaling branches mediated by three ER transmembrane proteins: inositol-requiring protein 1 (IRE1), protein kinase RNA-like ER kinase (PERK), activating transcription factor 6 (ATF6).

Using *Drosophila melanogaster* as a model, I studied the role of the three branches of the unfolded protein response by their ectopic activation. For this, I enhanced the expression of IRE1, XBP1s, PERK, or ATF6, respectively. Overexpression of XBP1s and of PERK in the fat body induced striking structural changes in cell shapes and nucleus sizes, while overexpression of IRE1 and ATF6 had only minor effects. Activation of XBP1s and of PERK in the trachea was lethal. Moreover, it could be found that ectopic activation of XBP1s and of PERK, both in trachea and in the fat body induced expression of the antimicrobial peptide genes *drosomycin*. Thus, a strong activation of the innate immune response might be part of the UPR in these tissues.

Insulin-like peptides (ILPs) act as key effectors regulating lifespan, metabolism, growth, development, reproduction, stress resistance and feeding behaviors in multicellular organisms. In this part, the focus was on the role of ectopic activation of the UPR in regulation of DILPs in Insulin producing cells (IPCs). In these experiments, obvious phenotypic changes of IPCs were observed in the adult brain, comprising of a decreased size of the IPC cluster in the pars intercerebralis, in animals experiencing specific XBP1s and PERK overexpression in the IPC. This reduction was more

pronounced in PERK overexpressing flies. The level of circulating DILP2 in XBP1s overexpressing flies was decreased, both in females and males, exactly as the level of total DILP2. The insulin level was associated with hyperglycemia, attenuated ability of glucose clearance, and an extension of life span. Conversely, in PERK-overexpressing flies, a marked down-regulation of total insulin level was detected compared to the control flies, but a normal level of circulating insulin and an unimpaired ability of glucose clearance was seen. In addition, a developmental delay and smaller body sizes were observed only in PERK-overexpressing flies. ORMDL3 is a protein associated with Type 1 diabetes, however the circulating and total DILP2 content in ORMDL overexpressing flies has no difference compare to controls. ORMDL flies possess a good capacity of glucose clearance after oral feeding of glucose, compared to control flies although the glucose levels were slightly higher. All these results suggest that ORMDL overexpression has a slight effect but the ectopic overexpression of XBP1s in IPCs is indeed a very useful type 1 diabetes model.

Zusammenfassung

In eukariotischen Zellen akkumulieren nicht korrekt gefaltete Proteine im Lumen des endoplasmatischen Reticulums (ER). Dieser ER-Stress kann in vielen humanen Geweben nachgewiesen werden und wird unter anderem mit Krebs, Diabetes, Fettleibigkeit und neurodegenerativen Krankheiten assoziiert. Durch ER-Stress wird die Unfolded Protein Response (UPR), ein phylogenetisch hochkonserviertes, intrazelluläres Signalsystem zum Erhalt der Gewebemöostase, ausgelöst. Die UPR besteht aus drei Signalkaskaden, die jeweils durch spezifische ER-Transmembranproteine reguliert werden: Inositol-Requiring Protein 1 (IRE1), Protein Kinase RNA-like ER Kinase (PERK) und Activating Transcription Factor 6 (ATF6).

Die vielfältigen genetischen Manipulationsmöglichkeiten der Taufliege *Drosophila melanogaster* erlauben es, dieses komplexe System des ER-Stresses und die damit verbundene physiologische Rolle der UPR detailliert zu untersuchen. In dieser Arbeit wurden die UPR-Signalkaskaden durch gewebespezifische ektopische Überexpression charakterisiert. Während die Überexpression von IRE1 und ATF6 im Fettkörper kaum phänotypische Veränderungen hervorrief, zeigte die Überexpression von PERK und XBP1s im gleichen Gewebe auffallende strukturelle Veränderungen, insbesondere der Zellform und der Zellkerngröße. Die Überexpression dieser beiden Gene in den Tracheen war letal. Es konnte gezeigt werden, dass die ektopische Aktivierung von PERK und XBP1s sowohl in den Tracheen, als auch im Fettkörper, zur Expression des antimikrobiellen Peptids drosomycin führt. Daraus kann geschlossen werden, dass die angeborene Immunabwehr in diesen Geweben eng mit der UPR verknüpft ist.

Insulin-Like Peptides (ILP) regulieren in multizellulären Organismen eine Vielzahl von Vorgängen wie zum Beispiel Entwicklung, Wachstum, Metabolismus, Reproduktion, Stressresistenz, Fressverhalten und die Lebensspanne. Es wurde hier der Einfluss der UPR auf die Regulation der *Drosophila* Insulin-Like Peptides (DILP) in Insulin Producing Cells (IPC) analysiert. Die Überexpression von XBP1s und insbesondere von PERK in

den IPCs adulter Taufliegen führte zu einer Reduktion des IPC Clusters im pars intercerebralis. Gleichzeitig sank das Level an zirkulierendem DILP2, als auch an absolutem DILP2, bei den XBP1s überexprimierenden Fliegen. Das verminderte Insulinlevel konnte mit einer Verminderung der Glukoseaufnahme aus der Hämolymphe und daraus resultierender Hyperglykämie assoziiert werden. Zudem zeigten diese Taufliegen eine längere Lebensspanne als die Kontrollfliegen. Im Gegensatz hierzu wurde bei einer PERK Überexpression zwar eine Verminderung des absoluten Insulins beobachtet, nicht aber eine Verminderung des zirkulierenden Insulins. Diese Fliegen zeigten zudem keine Beeinträchtigung der Glukoseaufnahme, wohl aber eine Verzögerung der Entwicklung und eine geringere Körpergröße. ORMDL3 ist ein mit Diabetes Typ 1 assoziiertes Protein. In der Taufliege zeigt eine Überexpression dieses Genes allerdings keinen Effekt auf zirkulierendes oder absolutes DILP2. Des Weiteren konnte kein Effekt auf die Glukoseaufnahmefähigkeit nach oraler Glukosegabe nachgewiesen werden. Insgesamt hat sich das XBP1s Überexpressionsmodell in den IPCs als ein wertvolles Modell in der Diabetes Typ 1 Forschung erwiesen.

Reference

- Affolter M, Montagne J, Walldorf U, Groppe J, Kloter U, LaRosa M (1994) Gehring W.J. The Drosophila SRF homolog is expressed in a subset of tracheal cells and maps within a genomic region required for tracheal development. *Development* 120:743–753.
- Allagnat F, Christulia F, Ortis F, et al (2010) Sustained production of spliced X-box binding protein 1 (XBP1) induces pancreatic beta cell dysfunction and apoptosis. *Diabetologia* 53(6): 1120-1130.
- Bai H, Kang P, Tatar M (2012) Drosophila insulin-like peptide-6 (dilp6) expression from fat body extends lifespan and represses secretion of Drosophila insulin-like peptide-2 from the. *Aging Cell* 11:978–985.
- Baker KD, Thummel CS (2007) Diabetic larvae and obese flies-emerging studies of metabolism in Drosophila. *Cell metabolism* 6:257-266.
- Barrett JC, Clayton DG, Concannon P (2009) Genome-wide association study and meta-analysis find that over 40 loci affect risk of type 1 diabetes. *Nature genetics* 41(6): 703-707.
- Bier E (2005) Drosophila, the golden bug, emerges as a tool for human genetics. *Genetics* 6(1): 9.
- Bellen HJ, Levis RW, Liao G, He Y, Carlson JW, Tsang G, Evans-Holm M, Hiesinger PR, Schulze KL, Rubin GM, Hoskins RA, Spradling AC (2004) The BDGP gene disruption project: single transposon insertions associated with 40% of Drosophila genes. *Genetics* 167:761-781.
- Bertolotti A, Zhang Y, Hendershot LM, Harding HP, Ron D (2000) Dynamic interaction of BiP and ER stress transducers in the unfolded-protein response. *Nature Cell Biology* 2:326–332.

- Bertolotti A, Wang X, Novoa I, Jungreis R, Schlessinger K, Cho JH, West AB, Ron D (2001) Increased sensitivity to dextran sodium sulfate colitis in ire1beta-deficient mice. *Journal of Clinical Investigation*, 107(5): 585.
- Bernards A, Hariharan I K (2001) Of flies and men—studying human disease in *Drosophila*. *Current opinion in genetics & development* 11(3): 274-278.
- Birse RT, Bodmer R (2011) Lipotoxicity and cardiac dysfunction in mammals and *Drosophila*. *Critical reviews in biochemistry and molecular biology* 46(5):376-385.
- Boden G, Duan X, Homko C, Molina EJ, Song W, Perez O, Cheung P, Merali S (2008) Increase in endoplasmic reticulum stress-related proteins and genes in adipose tissue of obese, insulin resistant individuals. *Diabetes* 57:2438–2444.
- Bouzigon E, Corda E, Aschard H, et al (2008) Effect of 17q21 variants and smoking exposure in early-onset asthma. *New England journal of medicine* 359(19): 1985-1994.
- Brand AH, Perrimon N (1993) Targeted gene expression as a means of altering cell fates and generating dominant phenotypes. *Development* 118:401-415.
- Broggiolo W, Stocker H, Ikeya T, Rintelen F, Fernandez R, Hafen E (2001) An evolutionarily conserved function of the *Drosophila* insulin receptor and insulin-like peptides in growth control. *Current biology* 11:213-221.
- Broughton S, Alic N, Slack C, Bass T, Ikeya T, Vinti G (2008) Reduction of DILP2 in *Drosophila* triages a metabolic phenotype from lifespan revealing redundancy and compensation among DILPs. *PLoS ONE* 3: e3721.
- Broughton SJ, Piper MD, Ikeya T, Bass TM, Jacobson J, Drieger Y (2005) Longer lifespan, altered metabolism, and stress resistance in *Drosophila* from ablation of cells making insulin like ligands. *Proceedings of the National Academy of Sciences of the United States of America* 102(8): 3105-3110.
- Brozzi F, Eizirik D L (2016) ER stress and the decline and fall of pancreatic beta cells in

- type 1 diabetes. *Uppsala journal of medical sciences* 121(2): 133-139.
- Bulet P, Stäcklin R, Menin L (2004) Anti-microbial peptides: From invertebrates to vertebrates. *Immunology Review* 184:198-169.
- Butler AE, Janson J, Bonner-Weir S (2003) β -Cell deficit and increased β -cell apoptosis in humans with type 2 diabetes. *Diabetes* 52(1): 102-110.
- Cao SS, Kaufman RJ (2014) Endoplasmic reticulum stress and oxidative stress in cell fate decision and human disease. *Antioxidants & redox signaling* 21(3): 396-413.
- Cantero-Recasens G, Fandos C, Rubio-Moscardo F (2009) The asthma-associated ORMDL3 gene product regulates endoplasmic reticulum-mediated calcium signaling and cellular stress. *Human molecular genetics* 19(1): 111-121.
- Chapman RF (1998) *The Insects Structure and Function*. Cambridge University Press
- Chen D, Ahlford A, Schnorrer F, Kalchauer I, Fellner M, Viragh E, Kiss I, Syvanen AC, Dickson BJ (2008) High-resolution, high-throughput SNP mapping in *Drosophila melanogaster*. *Nature methods* 5:323-329.
- Chen F (2016) Preparation and Immunofluorescence Staining of the Trachea in *Drosophila* Larvae and Pupae. *Bio-protocol* 6(9): e1797.
- Cnop Miriam, Nils Welsh, Jean-Christophe Jonas, Anne Jörns, Sigurd Lenzen, Decio L. Eizirik (2005) Mechanisms of Pancreatic β -Cell Death in Type 1 and Type 2 Diabetes. *Diabetes* 54: S97-S107.
- Cornejo V H, Pihán P, Vidal R L, et al (2013) Role of the unfolded protein response in organ physiology: lessons from mouse models. *IUBMB life* 65(12): 962-975.
- Cox JS, Shamu CE, and Walter P (1993). Transcriptional induction of genes encoding endoplasmic reticulum resident proteins requires a transmembrane protein kinase. *Cell* 73, 1197-1206.
- Demay Y, Perochon J, Szuplewski S, et al (2014) The PERK pathway independently triggers apoptosis and a Rac1/SIpr/JNK/Dilp8 signaling favoring tissue

- homeostasis in a chronic ER stress *Drosophila* model. *Cell death & disease* 5(10): e1452.
- Dietzl G, Chen D, Schnorrer F, Su KC, Barinova Y, Fellner M, Gasser B, Kinsey K, Oettel S, Scheiblaue S, Couto A, Marra V, Keleman K, Dickson BJ (2007) A genome-wide transgenic RNAi library for conditional gene inactivation in *Drosophila*. *Nature* 448:151-156.
- D Ron, P Walter (2007) Signal integration in the endoplasmic reticulum unfolded protein response. *Nat. Rev. Mol. Cell Biol* 8:519-529.
- Duffy JB (2002) GAL4 system in *Drosophila*: a fly geneticist's Swiss army knife. *genesis* 34(1-2): 1-15.
- Eizirik DL, L Colli M, Ortis F (2009) The role of inflammation in insulinitis and β -cell loss in type 1 diabetes. *Nat. Rev. Endocrinol* 5:219–226.
- Eizirik DL, Cnop M (2010) ER stress in pancreatic beta cells: the thin red line between adaptation and failure. *Sci Signal* 3-7.
- Eizirik DL, Miani M, Cardozo AK (2013) Signalling danger: Endoplasmic reticulum stress and the unfolded protein response in pancreatic islet inflammation. *Diabetologia* 56:234–241.
- Elliott DA, Brand AH (2008) The GAL4 system: a versatile system for the expression of genes. *Drosophila: Methods and Protocols*:79-95.
- Ferrandon D, Jung A, Cricqui M, Lemaitre B, Uttenweiler-Joseph S, á Michaut L, Reichhart JM, Hoffmann JA (1998) A drosomycin-GFP reporter transgene reveals a local immune response in *Drosophila* that is not dependent on the Toll pathway. *EMBO Journal* 17:1217-1227.
- Fridell YWC, Hoh M, Kréneisz O, et al (2009) Increased uncoupling protein (UCP) activity in *Drosophila* insulin-producing neurons attenuates insulin signaling and extends lifespan. *Aging (Albany NY)* 1(8): 699-713.

- Fonseca SG, Gromada J, Urano F (2011) Endoplasmic reticulum stress and pancreatic beta-cell death. *Trends in Endocrinology & Metabolism* 22(7): 266-274.
- Géminard C, Rulifson E J, Léopold P (2009) Remote control of insulin secretion by fat cells in *Drosophila*. *Cell metabolism* 10(3): 199-207.
- Ganz T, Lehrer B (2003) Antimicrobial peptides; in Ezekowitz RAB, Hoffmann JA (eds). *Innate Immunity. Infectious Diseases*. Totowa, Humana Press 303:287–303.
- Ghabrial AS, Krasnow MA (2006) Social interactions among epithelial cells during tracheal branching morphogenesis. *Nature* 441 (7094):746-749.
- Ghaemmaghami S, Huh WK, Bower K et al (2003) Global analysis of protein expression in yeast. *Nature* 425:37-741.
- Giannakou ME, Partridge L (2007) Role of insulin-like signalling in *Drosophila* lifespan. *Trends in biochemical sciences* 32:180-188.
- Grönke S, Partridge L (2010) The functions of insulin-like peptides in insects. In *IGFs: Local Repair and Survival Factors Throughout Life Span* 105-124.
- Guerra C, Navarro P, Valverde AM, Arribas M, Bruning J, Kozak LP, et al (2001) Brown adipose tissue-specific insulin receptor knockout shows diabetic phenotype without insulin resistance. *Journal of Clinical Investigation* 108(8): 1205.
- Guillemin K, Groppe J, Ducker K, Treisman R, Hafen E, Affolter M, Krasnow MA (1996) The pruned gene encodes the *Drosophila* serum response factor and regulates cytoplasmic outgrowth during terminal branching of the tracheal system. *Development* 122:1353–1362.
- Harding HP, Novoa I, Zhang Y, Zeng H, Wek R, Schapira M, and RonD (2000) Regulated translation initiation controls stress-induced gene expression in mammalian cells. *Cell* 6:1099–1108.
- Harrison JF (2003) *Encyclopedia of Tracheal system*. Academic Press.
- Hetz C (2012) The unfolded protein response: controlling cell fate decisions under ER

- stress and beyond. *Cell* 13:89–102.
- Hirschfield GM, Liu X, Xu C, et al (2009) Primary biliary cirrhosis associated with HLA, IL12A, and IL12RB2 variants. *New England Journal of Medicine* 360(24): 2544-2555.
- Hjelmqvist L, Tuson M, Marfany G, et al (2002) ORMDL proteins are a conserved new family of endoplasmic reticulum membrane proteins. *Genome biology* 3(6): research0027. 1.
- Hollien J, Weissman JS (2006) Decay of endoplasmic reticulum-localized mRNAs during the unfolded protein response. *Science* 313:104–107.
- Hoffmann J (2003) The immune response of *Drosophila*. *Nature*. 38:426-33.
- Hoffmann JA, Reichhart JM (2002) *Drosophila* innate immunity: an evolutionary perspective. *Nature Immunol* 3:121–126.
- Hotamisligil GS. (2010). Endoplasmic reticulum stress and the inflammatory basis of metabolic disease. *Cell* 140(6): 900-917.
- Ikeya T, Galic M, Belawat P, Nairz K, Hafen E (2002) Nutrient-dependent expression of insulin-like peptides from neuroendocrine cells in the CNS contributes to growth regulation in *Drosophila*. *Current Biology* 12(15):1293-1300.
- Inagi R, Ishimoto Y, Nangaku M (2014) Proteostasis in endoplasmic reticulum—new mechanisms in kidney disease. *Nature reviews Nephrology* 10(7): 369-378.
- Jarecki J, Johnson E, Krasnow MA (1999) Oxygen regulation of airway branching in *Drosophila* is mediated by branchless FGF. *Cell* 99 (2):211-20.
- Jamora C, Dennert G, Lee AS (1996) Inhibition of tumor progression by suppression of stress protein grp78/bip induction in fibro sarcoma b/c10me. *Proceedings of the National Academy of Sciences* 93:7690–7694.
- Janssens S, Pulendran B, Lambrecht BN (2014) Emerging functions of the unfolded protein response in immunity. *Nature immunology* 15(10): 910-919.

- Kadowaki H, Nishitoh H (2013) Signaling pathways from the endoplasmic reticulum and their roles in disease. *Genes* 4(3): 306-333.
- Kanapin A, Batalov S, Davis MJ et al (2003) Global analysis of protein expression in yeast. *Nature* 425(6959): 737.
- Korennykh AV, Egea PF, Korostelev AA et al (2009) The unfolded protein response signals through higher-order assembly of Ire1. *Nature* 457:687-693.
- Kozutsumi Y, Segal M, Normington K, Gething MJ, Sambrook J (1988) The presence of malfolded proteins in the endoplasmic reticulum signals the induction of glucose-regulated proteins. *Nature* 332:462-464.
- Lee J, Ozcan U (2014) Unfolded protein response signaling and metabolic diseases. *Journal of Biological Chemistry* 289(3): 1203-1211.
- Lemaitre B, Nicolas E, Michaut L, Reichhart JM, Hoffmann JA (1996) The dorsoventral regulatory gene cassette *spätzle/Toll/cactus* controls the potent antifungal response in *Drosophila* adults. *Cell* 86:973-83.
- Lehuen A, Diana J, Zaccane P, Cooke A (2010) Immune cell crosstalk in type 1 diabetes. *Nature Reviews Immunology* 10(7): 501-513.
- Linneweber GA, Jacobson J, Busch KE, Hudry B, Christov CP, Dormann D, Yuan M, Otani T, Knust E, de Bono M, Miguel-Aliaga I (2014) Neuronal control of metabolism through nutrient-dependent modulation of tracheal branching. *Cell* 156:69–83.
- Liu CY, Schroder M, Kaufman RJ (2000) Ligand dependent dimerization activates the stress response kinases IRE1 and PERK in the lumen of the endoplasmic reticulum. *Journal of Biological Chemistry* 275(32): 24881-24885.
- Lu M, et al (2014) Cell death. Opposing unfolded-protein response signals converge on death receptor 5 to control apoptosis. *Science* 345:98–101.
- Litman GW, Cannon JP, Dishaw LJ (2005) "Reconstructing immune phylogeny: new perspectives". *Nature Reviews. Immunology* 5 (11): 866–79.

- Marcu MG, et al (2002) Heat shock protein 90 modulates the unfolded protein response by stabilizing IRE1 α . *Journal of Biological Chemistry* 275(32): 24881-24885.
- Mathis D, Vence L, Benoist C (2001) β -Cell death during progression to diabetes. *Nature* 414:792–798.
- Miller M, Tam A B, Cho J Y, et al (2012) ORMDL3 is an inducible lung epithelial gene regulating metalloproteases, chemokines, OAS, and ATF6. *Proceedings of the National Academy of Sciences* 109(41): 16648-16653.
- McGovern DPB, Gardet A, Törkvist L, et al (2010) Genome-wide association identifies multiple ulcerative colitis susceptibility loci. *Nature genetics* 42(4): 332-337.
- Moffatt MF, Kabesch M, Liang L, et al (2007) Genetic variants regulating ORMDL3 expression contribute to the risk of childhood asthma. *Nature* 448(7152): 470.
- Moffatt MF, et al (2007) Genetic variants regulating ORMDL3 expression contribute to the risk of childhood asthma. *Nature* 448(7152):470–473.
- Moreno J A, Halliday M, Molloy C, Radford H, Verity N, Axten JM, Ortori CA, Willis AE, Fischer PM, Barrett DA, Mallucci GR (2013) "Oral Treatment Targeting the Unfolded Protein Response Prevents Neurodegeneration and Clinical Disease in Prion-Infected Mice". *Science Translational Medicine* 5 (206): 206ra138.
- Muralidharan, Sujatha, Pranoti Mandrekar (2013) "Cellular Stress Response and Innate Immune Signaling: Integrating Pathways in Host Defense and Inflammation." *Journal of Leukocyte Biology* 94.6: 1167–1184.
- Nakatsuji T, Gallo RL (2012) Antimicrobial peptides: Old molecules with new ideas. *J Invest Dermatol* 132:887–895.
- Niwa M, Sidrauski C, Kaufman RJ, Walter P (1999) A role for presenilin-1 in nuclear accumulation of Ire-1 fragments and induction of the mammalian unfolded protein response. *Cell* 99:691-702.

- Nolan CJ, Damm P, Prentki M (2011) Type 2 diabetes across generations: from pathophysiology to prevention and management. *Lancet* 378: 169–181.
- O'Byrne KJ, Dalgleish AG (2001) "Chronic immune activation and inflammation as the cause of malignancy". *British Journal of Cancer* 85 (4): 473–83.
- Osterwalder T, Yoon KS, White BH, Keshishian H (2001) A conditional tissue-specific transgene expression system using inducible GAL4. *Proceedings of the National Academy of Sciences of the United States of America* 98:12596-12601.
- Özcan U, Yilmaz E, Özcan L, et al (2006) Chemical chaperones reduce ER stress and restore glucose homeostasis in a mouse model of type 2 diabetes. *Science* 313(5790): 1137-1140.
- Ozcan U, Ozcan L, Yilmaz E, Düvel K, Sahin M, Manning BD, Hotamisligil GS (2008) Loss of the tuberous sclerosis complex tumor suppressors triggers the unfolded protein response to regulate insulin signaling and apoptosis. *Cell* 29:541–551.
- Pasupuleti M, Schmidtchen A, Malmsten M (2012) Antimicrobial peptides: Key components of the innate immune system. *Critical reviews in biotechnology* 32(2): 143-171.
- Parks AL et al (2004) Systematic generation of high-resolution deletion coverage of the *Drosophila melanogaster* genome. *Nature genetics* 36:288-292.
- Park K, et al (2011) Regulation of cathelicidin antimicrobial peptide expression by an endoplasmic reticulum (ER) stress signaling, vitamin D receptor-independent pathway. *Journal of Biological Chemistry* 286(39): 34121-34130.
- Park S, Alfa RW, Topper SM, et al (2014) A genetic strategy to measure circulating *Drosophila* insulin reveals genes regulating insulin production and secretion. *PLoS genetics* 10(8): e1004555.
- Pfaffl MW (2001) A new mathematical model for relative quantification in realtime RT–PCR. *Nucleic acids research* 29(9): e45-e45.

- Picher-Martel V, Valdmanis PN, Gould PV, et al (2016) From animal models to human disease: a genetic approach for personalized medicine in ALS. *Acta neuropathologica communications* 4(1): 70.
- Potter CJ, Tasic B, Russler EV, Liang L, Luo L (2010) The Q system: a repressible binary system for transgene expression, lineage tracing, and mosaic analysis. *Cell* 141:536–548.
- Prentki M, Nolan CJ (2006) Islet beta cell failure in type 2 diabetes. *Journal of Clinical Investigation* 116(7): 1802.
- Rabel D, Charlet M, Ehret-Sabatier L, Cavicchioli L, Cudic M, Otvos L, Bulet P (2004) Primary structure and in vitro antibacterial properties of the *Drosophila melanogaster* attacin C Prodomain. *Journal of Biological Chemistry*. 279:14853–14859.
- Ramirez-Alvarado M, Kelly JW, Dobson CM (2010) *Protein Misfolding Diseases: Current and emerging principles and therapies*. John Wiley & Sons.
- Reiter LT, Potocki L, Chien S, Gribskov M, Bier E (2001) A systematic analysis of human disease-associated gene sequences in *Drosophila melanogaster*. *Genome research* 11 (6):1114-25.
- Lloyd TE, Taylor JP (2010) Flightless flies: *Drosophila* models of neuromuscular disease. *Annals of the New York Academy of Sciences* 1184(1).
- Rincon-Limas DE, Jensen K, Fernandez-Funez P (2012) *Drosophila* models of proteinopathies: the little fly that could. *Current pharmaceutical design* 18(8): 1108-1122.
- Rulifson EJ, Kim SK, Nusse R (2002) Ablation of insulin-producing neurons in flies: growth and diabetic phenotypes. *Science* 296(5570):1118-1120.
- Ruiz OE, Nikolova LS, Metzstein MM (2012) *Drosophila* Zpr1 (Zinc Finger Protein 1) Is Required Downstream of Both EGFR And FGFR Signaling in Tracheal Subcellular

- Lumen Formation. PLoS ONE 7 (9): e45649 ().
- Rutkowski DT, Arnold SM, Miller CN, et al (2006) Adaptation to ER stress is mediated by differential stabilities of pro-survival and pro-apoptotic mRNAs and proteins. PLoS biology 4(11): e374.
- Rutkowski DT, Kaufman RJ (2007) That which does not kill me makes me stronger: adapting to chronic ER stress. Trends in biochemical sciences 32(10): 469-476.
- Rutkowski DT, Hegde RS (2010) Regulation of basal cellular physiology by the homeostatic unfolded protein response. The Journal of cell biology 189(5): 783-794.
- Sato-Miyata Y, Muramatsu K, Funakoshi M, et al (2014) Overexpression of dilp2 causes nutrient-dependent semi-lethality in Drosophila. Frontiers in physiology 5.
- Saucedo LJ, Gao X, Chiarelli DA, Li L, Pan D, Edgar BA (2003) Rheb promotes cell growth as a component of the insulin/TOR signaling network. Nature cell biology 5:566-571.
- Selsted ME, Ouellette AJ (2005) Mammalian defensins in the antimicrobial immune response. Nature Immunol 6:551–557.
- Sena LA, Chandel NS (2012) Physiological roles of mitochondrial reactive oxygen species. Molecular cell 48(2): 158-167.
- Sen-Lin L, Lee T (2006) Genetic mosaic with dual binary transcriptional systems in Drosophila. Nature neuroscience 9(5): 703.
- Shaw JE, Sicree RA, Zimmet PZ (2010) Global estimates of the prevalence of diabetes for 2010 and 2030. Diabetes research and clinical practice 87(1): 4-14.
- Suster ML, Seugnet L, Bate M, Sokolowski MB (2004) Refining GAL4-driven transgene expression in Drosophila with a GAL80 enhancer-trap. Genesis 39:240-245.
- Taguchi A, White MF (2008) Insulin-like signaling, nutrient homeostasis, and life span. Annu. Rev. Physiol 70: 191-212.

- Thomas Osterwalder, Kenneth S, Yoon, Benjamin H, White, Haig Keshishian (2001) A conditional tissue-specific transgene expression system using inducible GAL4. PNAS 98: 12596-12601.
- Tirasophon W, Welihinda AA, Kaufman RJ (1998) A stress response pathway from the endoplasmic reticulum to the nucleus requires a novel bifunctional protein kinase/endoribonuclease (Ire-1p) in mammalian cells. Genes 12:1812-24.
- Todd DJ, Lee AH, Glimcher LH (2008) The endoplasmic reticulum stress response in immunity and autoimmunity. Immunology 8(9):663–674.
- Tossi A, Sandri L (2002) Molecular diversity in gene-encoded, cationic antimicrobiapolypeptides. Current Pharmaceutical Design 8:743–761.
- Thibault ST et al (2004) A complementary transposon tool kit for *Drosophila melanogaster* using P and piggyBac. Nature genetics 36:283-287.
- Tzou P, Ohresser S, Ferrandon D, et al (2000) Tissue-specific inducible expression of antimicrobial peptide genes in *Drosophila* surface epithelia. Immunity 13(5): 737-748.
- Wang JW, Beck ES, McCabe BD (2012) A modular toolset for recombination transgenesis and neurogenetic analysis of *Drosophila*. PloS one 7(7): e42102.
- Wen L, Ley RE, Volchkov PV, et al (2008) Innate immunity and intestinal microbiota in the development of Type 1 diabetes. Nature 455(7216): 1109.
- WD Hertog, M. Maris, G. B. Ferreira, et al (2010) “Novel insights into the global proteome responses of insulin-producing INS-1E cells to different degrees of endoplasmic reticulum stress,” Journal of Proteome Research 9: 5142–5152.
- Yamamoto K, Sato T, Matsui T et al (2007) Transcriptional induction of mammalian ER quality control proteins are mediated by single, or combined action of ATF6alpha and xbp1. Cell 13:365-376.
- Ye J, et al (2000) ER stress induces cleavage of membrane bound ATF6 by the same

proteases that process SREBPs. *Cell* 6:1355–1364.

Yoshida H, Matsui T, Yamamoto A, Okada T, Mori K (2001) XBP1 mRNA is induced by ATF6 and spliced by IRE1 in response to ER stress to produce a highly active transcription factor. *Cell* 107:881–891.

Zasloff M (2002) Antimicrobial peptides of multicellular organisms. *Nature* 415(6870): 389-395.

Zhao L, Ackerman SL (2006) Endoplasmic reticulum stress in health and disease. *Current opinion in cell biology* 18(4): 444-452.

Zeng L, Zampetaki A, Margariti A, et al (2009) Sustained activation of XBP1 splicing leads to endothelial apoptosis and atherosclerosis development in response to disturbed flow. *Proceedings of the National Academy of Sciences* 106(20): 8326-8331.

Appendix

1. Sequence of *pBID-UASC (9394)* and insert site.

Target gene insert (5727-5746) (showed in gray color)

```

1 CTAAATTGTA AGCGTTAATA TTTTGTTAAA ATTCGCGTTA AATTTTTGTT AAATCAGCTC
61 ATTTTTTAAC CAATAGGCCG AAATCGGCAA AATCCCTTAT AAATCAAAAG AATAGACCGA
121 GATAGGGTTG AGTGTGTTC CAGTTTGGAA CAAGAGTCCA CTATTAAAGA ACGTGGACTC
181 CAACGTCAA GGGCGAAAAA CCGTCTATCA GGGCGATGGC CCACTACGTG AACCATCACC
241 CTAATCAAGT TTTTGGGGT CGAGGTGCCG TAAAGCACTA AATCGGAACC CTAAGGGAG
301 CCCCCGATTT AGAGCTTGAC GGGGAAAGCC GGCGAACGTG GCGAGAAAGG AAGGGAAGAA
361 AGCGAAAGGA GCGGGCGCTA GGGCGCTGGC AAGTGTAGCG GTCACGCTGC GCGTAACCAC
421 CACACCCGCC GCGCTTAATG CGCCGCTACA GGGCGCTCC CATTGCCAT TCAGGCTGCG
481 CAACTGTTGG GAAGGGCGAT CGGTGCGGGC CTCTTCGCTA TTACGCCAGC TGGCGAAAGG
541 GGGATGTGCT GCAAGGCGAT TAAGTTGGGT AACGCCAGGG TTTTCCAGT CACGACGTTG
601 TAAAACGACG GCCAGTGAAT TGTAATACGA CTCACTATAG GGCGAATTGG GTACGTACCG
661 GGCCCTAGT ATGTATGTAA GTTAATAAAA CCCATTTTTG CGGAAAGTAG ATAAAAAAA
721 CTTTTTTTTT TTTTACTGCA CTGGATATCA TTGAACTTAT CTGATCAGTT TAAATTTAC
781 TTCGATCCAA GGGTATTTGA TGTACCAGGT TCTTTCGATT ACCTCTCACT CAAAATGACA
841 TTCCAACCAA AGTCAGCGCT GTTTGCCTCC TTCTCTGTCC ACAGAAATAT CGCCGTCTCT
901 TTCGCCGCTG CGTCCGCTAT CTCTTTCGCC ACCGTTTGTG GCGTTACGTA GCGTCAATGT
961 CCGCCTTCAG TTGCATTTTG TCAGCGGTTT CGTGACGAAG CTCCAAGCGG TTTACGCCAT
1021 CAATTAACA CAAAGTGCTG TGCCAAAACCT CCTCTCGCTT CTTATTTTTG TTTGTTTTTT
1081 GAGTGATTGG GGTGGTGATT GGTTTTGGGT GGGTAAGCAG GGGAAAGTGT GAAAAATCCC
1141 GGCAATGGGC CAAGAGGATC AGGAGCTATT AATTCGCGGA GGCAGCAAAC ACCCATCTGC
1201 CGAGCATCTG ACAAATGTGA GTAGTACATG TGCATACATC TTAAGTTCAC TTGATCTATA
1261 GAACTGCGA TTGCAACATC AAATTGTCTG CGGCGTGAGA ACTGCGACCC AAAAAATCC
1321 CAAACCGCAA TTGCACAAAC AAATAGTGAC ACGAAACAGA TTATTCTGGT AGCTGTCTC
1381 GCTATATAAG ACAATTTTTG AGATCATATC ATGATCAAGA CATCTAAAGG CATTCATTTT
1441 CGACTATATT CTTTTTACA AAAAAATAA CAACCAGATA TTTAAGCTG ATCCTAGATG
1501 CACAAAAAAT AAATAAAAGT ATAAACCTAC TTCGTAGGAT ACTTCGGGGT ACTTTTTGTT
1561 CGGGGTTAGA TGAGCATAAC GCTTGTAGTT GATATTTGAG ATCCCCTATC ATTGCAGGGT
1621 GACAGCGGAG CGGCTTCGA GAGCTGCATT AACCAGGGCT TCGGGCAGGC CAAAAACTAC
1681 GGCACGCTCC GGCCACCCAG TCCGCCGGAG GACTCCGTT CAGGGAGCGG CCAACTAGCC
1741 GAGAACCTCA CCTATGCCTG GCACAATATG GACATCTTTG GGGCGGTCAA TCAGCCGGGC
1801 TCCGGATGGC GGCAGCTGGT CAACCGGACA CGCGGACTAT TCTGCAACGA GCGACACATA
1861 CCGGCGCCCA GGAACATTT GCTCAAGAAC GGTGAGTTTC TATTCGCACT CGGCTGATCT
1921 GTGTGAAATC TTAATAAAGG GTCCAATTAC CAATTTGAAA CTCAGTTTGC GGCCTGGCCT
1981 ATCCGGGCGA ACTTTTGGCC GTGATGGGCA GTTCCGGTGC CGGAAAGACG ACCCTGCTGA
2041 ATGCCCTTGC CTTTCGATCG CCGCAGGGCA TCCAAGTATC GCCATCCGGG ATGCGACTGC
2101 TCAATGGCCA ACCTGTGGAC GCCAAGGAGA TGCAGGCCAG GTGCGCCTAT GTCCAGCAGG
2161 ATGACCTCTT TATCGGCTCC CTAACGGCCA GGGAACACCT GATTTTCCAG GCCATGGTGC

```

2221 GGATGCCACG ACATCTGACC TATCGGCAGC GAGTGGCCCG CGTGGATCAG GTGATCCAGG
 2281 AGCTTTCGCT CAGCAAATGT CAGCACACGA TCATCGGTGT GCCCAGCAGG GTGAAAGGTC
 2341 TGTCCGGCGG AGAAAGGAAG CGTCTGGCAT TCGCCTCCGA GGCCTAACC GATCCGCCGC
 2401 TTCTGATCTG CGATGAGCCC ACCTCCGGAC TGGACTCATT TACCGCCAC AGCGTCGTCC
 2461 AGGTGCTGAA GAAGCTGTCTG CAGAAGGGCA AGACCGTCAT CCTGACCATT CATCAGCCGT
 2521 CTTCCGAGCT GTTTGAGCTC TTTGACAAGA TCCTTCTGAT GGCCGAGGGC AGGGTAGCTT
 2581 TCTTGGGCAC TCCCAGCGAA GCCGTCGACT TCTTTTCCTA GTGAGTTCGA TGTGTTTATT
 2641 AAGGGTATCT AGCATTACAT TACATCTCAA CTCCTATCCA GCGTGGGTGC CCAGTGTCTT
 2701 ACCAACTACA ATCCGGCGGA CTTTTACGTA CAGGTGTTGG CCGTTGTGCC CGGACGGGAG
 2761 ATCGAGTCCC GTGATCGGAT CGCCAAGATA TCGCACAATT TTGCTATTAG CAAAGTAGCC
 2821 CGGGATATGG AGCAGTTGTT GGCCACCAAA AATTTGGAGA AGCCACTGGA GCAGCCGGAG
 2881 AATGGGTACA CCTACAAGGC CACCTGGTTC ATGCAGTTCC GGGCGGTCCT GTGGCGATCC
 2941 TGGCTGTCTG TGCTCAAGGA ACCACTCCTC GTAAAAGTGC GACTTATTCA GACAACGGTG
 3001 AGTGGTTCCA GTGGAAACAA ATGATATAAC GCTTACAATT CTGGAAACA AATTCGCTAG
 3061 ATTTTAGTTA GAATTGCCTG ATTCCACACC CTCTTAGTT TTTTCAATG AGATGTATAG
 3121 TTTATAGTTT TGCAGAAAAT AAATAAATTT CATTAACTC GCGAACATGT TGAAGATATG
 3181 AATATTAATG AGATGCGAGT AACATTTTAA TTTGCAGATG GTTGCCATCT TGATTGGCCT
 3241 CATCTTTTGG GCCAACAAAC TCACGCAAGT GGGCGTGATG AATATCAACG GAGCCATCTT
 3301 CCTCTTCTG ACCAACATGA CCTTTCAAAA CGTCTTTGCC ACGATAAATG TAAGTCTTGT
 3361 TTAGAATACA TTTGCATATT AATAATTTAC TAACCTTCTA ATGAATCGAT TCGATTTAGG
 3421 TGTTACCTC AGAGCTGCCA GTTTTTATGA GGGAGGCCCG AAGTCGACTT TATCGCTGTG
 3481 ACACATACTT TCTGGGCAAA ACGATTGCCG AATTACCGCT TTTTCTCACA GTGCCACTGG
 3541 TCTTACGGC GATTGCCTAT CCGATGATCG GACTGCGGGC CGGAGTGCTG CACTTCTTCA
 3601 ACTGCCTGGC GCTGGTCACT CTGGTGGCCA ATGTGTCAAC GTCCTTCGGA TATCTAATAT
 3661 CCTGCGCCAG CTCCTCGACC TCGATGGCGC TGCTGTGGG TCCGCCGGTT ATCATACCAT
 3721 TCCTGCTCTT TGGCGGCTTC TTCTTGAAC CGGGCTCGGT GCCAGTATAC CTCAAATGGT
 3781 TGTCGTACCT CTCATGGTTC CGTTACGCCA ACGAGGGTCT GCTGATTAAC CAATGGGCGG
 3841 ACGTGGAGCC GGGCGAAATT AGCTGCACAT CGTCGAACAC CACGTGCCCC AGTTCGGGCA
 3901 AGGTCATCCT GGAGACGCTT AACTTCTCCG CCGCCGATCT GCCGCTGGAC TACGTGGGTC
 3961 TGGCCATTCT CATCGTGAGC TTCCGGGTGC TCGCATATCT GGCTTAAGA CTTCGGGCCC
 4021 GACGCAAGGA GTAGCCGACA TATATCCGAA ATAACCTGCTT GTTTTTTTTT TTTACCATTA
 4081 TTACCATCGT GTTACTGTT TATTGCCCCC TCAAAAAGCT AATGTAATTA TATTTGTGCC
 4141 AATAAAAACA AGATATGACC TATAGAATAC AAGTATTTCC CCTTCGAACA TCCCCACAAG
 4201 TAGACTTTGG ATTTGTCTTC TAACCAAAAG ACTTACACAC CTGCATACCT TACATCAAAA
 4261 ACTCGTTTAT CGCTACATAA AACACCGGGA TATATTTTTT ATATACATAC TTTTCAAATC
 4321 GCGCGCCCTC TTCATAATTC ACCTCCACCA CACCACGTTT CGTAGTTGCT CTTTCGCTGT
 4381 CTCCCACCCG CTCTCCGCAA CACATTCACC TTTTGTTCGA CGACCTTGGG GCGACTGTCC
 4441 TTAGTTCCGC GCGATTCCGT TCGCTCAAAT GGTTCCGAGT GGTTCAATTC GTCTCAATAG
 4501 AAATTAGTAA TAAATATTTG TATGTACAAT TTATTTGCTC CAATATATTT GTATATATTT
 4561 CCCTCACAGC TATATTTATT CTAATTTAAT ATTATGACTT TTTAAGGTAA TTTTTGTGA
 4621 CCTGTTCCGA GTGATTAGCG TTACAATTTG AACTGAAAGT GACATCCAGT GTTTGTTCTT
 4681 TGTGTAGATG CATCTCAAAA AAATGGTGGG CATAATAGTG TTGTTTATAT ATATCAAAAA
 4741 TAACAATAT AATAATAAGA ATACATTTAA TTAGAAAAT GCTTGGATTT CACTGGAAT
 4801 AGGCTAGCAT AACTTCGTAT AATGTATGCT ATACGAAGTT ATGCTAGCGG ATCCTGGCCA

4861 CGTAATAAGT GTGCGTTGAA TTTATTCGCA AAAACATTGC ATATTTTCGG CAAAGTAAAA
 4921 TTTTGTGCA TACCTTATCA AAAAATAAGT GCTGCATACT TTTTAGAGAA ACCAAATAAT
 4981 TTTTATTGC ATACCCGTTT TTAATAAAAT ACATTGCATA CCCTCTTTTA ATAAAAATA
 5041 TTGCATACTT TGACGAAACA AATTTTCGTT GCATACCCAA TAAAAGATTA TTATATTGCA
 5101 TACCCGTTTT TAATAAAATA CATTGCATAC CCTCTTTTAA TAAAAAATAT TGCATACGTT
 5161 GACGAAACAA ATTTTCGTTG CATACCCAAT AAAAGATTAT TATATTGCAT ACCTTTTCTT
 5221 GCCATACCAT TTAGCCGATC AATTGTGCTC GGCAACAGTA TATTTGTGGT GTGCCAACCA
 5281 ACAACAGATC CAAGCTGGCC GCGGCTCGAT CCGCTTGCAT GCCTGCAGGT CGGAGTACTG
 5341 TCCTCCGAGC GGAGTACTGT CCTCCGAGCG GAGTACTGTC CTCCGAGCGG AGTACTGTCC
 5401 TCCGAGCGGA GACTGTCTCT CCGAGCGGAA GCTTGCATGC CTGCAGGTCG GAGTACTGTC
 5461 CTCCGAGCGG AGTACTGTCC TCCGAGCGGA GACTGTCTCT CCGAGCGGAG TACTGTCTCT
 5521 CGAGCGGAGT ACTGTCTCTC GAGCGGAGAC TCTAGCGAGC TCGCCCGGGG ATCGAGCGCA
 5581 GCGGTATAAA AGGGCGCGGG GTGGCTGAGA GCATCAGTTG TGAATGAATG TTCGAGCCGA
 5641 GCAGACGTGC CGTGCCTTC GTTAAATATCC TTTGAATAAG CCAACTTTGA ATCACAAGAC
 5701 GCATACCAA CGAATTCGCA GATCTGCGGC CGCGGCTCGA GGGTACCTCT AGAGGATCTT
 5761 TGTGAAGGAA CCTTACTTCT GTGGTGTGAC ATAATTGGAC AAACCTA CAGAGATTTA
 5821 AAGCTCTAAG GTAAATATAA AATTTTTAAG TGTATAATGT GTTAAACTAC TGATTCTAAT
 5881 TGTTTGTGTA TTTTAGATTG CAACCTATGG AACTGATGAA TGGGAGCAGT GGTGGAATGC
 5941 CTTAATGAG GAAAACCTGT TTTGCTCAGA AGAAATGCCA TCTAGTGATG ATGAGGCTAC
 6001 TGCTGACTCT CAACATTCTA CTCCTCCAAA AAAGAAGAGA AAGGTAGAAG ACCCCAAGGA
 6061 CTTTCCTTCA GAATTGCTAA GTTTTTGAG TCATGCTGTG TTTAGTAATA GAACTCTTGC
 6121 TTGCTTTGCT ATTTACACCA CAAAGGAAAA AGCTGCACTG CTATACAAGA AAATTATGGA
 6181 AAAATATTG ATGTATAGTG CCTTGACTAG AGATCATAAT CAGCCATACC ACATTTGTAG
 6241 AGGTTTTACT TGCTTAAAA AACCTCCCAC ACCTCCCCCT GAACCTGAAA CATAAAATGA
 6301 ATGCAATTGT TGTGTTAAC TTGTTTATTG CAGCTTATAA TGGTTACAAA TAAAGCAATA
 6361 GCATCACAAA TTTACAAAAT AAAGCATTTT TTTCACTGCA TTCTAGTTGT GGTGTGCCA
 6421 AACTCATCAA TGTATCTTAT CATGTCTGGA TCTTGCCAC GTAATAAGTG TCGGTTGAAT
 6481 TTATTCGCAA AAACATTGCA TATTTTCGGC AAAGTAAAAA TTTGTTGCAT ACCTTATCAA
 6541 AAAATAAGTG CTGCATACTT TTTAGAGAAA CCAAATAATT TTTTATTGCA TACCCGTTTT
 6601 TAATAAAATA CATTGCATAC CCTCTTTTAA TAAAAAATAT TGCATACTTT GACGAAACAA
 6661 ATTTTCGTTG CATACCCAAT AAAAGATTAT TATATTGCAT ACCCGTTTTT AATAAAATAC
 6721 ATTGATACCT CTCTTTAAT AAAAAATATT GCATACGTTG ACGAAACAAA TTTTCGTTGC
 6781 ATACCCAATA AAAGATTATT ATATTGCATA CCTTTTCTTG CCATACCATT TAGCCGATCA
 6841 ATTGTGCTCG GCAACAGTAT ATTTGTGGTG TGCCAACCAA CAACGGATCC ACTAGTGTGC
 6901 ACGATGTAGG TCACGGTCTC GAAGCCGCGG TGCGGGTGCC AGGGCGTGCC CTTGGGCTCC
 6961 CCGGGCGCGT ACTCCACCTC ACCCATCTGG TCCATCATGA TGAACGGGTC GAGGTGGCGG
 7021 TAGTTGATCC CGGCGAACGC GCGGCGCACC GGAAGCCCT CGCCCTCGAA ACCGCTGGGC
 7081 GCGGTGGTCA CGGTGAGCAC GGGACGTGCG ACGGCGTCGG CGGGTGCGGA TACGCGGGG
 7141 AGCGTCAGCG GGTCTCGAC GGTACGGCG GGCATGTCGA CACTAGTTCT AGCCAGCTTT
 7201 TGTTCCCTTT AGTGAGGGTT AATTCGAGC TTGGCGTAAT CATGGTCATA GCTGTTTCT
 7261 GTGTGAAATT GTTATCCGCT CACAATTCCA CACAACATAC GAGCCGGAAG CATAAAGTGT
 7321 AAAGCCTGGG GTGCCTAATG AGTGAGCTAA CTCACATTAA TTGCGTTGCG CTCACTGCC
 7381 GCTTTCCAGT CGGGAAACCT GTCGTGCCAG CTGCATTAAT GAATCGGCCA ACGCGCGGG
 7441 AGAGGCGGTT TCGTATTGG GCGCTCTCC GCTTCTCGC TCACTGACTC GCTGCGCTCG

7501 GTCGTTCCGGC TCGGGCGAGC GGTATCAGCT CACTCAAAGG CGGTAATACG GTTATCCACA
7561 GAATCAGGGG ATAACGCAGG AAAGAACATG TGAGCAAAAG GCCAGCAAAA GGCCAGGAAC
7621 CGTAAAAAGG CCGCGTTGCT GGCGTTTTTC CATAGGCTCC GCCCCCCTGA CGAGCATCAC
7681 AAAAATCGAC GCTCAAGTCA GAGGTGGCGA AACCCGACAG GACTATAAAG ATACCAGGCG
7741 TTTCCCCTG GAAGCTCCCT CGTGCCTCT CCTGTCCGA CCCTGCCGCT TACCGGATAC
7801 CTGTCCGCT TTCTCCCTC GGAAGCGTG GCGCTTCTC ATAGCTCACG CTGTAGGTAT
7861 CTCAGTTCGG TGTAGTCTG TCGCTCCAAG CTGGGCTGTG TGCACGAACC CCCCCTTCAG
7921 CCCGACCGCT GCGCCTTATC CGGTAATAT CGTCTTGAGT CCAACCCGGT AAGACACGAC
7981 TTATCGCCAC TGGCAGCAGC CACTGGTAAC AGGATTAGCA GAGCGAGGTA TGTAGGCGGT
8041 GCTACAGAGT TCTTGAAGTG GTGGCCTAAC TACGGCTACA CTAGAAGAAG AGTATTTGGT
8101 ATCTGCGCTC TGCTGAAGCC AGTTACCTC GGAAAAAGAG TTGGTAGCTC TTGATCCGGC
8161 AAACAAACCA CCGCTGGTAG CGGTGGTTTT TTTGTTTGCA AGCAGCAGAT TACGCGCAGA
8221 AAAAAGGAT CTCAAGAAGA TCCTTTGATC TTTTCTACGG GGTCTGACGC TCAGTGGAAC
8281 GAAAACCTCAC GTTAAGGGAT TTTGGTCATG AGATTATCAA AAAGGATCTT CACCTAGATC
8341 CTTTTAAATT AAAAATGAAG TTTAAATCA ATCTAAAGTA TATATGAGTA AACTTGGTCT
8401 GACAGTTACC AATGCTTAAT CAGTGAGGCA CCTATCTCAG CGATCTGTCT ATTTTCGTTCA
8461 TCCATAGTTG CCTGACTCCC CGTCGTGTAG ATAACCTACG TACGGGAGGG CTTACCATCT
8521 GGCCCCAGTG CTGCAATGAT ACCGCGAGAC CCACGCTCAC CGGCTCCAGA TTTATCAGCA
8581 ATAAACCAGC CAGCCGGAAG GGCCGAGCGC AGAAGTGGTC CTGCAACTTT ATCCGCCTCC
8641 ATCCAGTCTA TTAATTGTTG CCGGGAAGCT AGAGTAAGTA GTTCGCCAGT TAATAGTTTG
8701 CGCAACGTTG TTGCCATTGC TACAGGCATC GTGGTGTAC GCTCGTCGTT TGGTATGGCT
8761 TCATTCAGCT CCGTTCCCA ACGATCAAGG CGAGTTACAT GATCCCCAT GTTGTGCAAA
8821 AAAGCGGTTA GCTCCTTCGG TCCTCCGATC GTTGTGAGAA GTAAGTTGGC CGCAGTGTTA
8881 TCACTCATGG TTATGGCAGC ACTGCATAAT TCTTCTACTG TCATGCCATC CGTAAGATGC
8941 TTTTCTGTGA CTGGTGAGTA CTCAACCAAG TCATTCTGAG AATAGTGTAT GCGGCGACCG
9001 AGTTGCTCTT GCCCGGCGTC AATACGGGAT AATACCGCGC CACATAGCAG AACTTTAAAA
9061 GTGCTCATCA TTGGAAAACG TTCTTCGGGG CGAAAACCTCT CAAGGATCTT ACCGCTGTTG
9121 AGATCCAGTT CGATGTAACC CACTCGTGCA CCCAACTGAT CTTGAGCATC TTTTACTTTC
9181 ACCAGCGTTT CTGGGTGAGC AAAAACAGGA AGGCAAAATG CCGCAAAAAA GGAATAAGG
9241 GCGACACGGA AATGTTGAAT ACTCATACTC TTCCTTTTTC AATATTATTG AAGCATTAT
9301 CAGGGTTATT GTCTCATGAG CGGATACATA TTTGAATGTA TTTAGAAAAA TAAACAAATA
9361 GGGGTTCCGC GCACATTTC CCGAAAAGTG CCAC

2.Template Atf6 Sequence.

Atf6, isoform B [Drosophila melanogaster] Sequence ID: ref|NP_610159.1|Length: 739

Protein Sequence 344(1032):

MTPCLFSDDLSSLGTEVNNYDNNIVHDILNSSAFYNDTSLDLSELIPDLQKEAFGLHFSSNPITSE
FSLSSPISGLKQIPSA CSGEFKRVNDNNFQLDLTNSRNDLPEPNSSPTRSLNRSNVNGCSN EEA V
YPLLVDSDKFDPPFEPKVRSPNKEFNSTISNLSDIKNELPETSQDLGFNSYNTSRNNSTLTKSWPI

NTELNLDNQVPKTVLPLSRTIYLPSHDYKGLLPTVKCNGDRTLKKNVNVRSKISNIVIKKNATFIQ
 SLKESTPSHTMDDKIYKQYQRMKNRESASLSRKKRKEYVVSLETRINKLEKECDLKAENITLRDQI
 FLLATSCQR

2. Blast result on NCBI

[Download](#) [GenBank](#) [Graphics](#)

Drosophila melanogaster Atf6 (Atf6), transcript variant B, mRNA
 Sequence ID: [ref|NM_136315.3|](#) Length: 3959 Number of Matches: 1

Range 1: 1014 to 2045 [GenBank](#) [Graphics](#) ▼ Next Match ▲ Previous Match

Score	Expect	Identities	Gaps	Strand
1906 bits(1032)	0.0	1032/1032(100%)	0/1032(0%)	Plus/Plus
Query 1	ATGACGCCATGTTTATTTTCAGACGATTTATCGCTGTTGGGAGAAGTGACTGAAAATAAC	60		
Sbjct 1014	ATGACGCCATGTTTATTTTCAGACGATTTATCGCTGTTGGGAGAAGTGACTGAAAATAAC	1073		
Query 61	TACGACAATAATATTGTACACGACATTCTGAACTCATCAGCATTCTACAATGATACATCG	120		
Sbjct 1074	TACGACAATAATATTGTACACGACATTCTGAACTCATCAGCATTCTACAATGATACATCG	1133		
Query 121	TTAGATCTAAGTGAATTAATACCTGATCTTCAAAAAGAAGCCTTTGGATTGCATTTCTCG	180		
Sbjct 1134	TTAGATCTAAGTGAATTAATACCTGATCTTCAAAAAGAAGCCTTTGGATTGCATTTCTCG	1193		
Query 181	TCAAACCCAATAACTTCAGAATTTAGCTTGAGTTCCCGATTTCTGGTTTGAACAAATT	240		
Sbjct 1194	TCAAACCCAATAACTTCAGAATTTAGCTTGAGTTCCCGATTTCTGGTTTGAACAAATT	1253		
Query 241	CCTTCAGCGTGTTCTGGTGAATTTAAAAGAAATGTAATGACAATAATTTTCAATTGGAT	300		
Sbjct 1254	CCTTCAGCGTGTTCTGGTGAATTTAAAAGAAATGTAATGACAATAATTTTCAATTGGAT	1313		
Query 301	CTTACCAACAGTAGAAATGATTTACCTGAGCCTAATTCGTCTCCCAAGAAGCTTAAAT	360		
Sbjct 1314	CTTACCAACAGTAGAAATGATTTACCTGAGCCTAATTCGTCTCCCAAGAAGCTTAAAT	1373		
Query 361	CGTTCAAATGTAATGGATGTTCTAACGAAGAGGCGGTCTATCCACTCTTAGTCGATTCA	420		
Sbjct 1374	CGTTCAAATGTAATGGATGTTCTAACGAAGAGGCGGTCTATCCACTCTTAGTCGATTCA	1433		
Query 421	GATAAGTTTGATCCATTTTTTGAACCTGCTAAAGTTCGGAGCCCCAACAAAGAATTC AAC	480		
Sbjct 1434	GATAAGTTTGATCCATTTTTTGAACCTGCTAAAGTTCGGAGCCCCAACAAAGAATTC AAC	1493		
Query 481	AGCACGATTTCTAATCTATCAGATATAAAAAACGAACTTCCGGAAACTTCCCAAGACTTG	540		
Sbjct 1494	AGCACGATTTCTAATCTATCAGATATAAAAAACGAACTTCCGGAAACTTCCCAAGACTTG	1553		
Query 541	GGTTTTAATTCATATAACACTTCAAGGAATAATTCAACTTTAACCAAAAGCTGGCCAATA	600		
Sbjct 1554	GGTTTTAATTCATATAACACTTCAAGGAATAATTCAACTTTAACCAAAAGCTGGCCAATA	1613		
Query 601	AATACTGAGCTGAATCTAGATAATCAAGTTCCAAAAACAGTTTTACCTTTGTCAAGGACA	660		
Sbjct 1614	AATACTGAGCTGAATCTAGATAATCAAGTTCCAAAAACAGTTTTACCTTTGTCAAGGACA	1673		
Query 661	ATTTATTTACCTTCACATGATTACAAAGGCTTTTGCCAACAGTGAAATGTAAACGGTGAT	720		
Sbjct 1674	ATTTATTTACCTTCACATGATTACAAAGGCTTTTGCCAACAGTGAAATGTAAACGGTGAT	1733		

Acknowledgement

Firstly, I would like to express my sincere gratitude to my advisor Prof. Dr. Reoder for the continuous support of my Ph.D study and related research, for his patience, motivation, and immense knowledge. His guidance helped me in all the time of research and writing of this thesis. I could not have imagined having a better advisor and mentor for my Ph.D study. Besides my advisor, I deeply appreciate to Dr. Christine Fink, Dr. Yong Li and Dr. Yang Li for guiding me into the experimental work. I would also like to thank Britta Laubenstein and Christiane Sandberg for excellent technical assistance. I am deeply grateful for all the kindness and help from all the other colleagues. Last but not the least, I would like to thank my parents for supporting me spiritually throughout writing this thesis and my life in general.

Curriculum vitae

Personal data:

Name: Gu Tian

Gender: Female

Data of birth: June 27, 1986

Place of birth: Heilongjiang, China

Marital status: Married

Email: gutian0627@gmail.com

Education:

11.2013-date: PhD at the Institute of Zoophysiology II, Faculty of mathematics and natural science, Christian–Albrechts University, Kiel, Germany. Title of my thesis: “Effects of activation of the Unfolded Protein Response in *Drosophila melanogaster*”.

09.2009-06.2012: M.Sc. in Microbiology, Department of resource and environment, Northeast Agriculture University, China. Thesis: “Gene clone of xylanase in *Penicillium citrinum* and protein expression in yeast.”

09.2005-06.2009: B.Sc. in Microbiology, Department of resource and environment, Northeast Agriculture University, China. Thesis: “Comparison of three methods for total DNA extraction from soil microorganisms.”

Declaration

I, Gu Tian, here declare that my doctoral thesis entitled “Effects of activation of the Unfolded Protein Response in *Drosophila melanogaster*” and the work presented in it are my own work apart from supervisor’s guidance and design of the paper. This dissertation has not been submitted for the award of doctoral degree to another examining body and was prepared according to the Rules of Good Scientific Practice of the German Research Foundation.

Erklärung

Hiermit erkläre ich, Gu Tian, dass diese Dissertation mit dem Titel: “ Effects of activation of the Unfolded Protein Response in *Drosophila melanogaster*”, sowie die darin beschriebenen Arbeiten, abgesehen von der Beratung durch meinen akademischen Lehrer, nach Inhalt und Form meine eigene Arbeit ist. Diese Arbeit wurde weder im Ganzen noch zum Teil an anderer Stelle im Rahmen eines Promotionsvorhabens eingereicht. Sie wurde nach den Regeln guter wissenschaftlicher Praxis der Deutschen Forschungsgemeinschaft angefertigt.

Kiel,

Gu Tian